Mucin-linked regulatory factors in *C. jejuni* infections and advances in spheroid modeling

Inaugural-Dissertation

to obtain the academic degree

Doctor rerum naturalium (Dr. rer. nat.)

submitted to the Department of Biology, Chemistry, Pharmacy

of Freie Universität Berlin

by

Angelina Kraski

2024

This thesis was conducted in the group of PD Dr. Soroush Sharbati at the Freie Universität Berlin, Institute of Veterinary Biochemistry from October 2021 to October 2024. Parts of the following thesis were published in Gut Pathogens.

1st reviewer:	PD Dr. Soroush Sharbati School of Veterinary Medicine Institute of Veterinary Biochemistry
2nd reviewer:	Prof. Dr. Burkhard Kleuser Department of Biology, Chemistry and Pharmacy Institute of Pharmacy
Date of Defense:	16.01.2025

Declaration of Independence

I hereby declare that I alone am responsible for the content of my doctoral dissertation and that I have only used the sources or references cited in the dissertation.

Angelina Kraski

Table of Content

List of Figures

List of Abbreviation

2D	two-dimensional
3D	three-dimensional
AGO	Argonaute protein family
AKT	Protein kinase B
AMP	antimicrobial peptides
B3GNT6	3-N-acetylglucosaminyltransferase 6
B4GALT1	beta -1,4-galactosyltransferase 1
BMZ	German Federal Ministry for Economic Cooperation and Development
C. jejuni	*Campylobacter jejuni*
C1GalT1	N-acetylgalactosamine 3-beta-galactosyltransferase 1
CadF	*Campylobacter* adhesion to fibronectin
CMP-NeuAc	CMP-N-acetylneuraminate
CMP-SA	CMP-N-acetyl-neuraminate
DCS	deep crypt secretory
DGCR8	DiGeorge Syndrome Critical Region 8
EFNB	EphrinB
EFSA	European Food Safety Authority
EGF	Epidermal Growth Factor
EGFR	Epidermal Growth Factor Receptor
EPHB2	ephrin B receptor 2
FlpA	fibronectin-like protein A
Fuc	fucose
Gal	galactose
GalNAc	N-acetyl galactosamine
GalNAc-T	UDP-GalNAc:polypeptide *N*-acetylgalactosaminyltransferases
GCNT	Glucosaminyl (N-Acetyl) Transferases
GlcNAc	N-acetyl glucosamine
H. pylori	*Helicobacter pylori*
IFNγ	interferon gamma
IL	Interleukin

LOS	Lipooligosaccharide
M cells	microfold cells
miRISC	miRNA induced silencing complex
miRNA	microRNA
MRE	miRNA response element
mRNA	messenger RNA
MUC	Mucin
ncRNA	non-coding RNA
NeuAc	N-acetyl neuramic acid
NF-κB	nuclear factor 'kappa-light-chain-enhancer' of activated B-cells
OMPs	outer membrane proteins
OoC	organ-on-a-chip
PEPT1	peptide transporter 1
PI3K	phosphoinositide 3-kinase
PIP2	phosphatidylinositol-4,5-bisphosphate
PIP3	phosphatidylinositol-3,4,5-trisphosphate
pre-miRNA	precursor-miRNA
pri-miRNA	primary miRNA
PRR	Pattern Recognition Receptor
PTS	proline, threonine and serine
ROS	reactive oxygen species
S. flexneri	*Shigella flexneri*
SGLT1	sodium-dependent glucose cotransporter 1
shRNA	small hairpin RNAs
SMIS	structured multicellular intestinal spheroids
ST3GAL	ST3-beta-galactoside alpha-2,3-sialyltransferase
ST6GAL	beta-galactosidase alpha-2,6 sialyltransferase
ST6GALNAC	ST6-*N*-acetyl-galactosaminide alpha-2,6-sialyltransferase
ST8SIA	ST8 alpha-*N*-acetyl-neuraminide alpha-2,8-sialyltransferase
TFF3	Trefoil factor 3
TLR	Toll-like receptor
TNF-α	tumor necrosis factor alpha

TRBP	transactivation response element RNA-binding protein
T-synthase	N-acetylgalactosamine 3-beta-galactosyltransferase 1
ULA	Ultra Low Attachment
WHO	World Health Organization

1. Summary

Campylobacter jejuni is a prevalent zoonotic pathogen and the most common source of bacterial intestinal infections worldwide. However, the pathogenesis of the infection is not fully understood and detailed research on the underlying molecular mechanisms of many host-pathogen factors involved in colonization and infection is needed. *C. jejuni* has adapted several methods to penetrate the double mucus layer in the human colon, infect the epithelium and cause acute inflammation processes. Main component of this protecting barrier is MUC2, which is highly glycosylated by mucin-type *O*-glycosylations through specific glycosyltransferases. The expression of several glycosyltransferases involved in mucin-type *O*-glycosylation is dysregulated in *C. jejuni* infections, which may affect the mucosal defense mechanisms and influence the severity of the infection.

miRNAs play an important role in controlling mammalian host cell responses to bacterial infections. It was shown that the mucin-associated miRNAs miR-125a-5p and miR-615-3p are dysregulated in *C. jejuni* infections. Moreover, a potential regulation of miR-125a-5p on the expression of the sialyltransferase *St3gal1* and the glycosyltransferase *B4galt1* was demonstrated by combining *in silico*, *in vitro* and *in vivo* approaches. *St3gal1* and *B4galt1* are both involved in mucin-type *O*-glycosylations and significantly upregulated in an infection-dependent manner in the colon of *C. jejuni* infected mice compared to naïve control animals. Hence, miR-125a-5p possibly participates in regulating the glycosylation pattern of important host cell response proteins like MUC2 upon infection.

For further investigations, human structured multicellular intestinal spheroids (SMIS) were generated. This advanced 3D cell culture model comprises of four relevant cell lines, with a fibroblast core that is surrounded by a single layer of enterocytes, goblet cells and activated monocytes. SMIS thereby replicate the microarchitecture of the luminal surface of the human intestinal mucosa. Further, the spheroids show differentiated morphological characteristic like microvilli after only two days in culture. SMIS were specifically designed to study molecular mechanisms following the infection by intestinal pathogens. After *C. jejuni* infections, they exhibit regulatory patterns of immunological markers that surpass 2D monolayers and closely align with *in vivo* responses to the infection. The human SMIS protocol is adaptable to the species mouse and pig, demonstrating its versatility.

2. Zusammenfassung

Campylobacter jejuni ist ein weit verbreitetes zoonotisches Pathogen und die häufigste Ursache bakterieller intestinaler Infektionen weltweit. Die Pathogenese der Infektion ist jedoch unzureichend erforscht und bedarf weiterführender Untersuchungen hinsichtlich der zugrundeliegenden molekularen Mechanismen von Wirt und Pathogen, die an Kolonisation und Infektion beteiligt sind. *C. jejuni* hat verschiedene Methoden entwickelt, um die schützende doppelte Mucus-Schicht im menschlichen Colon zu durchdringen, um dann das Epithelium zu infizieren und akute Inflammationsprozesse auszulösen. Hauptbestandteil dieser schützenden Barriere ist MUC2, das durch muzinartige *O*-Glykosylierungen, die von spezifischen Glykosyltransferasen katalysiert werden, stark glykosyliert ist. Die Expressionen mehrerer Glykosyltransferasen, die an muzinartigen *O*-Glykosylierungen beteiligt sind, sind bei *C. jejuni* Infektionen dysreguliert. Diese Veränderung kann die mukosalen Abwehrmechanismen beeinträchtigen und die Schwere der Infektion beeinflussen.

miRNAs spielen in Säugetieren bei der Kontrolle der Wirtszellantwort auf bakterielle Infektionen eine wichtige Rolle. Es konnte gezeigt werden, dass die muzin-assoziierten miRNAs miR-125a-5p and miR-615-3p in *C. jejuni* Infektionen dysreguliert sind. Darüber hinaus konnte eine mögliche Regulation von miR-125a-5p auf die Expression von der Sialyltransferase *St3gal1* und die Glykosyltransferase *B4galt1* durch die Kombination von *in silico*, *in vitro* und *in vivo* Methoden nachgewiesen werden. *St3gal1* und *B4galt1* sind beide an muzinartigen *O*-Glykosylierungen beteiligt und bei einer Infektion im Colon von *C. jejuni* infizierten Mäusen verglichen mit nicht-infizierten Kontrolltieren signifikant hochreguliert. Daraus ist zu schließen, dass miR-125a-5p Teil der Regulationsprozesse von Glykosylierungsmustern wichtiger Wirtszellenproteine als Antwort auf Infektionen ist.

Für weiterführende Untersuchungen wurden menschliche strukturierte multizelluläre intestinal Sphäroide (SMIS) entwickelt. Dieses 3D-Zellkulturmodell besteht aus vier relevanten Zelllinien mit einem Fibroblastenkern, der von einer Einzelschicht aus Enterozyten, Becherzellen und aktivierten Monozyten umgeben ist. Damit repliziert SMIS die Mikroarchitektur der luminalen Oberfläche der menschlichen intestinalen Mukosa. Zusätzlich weisen die Sphäroide bereits nach zwei Tagen in Kultur differenzierte morphologische Merkmale wie Mikrovilli auf. SMIS wurden speziell dafür entwickelt, molekulare

Mechanismen nach Infektionen mit Darmpathogenen zu untersuchen. Nach *C. jejuni* Infektion zeigen sie regulatorische Muster immunologischer Marker, die die von 2D-Monolayern übertreffen und die den *in vivo* Reaktionen auf die Infektion stark ähneln. Das menschliche SMIS-Protokoll ist auf die Spezies Maus und Schwein übertragbar, was dessen Vielseitigkeit demonstriert.

3. Introduction

3.1 The Mammalian Intestinal Mucosa

The main function of the mammalian intestinal tract is digesting and absorbing ingested nutrients and water while simultaneously excreting waste products. To achieve this, the intestine has a specialized functional anatomy, divided in four main layers: the Tunica mucosa (short mucosa), Tela submucosa, Tunica muscularis and Tunica serosa. The most crucial layer for investigating intestinal absorption but also bacterial infections is the mucosa, the first layer facing the lumen. As presented in Figure 1, the mucosa comprises the Lamina epithelialis mucosae, Lamina propria mucosae and Lamina muscularis mucosae.

The Lamina epithelialis is a simple layer of absorptive and secretory columnar epithelial cells that provides a physical and biochemical barrier between host intestinal tissue and the external environment. The absorptive epithelial cells are known as enterocytes, or colonocytes in the colon, and make up the majority of cells in the Lamina epithelialis. Integrated in the epithelial monolayer are goblet cells, enteroendocrine cells, Tuft cells and microfold cells (M cells). Goblet cells are specialized mucus-producing epithelial cells, while enteroendocrine cells, predominantly found in the small intestine, generate and secrete intestinal hormones and peptides. Tuft cells serve as chemosensory antiparasitic cells and M cells are part of the gut-associated lymphoid tissue and located in Peyer's Patches, which are organized lymphoid follicles concentrated in the ileum. Primary function of the M cells is facilitating mucosal immune surveillance by selectively transporting antigens from the intestinal lumen to underlying immune cells. Individual epithelial cells are connected by intercellular junctions, including tight junctions, adherens junctions and desmosomes, to seal the space between the cells paracellularly and prevent leakage of solutes. These cell-cell connections are also important for the structure of the epithelium and intercellular communication.

The surface area in the small intestine is expanded by villi - numerous finger-like structures protruding into the lumen and covered by the epithelial monolayer for enhanced nutrient absorption. Similar bristle like protrusions, the microvilli, are located on the luminal surface of the absorptive epithelial cells, forming brush borders to maximize the cell surface area to facilitate absorption. Microvilli are also found on colonic epithelial cells, villi on the other hand

are absent in the colon as the main function here is not the absorption and digestion of nutrients but rather dehydration of the digested food by slowly absorbing water and remaining electrolytes. Tubular invaginations called crypts of Lieberkühn (short crypts) can be found in the colon and in the small intestine acting as regulators for epithelial regeneration and homeostasis. Paneth cells in the small intestine and equivalently deep crypt secretory cells (DCS) in the colon as part of the innate immune system are found in the crypts. They secrete anti-microbial compounds into the intestinal lumen and thereby modulate host-defense and immunity. Paneth cells and DCS cells intercalate between actively proliferating pluripotent intestinal stem cells that reside at the bottom of the crypts and continuously regenerate intestinal cells that differentiate into specialized epithelial cells as they move up the crypt. This leads to a constantly renewing system of proliferating and differentiated cells in the mammalian epithelium. Enterocytes, colonocytes and M cells originate from non-secretory stem cell lineages whereas the other primary specialized types of intestinal epithelial cells - goblet cells, Paneth cells, DCS cells, enteroendocrine cells and Tuft cells - arise from shared secretory stem cell lineages.

Above the epithelium is the intestinal double mucus layer which creates a protective barrier for the mucosa. For additional protection, epithelial cells produce the glycocalyx, a multifunctional surface layer composed of tightly packed glycans of glycoproteins and glycolipids.

Beneath the Lamina epithelialis mucosae lies the Lamina propria mucosae, a thin loose connective tissue layer consisting of mesenchymal and immune cells. Mesenchymal cells are represented by fibroblasts and myofibroblasts and the immune cells include granulocytes, mononuclear phagocytes (monocytes and macrophages), T-cells and B-cells. It is richly vascularized, thereby supplying the epithelium with nutrients. The Lamina propria provides structural support and significantly impacts the intestinal immune response.

Lastly, the Lamina muscularis mucosae is the outermost layer of the mucosa and consists of smooth muscle cells, arranged in an inner circular and outer longitudinal layer, along with elastic fibers. Muscle contractions facilitate absorption by moving the mucosa and mucus.

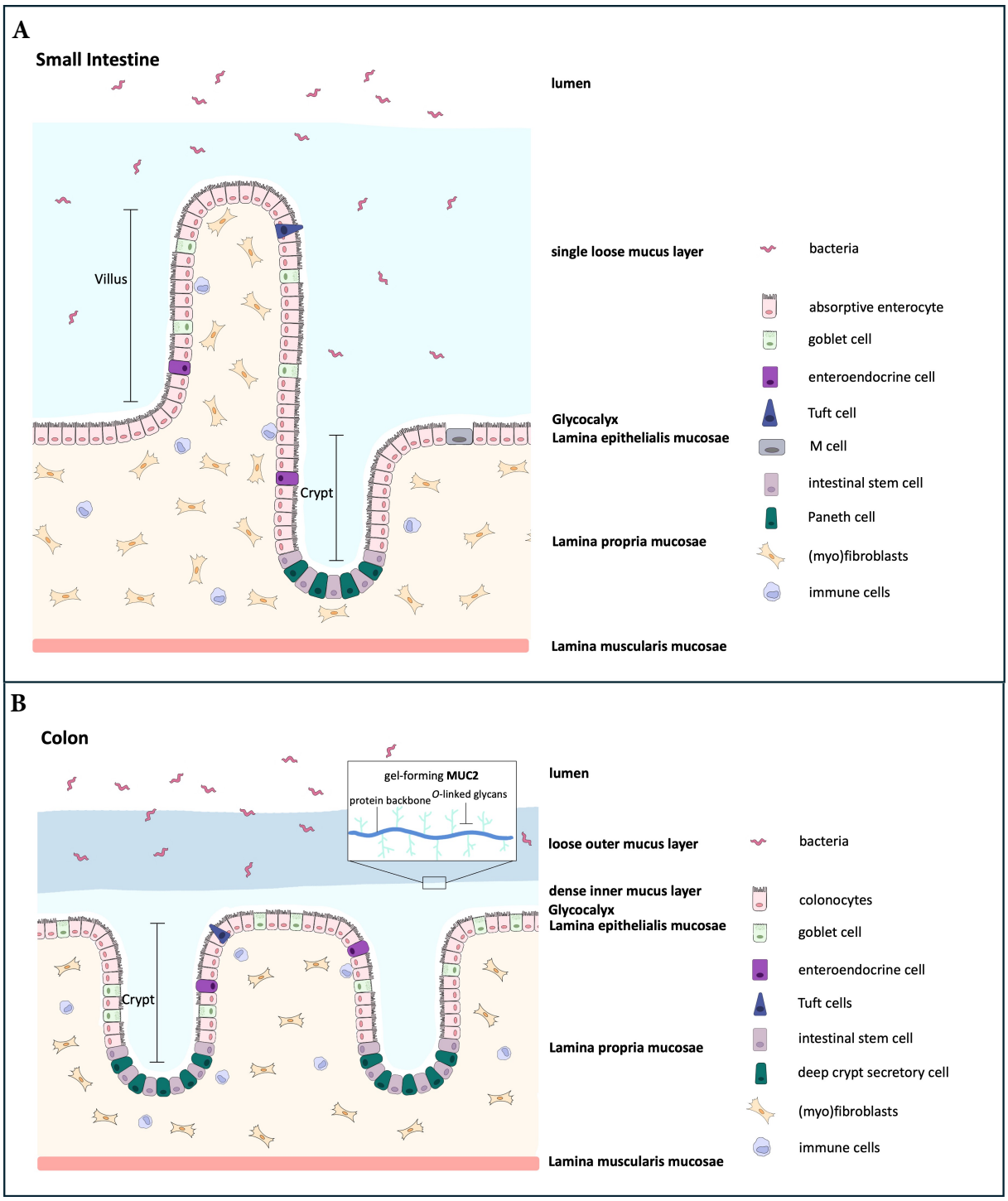

Figure 1: Schematic representation of the mammalian intestinal mucosa. The mucosa in the small intestine and colon comprises the Lamina epithelialis mucosae, Lamina propria mucosae and Lamina muscularis mucosae. (A) Structure of the mucosa of the small intestine. Relevant cell types of the Lamina epithelialis mucosae are absorptive enterocytes, goblet cells, enteroendocrine cells, Tuft cells and M cells. Additionally, intestinal stem cells and Paneth cells reside at the base of the crypts. Only a single, loosely attached mucus layer that is penetrable by the intestinal microbiota covers the Lamina epithelialis mucosae. (B) Structure of the mucosa in the colon. The Lamina epithelialis mucosae is composed of a monolayer of colonocytes, goblet cells, enteroendocrine cells and Tuft cells as well as intestinal stem cells and deep crypt secretory cells in the crypt base. The colonic mucosa consists of a

double mucus layer with an outer, loose and an inner, densely packed layer. While the outer layer is penetrable, the inner layer is impenetrable to the intestinal microbiota. Main component of both colonic mucus layers is the gel-forming MUC2, a highly *O*-glycosylated protein. An additional protective layer, the glycocalyx, can be found above the epithelium in the small intestine and colon. Cells of the Lamina propria mucosae in small intestine and colon include immune cells and (myo)fibroblasts. This figure is adapted from [1].

3.2 Colonic Mucus

3.2.1 Mucus

The mucus is a complex, viscoelastic and gel-like secretion that is produced and released by specialized secretory cells. It is found on the luminal side of the columnar epithelial lining in various organs, including the respiratory, intestinal and reproductive tract, that have contact with the external environment. The combination of viscous and elastic properties allows the mucus to adhere to surfaces and form a protective physicochemical barrier. The structural framework of the mucus barrier is formed by mucins (MUC), which serve as the primary architectural component. Mucins are a family of high molecular weight, heavily *O*-glycosylated proteins (glycoproteins) that can be divided into two subfamilies: the cell surface or transmembrane and secreted mucins. Cell surface mucins are bound to and integrated in the cellular membrane and form a carbohydrate-rich protective layer while secreted mucins are released into the lumen and contribute to the viscous properties of the mucus. Mucus layer dysfunctions are linked to various diseases across multiple organ systems, underlining the critical role of properly function mucus to maintain overall health. Diseases associated with an imbalanced mucus layer include Inflammatory Bowel Disease in the intestinal tract, Chronic Constructive Pulmonary Disease in the respiratory tract or Bacterial vaginosis in the reproductive tract [2-4].

3.2.2 Gastrointestinal Mucins

The entire luminal surface of the mammalian gastrointestinal tract is coated by a protective layer of intestinal mucus. This mucus layer serves multiple crucial functions including facilitating a smooth passage of food by acting as a natural lubricant, protecting the underlying

host epithelium from the commensal or pathogenic bacteria, toxins and other environmental irritants and participating in cell signaling pathways [1]. The composition of the mucus varies throughout the gastrointestinal tract, adapting to the need of each organ or specific section of the organ. Main mucins expressed in the stomach are the membrane bound, cell surface mucin MUC1 and the secreted MUC5AC and MUC6 that form a double mucus layer. The small intestine on the other hand, only contains a single mucus layer primarily composed of MUC2 and MUC6, that is penetrable by bacteria. The transmembrane mucins of the small intestine and colon, including MUC3, MUC12, MUC13, MUC15 and MUC17 predominantly form the glycocalyx. The mammalian colon features a constantly renewing double mucus layer. The predominant component of both layers is MUC2, which is produced, stored and secreted by goblet cells and structurally resembles a bottle brush (Figure 1). Under healthy conditions, the outer loosely adherent layer harbors a diverse community of microorganisms collectively known as the microbiota which co-evolve in a mutually beneficial relationship with the host. In contrast, the inner densely packed mucus layer is sterile and impenetrable for the microbiota. Additionally, antimicrobial peptides (AMP), bioactive compounds produced by various intestinal cells like epithelial or immune cells, are integrated into the mucus barrier to enhance the host's defense mechanisms against microorganisms while maintaining tolerance to commensal microbiota [5].

3.2.3 Colonic MUC2 *O*-Glycosylation

MUC2 is a high molecular weight glycoprotein with repeating domains of the amino acids proline, threonine and serine (PTS-domains) on the protein backbone. These PTS domains create binding sites for *O*-glycosylation by *O*-linked oligosaccharides (the mucin-type *O*-glycans, hereafter referred to as *O*-glycans), which can constitute up to 80% of the total MUC2 mass (Figure 2) [1, 6]. MUC2 also contains *N*-linked glycans in addition to *O*-linked glycans, although they only play a minor role.

Once secreted, MUC2 unfolds its gel-forming, viscous properties due to the hydration and high water-binding capacity of its *O*-glycans and builds a polymeric network by binding to other hydrated MUC2 molecules. This represents one of the various functions of the *O*-glycans on mucins. The glycans additionally aid in the tight packaging and storage of MUC2, serve as carbon and energy sources for mucus residing commensal bacteria and play essential roles in biological processes like cell adhesion, cell growth, immunity and intestinal homeostasis [7,

8]. The mucus undergoes a continuously high turnover rate that increases in response to stress stimuli, such as pathogenic invasion or toxins to eliminate them by rapidly flushing them away [1]. Furthermore, inflammatory cytokines, such as the interleukins (IL) IL-1, IL-6 and IL-8 or tumor necrosis factor alpha (TNF-α) can actively influence MUC2 expression [9, 10]. Interestingly, MUC2 gene promotor is shown to have binding sites for the transcription factor nuclear factor 'kappa-light-chain-enhancer' of activated B-cells (NF-κB), a key transcription factor regulating the immune response to infections. When lipopolysaccharides from enteropathogens activate NF-κB, it simultaneously increases MUC2 transcription in colonic epithelial cells [11]. This mechanism demonstrates an indirect connection between pathogen detection and mucin production.

The MUC2 glycosylation is a post-translational modification that occurs as a stepwise process in the Golgi apparatus (Figure 2). In the initial step, the monosaccharide N-acetyl galactosamine (GalNAc) is *O*-linked to hydroxyl groups of serine (serine-linked) and threonine (threonine-linked) in the PTS domains, forming the Tn-antigen (GalNAc-*O*-Ser/Thr) [12]. Subsequent steps involve the binding of different sugar molecules to GalNAc, generating various core structures that vary depending on the monosaccharide extension pattern. The majority of the glycans are composed of GalNAc, N-acetyl glucosamine (GlcNAc), galactose (Gal) and fucose (Fuc), which are bound by specific enzymes called glycosyltransferases [6]. It has been shown that inhibition of glycosyltransferases results in increased mucus permeability, highlighting the significance of the *O*-glycan binding for adequate mucus function [13]. There are eight different mucin core structures, although only four are commonly found. The most prevalent extension structure is the core 1, characterized by a β-1,3 linkage between Gal and GalNAc on the Tn-antigen. This bond is catalyzed by the glycosyltransferase N-acetylgalactosamine 3-beta-galactosyltransferase 1, also known as T-synthase or C1GalT1 [14]. Core 3 formation involves the attachment of GlcNAc to GalNAc mediated by the beta-1, 3-N-acetylglucosaminyltransferase 6 (B3GNT6) [14]. These two primary core structures can be further extended to form Core 2 and Core 4, respectively. This extension process is facilitated by a family of enzymes called Glucosaminyl (N-Acetyl) Transferases (GCNT1-4). All four core structures can then be further elongated, for example by transferring galactose in a β-1,4 linkage to similar acceptor sugars of the core 2 structures by beta -1,4-galactosyltransferase 1 (B4GALT1), creating a wide variety of differently

composed *O*-glycans. The elongated sugar chains restrict access to the MUC2 protein backbone, preventing mucus degradation by host digestive and bacterial proteases.

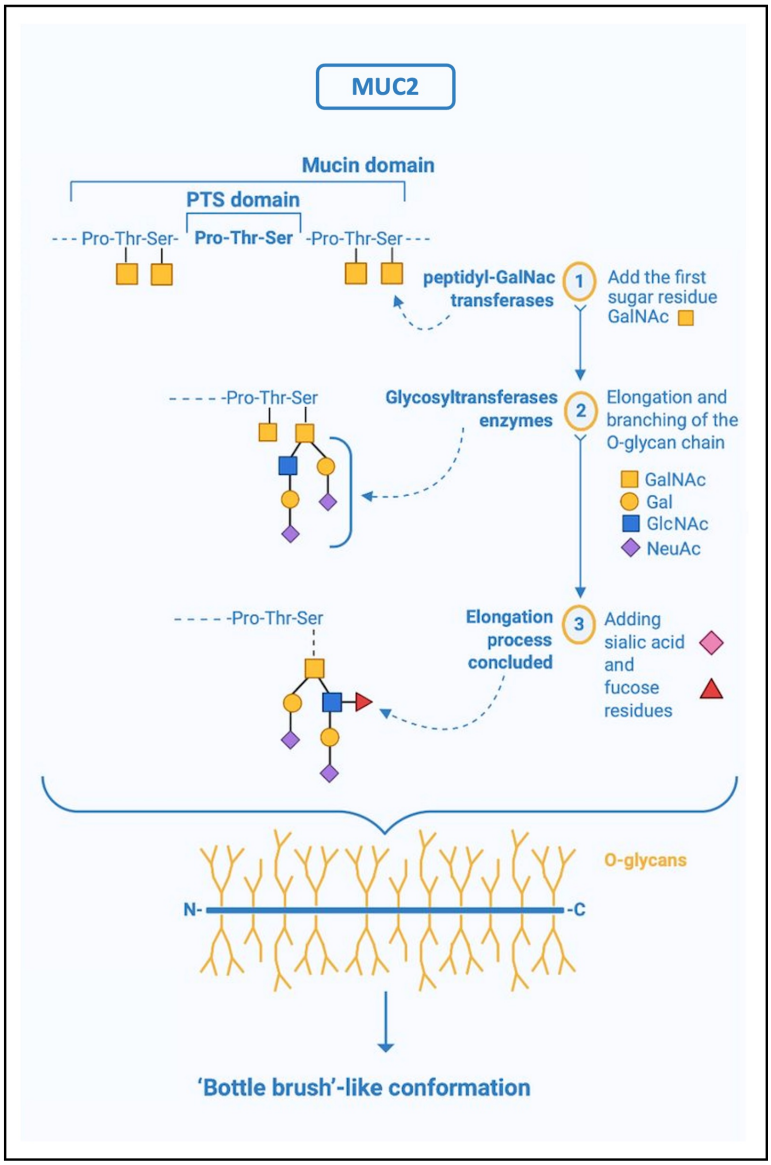

Figure 2: Different steps in MUC2 *O*-glycosylation. The initial step in MUC2 *O*-glycosylation involves the addition of the *O*-glycan GalNAc to serine and threonine residues in the PTS domain on the MUC2 protein backbone. Subsequent elongation and branching by different *O*-glycans including GalNAc, Gal, GlcNAc or NeuAc is catalyzed by specific glycosyltransferases. The *O*-glycosylation of MUC2 leads to a "bottle brush"-like conformation. Pro - proline; Ser - serine; Thr – threonine; GalNAc - N-acetyl galactosamine; Gal - galactose, GlcNAc - N-acetyl glucosamine; NeuAc - N-acetyl neuramic acid. This Figure is adapted from [15].

Interestingly, glycans are not just found on secreted and cell-membrane host glycoproteins but also on the surface of various pathogenic bacteria where they play a crucial role in host-pathogen interactions. The presence of glycans on pathogens can significantly influence the course of infection as the microorganisms are not only able to recognize host glycans but can engage in specific glycan-glycan connections between host and pathogen. These interactions facilitate the transport of the pathogen and lead to adhesion and invasion of the epithelium [16]. Bacterial pathogens present a variety of glycosylated molecules, including capsular polysaccharides, glycoproteins, lipooligosaccharides (LOS) or lipopolysaccharides. Many bacterial lectins act as adhesins to secure the attachment of the pathogen to host cells [16]. One pathogen that uses glycan interactions to promote colonization and infection is the intestinal *Campylobacter jejuni* (*C. jejuni*). The surface glycans of the bacterium bind to complementary host glycans in the intestinal tract to enhance and establish the infection [16, 17]. This glycan-mediated adhesion is a critical step in the pathogenesis of *C. jejuni* as it can subsequently lead to the invasion of epithelial cells. Despite the importance of these interactions, the processes remain largely unclear and future research is necessary to provide novel insides in order to understand the exact mechanisms.

3.2.4 MUC2 Sialylation

The sugar chains on MUC2 are commonly branched and elongation terminated by sialic acids, mainly N-acetyl neuramic acid (NeuAc), on non-reducing ends of an acceptor substrate on the sugar molecule. These sialylations have been recently shown to protect the mucin barrier against microbiota-dependent degradation [18, 19]. The negative charge of the sialic acids on MUC2 enhances mucin network structure formation, thereby preventing bacterial invasion in the colon and preserving intestinal homeostasis [19]. Moreover, reduced MUC2 sialylation is associated with inflammatory diseases [19]. Sialylations are catalyzed by specific glycosyltransferases, known as sialyltransferases. These enzymes can be divided into the four subfamilies based on substrate specificity and positions of sialyl-linkages in the sialylated product. These subfamilies are ST3-beta-galactoside alpha-2,3-sialyltransferase (ST3GAL), beta-galactosidase alpha-2,6 sialyltransferase (ST6GAL), ST6-*N*-acetyl-galactosaminide alpha-2,6-sialyltransferase (ST6GALNAC) and ST8 alpha-*N*-acetyl-neuraminide alpha-2,8-sialyltransferase (ST8SIA) [20]. Representatives of the ST3GAL subfamily transfer the sialyl

group from CMP-N-acetyl-neuraminate (CMP-SA) in an α-2,3 linkage to the galactosyl residue of glycans [20, 21]. ST3GAL1, one of five subtypes of ST3GAL, predominantly adds sialic acid to the core 1 *O*-glycan structures often found in mucin-type *O*-glycans [20, 21]. ST3GAL2, on the other hand, is crucial for the biosynthesis of gangliosides by adding sialic acid from CMP-N-acetylneuraminate (CMP-NeuAc) to the Gal-beta-1-3GalNAc terminus of the gangliosides [22]. Gangliosides are sialylated glycosphingolipids that regulate cell function and intracellular recognition and are usually abundant in the brain but are also expressed in epithelial cells of the intestinal tract [22, 23].

Research also revealed a connection between sialylations and *C. jejuni* regarding the impact on phagocytosis and immune modulator production in mice. More specifically, sialylated LOS of *C. jejuni* was more efficiently phagocytosed and increased the production of specific cytokines *in vivo* and *in vitro* [24].

3.3 Campylobacter jejuni

3.3.1 *Campylobacter*: A Global Zoonotic Threat

The zoonotic *Campylobacter* species causes intestinal infections in humans worldwide with alarmingly high numbers. Zoonoses are defined as infectious diseases transmitted directly or indirectly by an animal to humans (WHO). Noteworthy diseases associated with zoonosis include Rabies, Ebola, avian and swine influenza, and SARS-CoV-2. Causative pathogens can be bacteria, viruses, parasites, fungi and prions. Additionally, factors such as climate change, globalization and urbanization significantly influence the occurrence of zoonotic diseases [25, 26]. Zoonotic pathogens pose a substantial public and global health concern, since they account for over 60% of all infectious diseases with numbers rising.

The foodborne *Campylobacter* species are gram-negative, microaerophilic, spirally shaped and motile. They induce campylobacteriosis after infection, characterized by symptoms such as diarrhea, abdominal pain, vomiting, fever and headaches that last for three to six days. With approximately 140.000 human cases annually in the EU (2022, [27]), they represent the most common bacterial cause of human gastroenteritis in the EU but also globally and thus one of the most important zoonotic bacteria.

3.3.2 Routes of Infection

Despite the relevance of *Campylobacter* species as zoonotic pathogens, the pathomechanisms of these bacteria remain largely unknown, requiring further research. To date, over 30 species of the zoonotic genus *Campylobacter* were identified, with *C. jejuni* responsible for over 80% of all *Campylobacter* infections [28]. As a foodborne pathogen, the main route of transmission to humans is the consumption of contaminated food. Here, raw and undercooked meat and meat products, especially poultry, are linked to the majority cases in humans [29]. However contaminated, raw or improperly pasteurized milk, other cross-contaminated food and water or contact with pets and other animals have also been considered as adequate risk factors [29].

C. jejuni commonly colonizes the intestinal tract of many wild animals and livestock, such as poultry, cattle and pigs, asymptomatically without causing a disease. In humans, however, research suggests that the pathogen interacts with glycans of MUC2 in the colon and thereby penetrates the protecting double mucus layer to infect the underlying epithelium [16]. By binding to mucus glycans *C. jejuni* not only facilitates colonization, but also is the pathogen beneficially altering glycan pattern to decrease defense mechanisms through mucin-modifying enzymes like endogenous glycosyltransferases and glycosidases [16, 17]. Additionally, mucus components can be chemotactic and promote flagellar motility to facilitate transport through the inner layer and thereby enhance pathogenicity [30].

3.3.3 Adhesion, Invasion and Intracellular Survival in Humans

Once *C. jejuni* crosses the colonic mucus layers, it adheres to the host epithelial cells. This adhesion process involves complex molecular mechanisms, and the pathogen uses several methods simultaneously to secure success. Next to motility and chemotaxis, which are crucial for the interaction between the pathogen and host cells, the structures of microbial surface components are also of significant importance. Here, most widely studied is the adhesion through the outer membrane proteins by *Campylobacter* adhesion to fibronectin (CadF) and fibronectin-like protein A (FlpA). Both proteins enable binding to fibronectin, a glycoprotein on the extracellular matrix of polarized intestinal epithelial cells [31-33]. Following adhesion, subpopulations of the pathogen invade the host cells. As displayed in Figure 3, *C. jejuni* migrates either transcellularly, paracellularly - by opening tight and adherens junctions

between the epithelial cells through endogenous proteases- or by surviving intracellularly in vacuoles [33, 34]. Studies have demonstrated that *C. jejuni* is able to survive intracellularly in phagocytes and intestinal epithelial cells for an extended period of time [35, 36]. It is hypothesized that invasion factors of the pathogen actively induce host cell plasma membrane invaginations (late endosome marker LAMP-1), that express an endosomal compartment, that transports the *Campylobacter*-containing vacuoles from the apical to the basolateral surface [33, 36-38].

Adherence, invasion and intracellular survival facilitate *Campylobacter* translocation (endocytosis and exocytosis) across the intestinal epithelial barrier. Translocation and toxin released by *C. jejuni* are crucial in pathophysiology and the development of infections in humans.

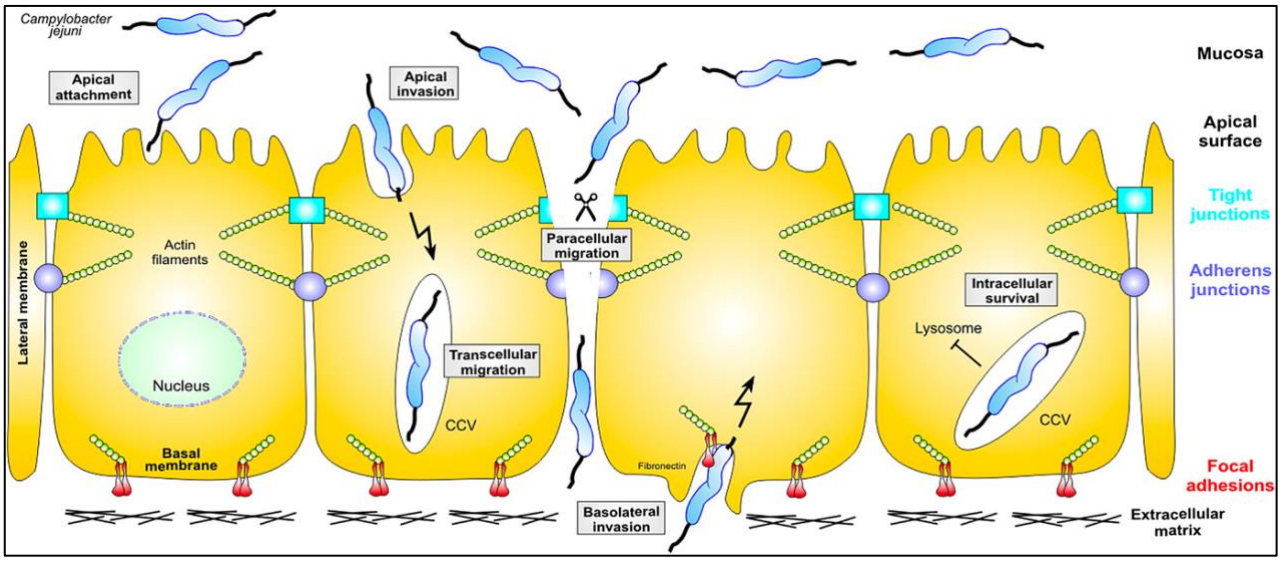

Figure 3: Illustrated model for mechanisms of *C. jejuni* infections. *C. jejuni* can invade the intestinal epithelium through multiple mechanisms. After attachment to the apical surface and invasion of epithelial cells, the pathogen either migrates transcellularly or survives intracellularly. *C. jejuni* can also migrate paracellularly by disrupting tight and adherens junctions between the epithelial cells, catalyzed by endogenous proteases. This figure is reproduced from [33].

3.3.4 Immune responses to *Campylobacter jejuni* Infections

C. jejuni exhibits the endotoxin LOS, a glycolipid consisting of an inner and outer oligosaccharide core, as an integral component of the membrane, and Lipid-A. The outer core structurally resembles human neuronal gangliosides and is recognized by the human innate immune system by the Toll-like receptor 4 (TLR4) [39, 40]. In response to LOS, downstream signaling pathways enable dendritic cells and macrophages to recruit neutrophilic granulocytes, producing toxic reactive oxygen species (ROS) and inflammatory mediators, that cause intestinal epithelial damage through apoptosis induction [41]. Important immune responses further include the secretion of immune modulators by macrophages, most relevantly the cytokines IL-6, IL-8, IL-1b, IL-12 and IL-23a and TNFα that promote inflammatory processes [41]. Activated T-cells additionally produce pro-inflammatory interferons (IFNγ) and interleukins IL-17 and IL-22 as well as the anti-inflammatory cytokines IL-4 and IL-10 to modulate the immune response and prevent a severe course of the disease. Symptoms typically range from mildly inflamed and self-limitating to severe, highly inflamed, bloody diarrhea accompanied by strong abdominal cramps and fever, depending on the host's immune status [40, 41]. The bloody diarrhea results from ulcerative tissue destruction due to epithelial apoptosis.

After *C. jejuni* invades the epithelial layer into underlying tissues such as the Lamina propria, it can enter the bloodstream, and potentially reach distinct organs such as liver, spleen or mesenteric lymph nodes [33]. *C. jejuni* rarely induces post-infection autoimmune diseases like the neurological Guillain-Barré-Syndrome in which the peripheral nerve system is damaged, Miller-Fischer syndrome or reactive arthritis, mediated by the immune system [42]. These autoimmune diseases may be caused due to structural similarity of LOS to neuronal gangliosides, leading to the production of antibodies in some patients [43, 44].

3.3.5 *Campylobacter jejuni* Infection Models

Despite the significance of *C. jejuni*, suitable experimental models to investigate the molecular mechanisms of adhesion, invasion and infection in humans are very limited. Vertebrate *in vivo* models often use mice due to their suitability for studying bacterial pathogenicity. However, murine models have limitations, including sporadic colonization and a lack of intestinal immunopathology and clinical disease manifestations [45]. This is partly because conventional

mice with normal commensal microflora exhibit colonization resistance against *C. jejuni* [46]. To address these challenges, a novel murine *in vivo* model using secondary abiotic mice was developed, in which the intestinal microbiota is eliminated using antibiotic treatment [46, 47]. This model retains susceptibility to *C. jejuni* infections and exhibits a physiologically developed immune system, transforming it in an appropriate model for studying host adaptation of *C. jejuni* and the long-term evolution *in vivo* [46]. The mice are also genetically modified to be deficient in IL-10 as it is an important anti-inflammatory mediator and is found to decrease *C. jejuni*-induced immunopathology [45, 48]. Secondary abiotic IL-$10^{-/-}$ mice were shown to develop acute enterocolitis similar to human campylobacteriosis, have been well-established, standardized, and reproduced in research (see [45, 49-51] and the *in vivo* investigations presented in this thesis).

Most human *in vitro* models for studying *C. jejuni* infections have traditionally relied on two-dimensional cell culture systems. Among the most frequently used cell lines are Caco-2, T84 and INT-407 cells [33]. Caco-2 cells are derived from a human colorectal adenocarcinoma and have been widely employed to study intestinal epithelial cell function and bacterial interactions. For instance, Everest et al. (1992) already used Caco-2 as a model to study *C. jejuni* invasion over thirty years ago [52]. T84 cells, a human colonic epithelial cell line, are often used to investigate intestinal barrier function and secretory responses. Research with T84 from 2008 showed that *C. jejuni* is able to disrupt epithelial tight junctions [53]. INT-407 cells are also known as HeLa derived cells and have been used in early *C. jejuni* invasion studies such as demonstrated in the work by Konkel and Cieplak (1992) in which the authors identified *C. jejuni* proteins involved in host cell invasion [54]. More recent studies have continued to expand and refine the findings with these cell lines for research on *C. jejuni*. Caco-2 cells were used for instance by Montanari et al. (2022) to study the role of outer membrane vesicles in *C. jejuni* pathogenesis or by Šikić Pogačar et al. (2020) to investigate the anti-adhesion and anti-invasion effects of natural compounds on *C. jejuni* [55, 56].

To further advance infection models, 2D co-culture systems were applied. A co-culture model consisting of human epithelial cells and THP-1 macrophages was developed to explore protective effects of curcumin against immune-induced epithelial barrier dysfunction in *C. jejuni* infections [57]. These co-culture systems allow the examination of the interplay between different cell types during infections.

While the 2D models have provided valuable insights in *C. jejuni* research, they have limitations in replicating the complex *in vivo* environment. Researchers have consequently been exploring more advanced models, including primary epithelial cells derived from tissue biopsies or 3D cell culture models such as spheroids and organoids. For example, Aguirre Garcia et al. (2022) developed a human intestinal organoid model to study *C. jejuni* infections and provide a more physiologically relevant system [58]. However, 3D models are only rarely used to study *C. jejuni* infections as researchers still prefer 2D monolayers.

The recent studies demonstrate that a trend towards more complex and physiologically relevant models, while established cells lines are still frequently used for specific research questions. Nonetheless, there is still only a limited amount of advanced cell models and more research is needed.

3.4MicroRNAs (miRNAs)

3.4.1 The Role of miRNAs

Gene expression is a strongly regulated process with numerous existing mechanisms to either increase or decrease the quantity and production of gene products (protein or RNA). One of the most relevant eucaryotic gene regulators are microRNAs (miRNAs). These small conserved and non-coding RNA (ncRNA) molecules play an important role in the post-transcriptional regulation of gene expression. By interfering with their target messenger RNAs (mRNAs), they control various biological processes like cell differentiation and proliferation, energy metabolism, apoptosis, cell growth and immune responses and are crucial for cellular homeostasis [59, 60]. 1917 miRNAs are identified within the human genome to date (https://www.mirbase.org, accessed October 1st, 2024 [33, 61]) collectively influencing more than half of the human protein-coding genes [62, 63]. While on the one hand one miRNA can regulate multiple genes, on the other hand one gene can be regulated by multiple miRNAs, thereby creating a complex regulatory network.

3.4.2 Biogenesis of miRNAs

The biogenesis of the approximately 18 to 24 nucleotides long small RNAs begins by the processing of Polymerase II/III transcripts post- or co-transcriptionally and can be divided into canonical and non-canonical pathways (Figure 4) [64]. The dominant canonical pathway starts in the nucleus with the primary miRNA (pri-miRNA) transcript from miRNA genes encoded in intronic, exonic and intergenic regions, that is recognized and cleaved by a microprocessor complex composed of RNase III Drosha and the double-stranded RNA binding protein DiGeorge Syndrome Critical Region 8 (DGCR8) to the precursor-miRNA (pre-miRNA) [65, 66]. The pre-miRNA, still approximately 70 nucleotide in length, is exported from the nucleus through the pores of the nuclear membrane to the cytoplasm by an exportin-5/RanGTP complex [67]. The pre-miRNA is then processed by the RNase III endonuclease Dicer in a mature miRNA duplex. Here, transactivation response element RNA-binding protein (TRBP) is an RNA-binding cofactor of the Dicer complex in human cells that increases RNA-binding affinity to the Dicer while enhancing cleavage accuracy. The miRNA duplex is loaded into Argonaute (AGO) protein family, and the passenger strand cleaved. The resulting mature single stranded miRNA bound to AGO forms the activated miRNA induced silencing complex (miRISC) regulating gene expression [68]. On the other hand, multiple non-canonical miRNA pathways exist in which various endogenous substrates like mirtrons or small hairpin RNAs (shRNAs) are processed into pre-miRNAs by splicing, debranching, and trimming of short introns. Here, different combinations of the proteins of the canonical pathway like Dicer, exportin-5 and AGO2 are involved leading to the same activated miRISC [65]. Upon activation, the miRNA on the miRISC can bind to a specific complementary sequence at the 3' untranslated region of the target mRNA, the so-called miRNA response element (MREs) [65]. Genetic silencing is regulated depending on the degree of complementarity. The more common partial complementarity between target mRNA and miRNA leads to translational inhibition whereas perfect complementarity activates the endonuclease activity of AGO2 resulting in mRNA cleavage and its degradation [65, 69].

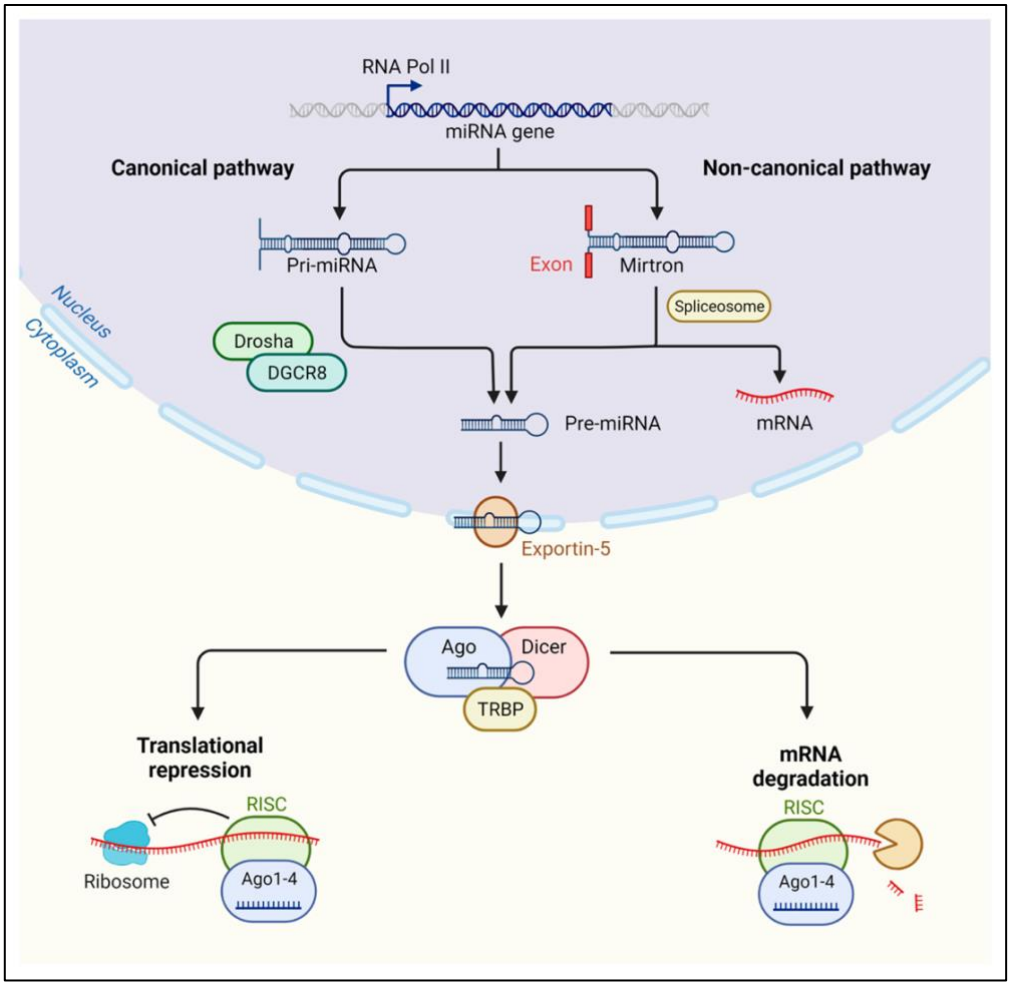

Figure 4: Biogenesis and mechanisms of action of miRNAs. Transcripts of the RNA Polymerase II or III are processed post- or co-transcriptionally through either the canonical or the non-canonical pathway. In the canonical pathway, the pri-miRNA is recognized and cleaved by the microprocessor complex, composed of Drosha and DGCR8, to form the pre-miRNA. In the non-canonical pathway, endogenous substrates like mirtrons or small hairpin RNAs are processed into pre-miRNAs by splicing, debranching and trimming of short introns. The pre-miRNA of both pathways is then exported from the nucleus by exportin-5 and further processed in the cytoplasm by the RNase III enzyme Dicer, which generates a smaller double-stranded miRNA molecule. An interaction between Dicer and TRBP enhances RNA-binding affinity of the Dicer while improving cleavage accuracy. The miRNA duplex is loaded onto a protein of the AGO family, which leads to the cleavage of the passenger strand and results in a mature single stranded miRNA. This miRNA-AGO complex forms activated miRISC, which regulates gene expression by either translational repression or mRNA degradation. pri-miRNA – primary miRNA; pre-miRNA - precursor miRNA; DGCR8 - DiGeorge Syndrome Critical Region; TRBP -transactivation response element RNA-binding protein; AGO - Argonaute protein; miRISC - miRNA induced silencing complex. This figure is reproduced from [70].

3.4.3 miRNA Regulation in Pathogenesis

Research has shown that the negative regulation of gene expression by miRNAs is not only essential for maintaining various cellular functions in health but also plays a crucial role in disease development. Alterations in genetic (mutations) and epigenetic factors (DNA modification) play a major role during pathogenesis and drug resistance, alongside aberrant expression of miRNAs [60, 65]. Most remarkable changes in miRNA expression are observed in cancer, in which cellular proliferation, differentiation and apoptosis are influenced by dysregulated miRNAs that might contribute to tumorigenesis [60]. On top of that are miRNAs associated with infectious diseases. As stat0poed above, miRNAs can indirectly modulate immunological functions and thereby mediate the host's immune responses of both, the innate and adaptive immune system, transforming them into significant molecules to prevent and fight infections [71]. Here, the recognition of different pathogens results in an aberrant expression of specific miRNAs leading to a regulation of a distinct set of genes involved in immune responses. This way, these molecules indirectly interfere with pathogens as an early or late response and exhibit a core temporal response that are either common to all pathogens or pathogen specific [72]. Their regulating role in immune responses ranges from the differentiation of immune cells to antigen presentation, secretion of cytokines to T-cell and TLR signal transduction [73].

For example, the miRNAs miR-155 and miR-146 are two key miRNAs involved in bacterial immunity. They are activated by the NF-κB pathway when Pattern Recognition Receptors (PRR) sense pathogen motifs and promote or dampen inflammation through their targets, including various cytokines [72]. Moreover, miR-125a-5p, which plays an important role in cell differentiation, is downregulated in several types of tumors (e.g. colon, breast, gastric) and has been associated with *C. jejuni* infections [50, 74]. In this context, research has elucidated an interaction between *C. jejuni* infections, certain dysregulated miRNAs and glycosyltransferases relevant for mucin-type *O*-glycosylations [50].

It has been suggested that in bacterial infections, pathogens have evolved sophisticated strategies involving host miRNAs to enhance survival, multiplication and colonization within the host organism. These microorganisms indirectly disrupt and interfere with various biological processes and functions, creating an environment that favors their persistence

throughout the course of infection [75]. Furthermore, the pathogens have developed mechanisms to reprogram host cells by altering the expression patterns of miRNAs. This allows the bacteria to modify the cellular responses by the host to the infection and effectively change microenvironment to their advantage [76, 77]. Interestingly, *Salmonella* has been shown to even produce miRNA-like RNA fragments within infected cells to facilitate their intracellular survival [78]. This illustrates the adaptivity of pathogens in repurposing the host cellular system for their own benefit. All of the aforementioned factors convert miRNAs into critical molecules to study when investigating infections and immune responses. More complex research is still necessary to identify regulating mechanisms regarding infections and the role of pathogens in the process.

3.5 3D Cell Culture Models

3.5.1 Advances in Cell Culture Models: From 2D to 3D Systems

Cell culture models have been an essential tool for studying complex molecular and cellular biology for a long time. In these models, cells are cultured outside a living organism under controlled physiological conditions. Initially, cell culture models were predominantly two-dimensional (2D), where cells were grown in monolayers on flat surfaces, providing length and width dimensions. However, as research advanced and limitations of 2D cultures were demonstrated, novel three-dimensional (3D) methods were explored. These models added depth to the culture environment, allowing cells to grow and interact in all three spatial dimensions (height, width and length) resulting in a higher physiological relevance, tissue complexity and increased cellular interactions compared to traditional 2D monolayers. While 2D models have strict limitations in mimicking the organ of interest, 3D models overcome these limitations by resembling *in vivo* organ morphology, physiology and microenvironment more closely. Nonetheless, animal models are still considered as the golden standard in biomedical research due to their genetical and biological similarity to the human organism [79, 80]. These *in vivo* models have contributed significantly to understand pathophysiological processes, however, the ethical concerns regarding animal welfare as well as poor validity and translation to humans have been criticized [81]. These 3D cell culture models bridge the gap between 2D and *in vivo* animal models by following the 3R principle of Reduction (the number

of animals), Refinement (limiting animal suffering to a minimum) and Replacement (of animal experiments).

3.5.2 3D Cell Culture Models: Organoids, OoC Systems, Bioprinting and Spheroids

As shown in Figure 5, various 3D cell culture models have been developed, including organoids, organ-on-a-chip (OoC) systems, bioprinting and spheroids. Organoids are self-organized 3D models derived from (induced) pluripotent stem cells or from organ-specific adult or fetal stem cells collected from tissue biopsies. In culture, organoids differentiate into specialized and tissue-specific cells that organize themselves into a 3D complex mimicking structure and function of the corresponding organ of interest. This includes the formation of tissue specific structures like crypts or villi in intestinal organoids [82]. OoC systems culture miniature tissues inside a microfluidic chip in which tissue-specific functions are maintained and the microenvironment is controlled [83]. In 3D bioprinting, also called additive manufacturing, biocompatible materials, cells and supporting components are printed layer-by-layer into 3D structures, with spatial control of the placement of functional components [84].

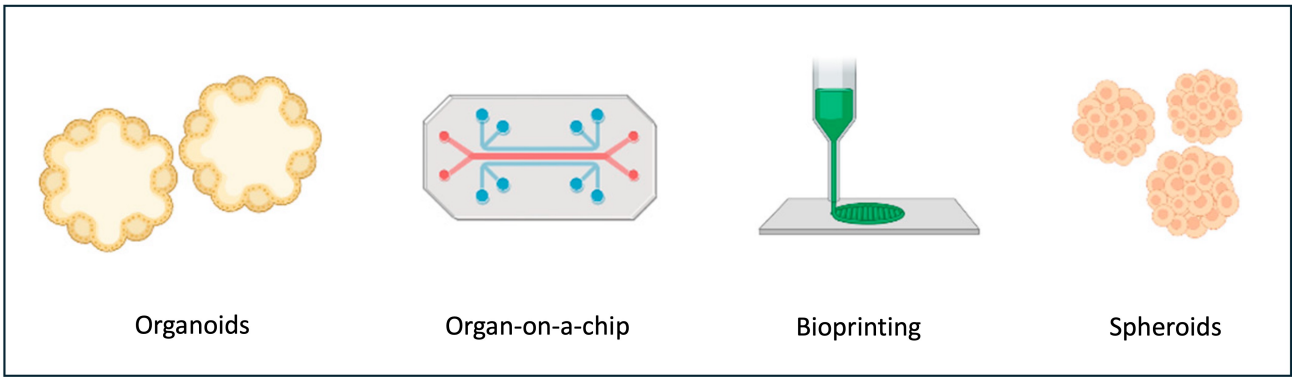

Figure 5: Schematic illustration of different 3D cell culture models. Strategies for 3D cell culture include Organoids, Organ-on-a-chip, Bioprinting or Spheroids. This figure is adapted from [85].

Although all three models mentioned offer significant advantages in resembling the organ of interest, they are relatively costly, time-consuming and their availability is limited as they often require human or animal biopsies. Additionally, standardization and harmonization can be challenging. In contrast, spheroids are easier to reproduce, standardize and harmonize with

lower cost and labor requirements by retaining a resemblance to the representing tissue. Spheroids are produced by using cell lines or, less commonly, primary cells from tissue biopsies wherein cells aggregate and, through self-assembly, form spherical 3D clusters. This facilitates cell-cell and cell-matrix interactions while mimicking the physiochemical environment and *in vivo* architecture [86].

3.5.3 Spheroid Culture Methods

Figure 6 illustrates four exemplary techniques for producing spheroids: Hanging Drops, Ultra Low Attachment (ULA)-Plates, Rotation Bioreactor Culture and Magnetic Levitation. In Hanging Drops, spheroids are formed through gravitational forces and surface tensions by suspending cells in small drop of culture medium and hanging them from the lid of a petri dish [86, 87]. Conversely, ULA-Plates involve seeding cells on a well plate coated with a specific hydrophobic, cell-repelling surface to prevent cell attachment at the well bottom, assisting cell aggregation and spontaneous spheroid formation [86]. Rotation Bioreactor Culture requires positioning of high density cell suspensions in a rotating bioreactor exposing the cells to constant stirring that prevents adherence to the reactor wall [88]. The extensive stress of the cells leads to the formation of 3D structures. Lastly, magnetic levitation-based spheroid formation relies on magnetic forces. Here, the cells are mixed with magnetic beads and incubated under magnetic forces causing cell aggregation by overcoming gravitational forces and allowing levitation [89]. All of the mentioned techniques have their advantages and disadvantages regarding spheroid shape and size homogeneity, cell damage, reproducibility and efficiency. However, ULA-plates can be considered as a suitable method of choice due to their favorable attributes.

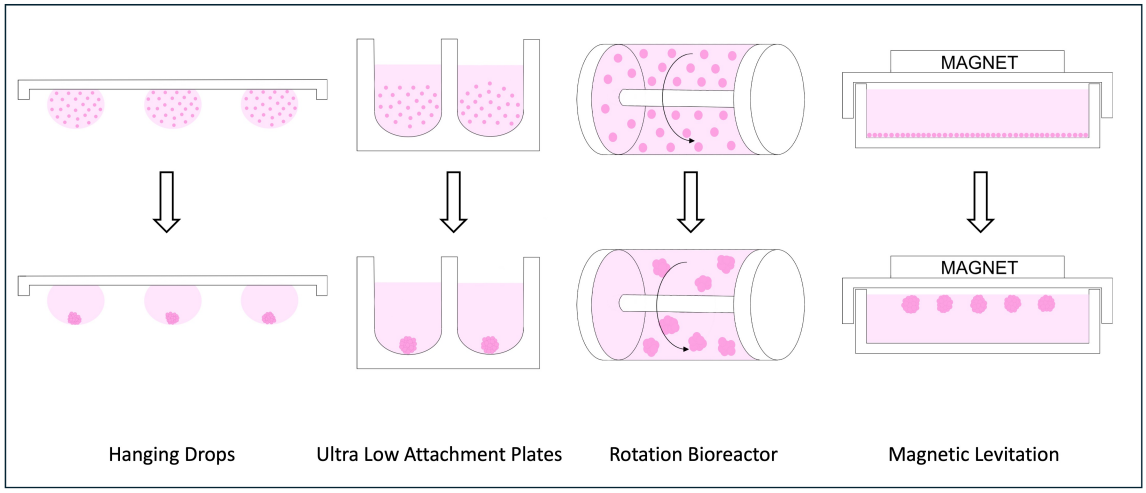

Figure 6: Different technical methods for spheroid formation. There are various methods for spheroid formation, including using Hanging Drops, Ultra Low Attachment Plates, Rotation Bioreactor or Magnetic Levitation. This figure was recreated from [86].

4. Aims and Objectives

Our understanding of underlying molecular mechanisms in infections caused by the prevalent zoonotic *C. jejuni* remains limited compared to what is known about less prevalent pathogens. This thesis aimed to identify and investigate new insights into *C. jejuni*-associated regulatory networks mediated by miRNAs that might influence mucin modification in the colon and thereby affecting pathogen invasion. Here, a comprehensive and extensive analysis using *in silico*, *in vivo* and traditional 2D *in vitro* approaches were intended to be carried out. For more advanced research on *C. jejuni* specifically and infection biology in general, a novel three-dimensional intestinal spheroid model was established. Primary goal of the model was to incorporate relevant intestinal cell types that are arranged in a directed order to mimic the intestinal mucosal microarchitecture and surpass conventional cell culture methods. The spheroids were aimed to exhibit regulatory immunological pattern comparable to *in vivo* conditions upon infection and therefore potentially reduce or replace animal models. The method was supposed to be adaptable to other species as well. Objectives of this study included:

1. Identification of potential overlapping targets of the miRNAs miR-125a-5p and miR-615-3p associated with mucin-type *O*-glycosylation that are conserved in the species human and mice

2. Determination and investigation of the interaction between *C. jejuni* infections, miR-125a-5p expression and the mucin-associated glycosyltransferases ST3GAL1 and B4GALT1 as targets of the miRNA to analyze potential mucin regulation in the colon upon infection

3. Development of a standardized, reproducible and scalable intestinal human 3D spheroid model comprising relevant cell types to resemble the intestinal mucosal *in vivo* microarchitecture and show differentiated morphological characteristics

4. Application of the spheroid model in *C. jejuni* infection biology to mimic the immune responses in *in vivo* infections more closely compared to conventional 2D cell culture methods

5. Successful adaptation of the spheroid formation protocol to the species mouse and pig

5. Published Work

5.1 Publication 1: miR-125a-5p regulates the sialyltransferase ST3GAL1 in murine model of human intestinal campylobacteriosis

Kraski, A., Mousavi, S., Heimesaat, M.M. *et al.* miR-125a-5p regulates the sialyltransferase ST3GAL1 in murine model of human intestinal campylobacteriosis.*Gut Pathog* **15**, 48 (2023).

DOI: https://doi.org/10.1186/s13099-023-00577-6

Gut Pathogens

RESEARCH Open Access

miR-125a-5p regulates the sialyltransferase ST3GAL1 in murine model of human intestinal campylobacteriosis

Angelina Kraski[1], Soraya Mousavi[2], Markus M. Heimesaat[2], Stefan Bereswill[2], Ralf Einspanier[1], Thomas Alter[3], Greta Gölz[3†] and Soroush Sharbati[1*†]

Abstract

Background Zoonotic microorganisms are increasingly impacting human health worldwide. Due to the development of the global population, humans and animals live in shared and progressively crowded ecosystems, which enhances the risk of zoonoses. Although *Campylobacter* species are among the most important bacterial zoonotic agents worldwide, the molecular mechanisms of many host and pathogen factors involved in colonisation and infection are poorly understood. *Campylobacter jejuni* colonises the crypts of the human colon and causes acute inflammatory processes. The mucus and associated proteins play a central host-protective role in this process. The aim of this study was to explore the regulation of specific glycosyltransferase genes relevant to differential mucin-type *O*-glycosylation that could influence host colonisation and infection by *C. jejuni*.

Results Since microRNAs are known to be important regulators of the mammalian host cell response to bacterial infections, we focussed on the role of miR-125a-5p in *C. jejuni* infection. Combining in vitro and in vivo approaches, we show that miR-125a-5p regulates the expression of the sialyltransferase ST3GAL1 in an infection-dependent manner. The protein ST3GAL1 shows markedly increased intestinal levels in infected mice, with enhanced distribution in the mucosal epithelial layer in contrast to naïve mice.

Conclusion From our previous studies and the data presented here, we conclude that miR-125a-5p and the previously reported miR-615-3p are involved in regulating the glycosylation patterns of relevant host cell response proteins during *C. jejuni* infection. The miRNA-dependent modulation of mucin-type *O*-glycosylation could be part of the mucosal immune response, but also a pathogen-driven modification that allows colonisation and infection of the mammalian host.

Keywords *Campylobacter jejuni*, *O*-glycosylation, microRNA, Mucin, Infection, Colonisation

†Greta Gölz and Soroush Sharbati contributed equally to this work.

*Correspondence:
Soroush Sharbati
Soroush.sharbati@fu-berlin.de
Full list of author information is available at the end of the article

Background

The mammalian colon is covered by a constantly renewing, double mucus layer that forms the first line of defence in the colon. The main component of both layers is the highly glycosylated Mucin 2 (MUC2) which is produced, stored and secreted by goblet cells [1]. Increased mucus secretion in the crypts is a response to stress stimuli such as bacterial invasion [2, 3]. The elevated secretion facilitates the elimination of the pathogens by quickly flushing them away. Once secreted, MUC2 unfolds and builds a polymeric and viscous network due to numerously hydrated *O*-glycosylations connected to repeating domains rich in the amino acids proline, threonine, and serine (PTS-domains) [4]. The MUC2 glycosylation is a post-translational modification that takes place as a stepwise process in the Golgi apparatus [5]. Firstly, the Tn-antigen is created by *N*-acetylgalactosamine binding to serine or threonine of the protein backbone, then the galactosaminyltransferase C1GALT1 and *N*-acetylglucosaminyltransferases B3GNT6 and GCNT1-4 catalyse the elongation of the *O*-linked oligosaccharide chains [5, 6]. Various *O*-glycans can be bound by specific glycosyltransferases, forming long carbohydrate chains and different core structures with different functions. Mucin-type *O*-glycan chains can be expanded or branched by sialic acids on terminal, non-reducing ends expressed both on cell-surfaces and secreted glycoproteins. The transfer of sialic acid residues from a sugar nucleotide donor, mainly *N*-acetylneuraminic acid, to an acceptor substrate is catalysed by sialyltransferases such as ST3 beta-galactoside alpha-2,3-sialyltransferase 1 (ST3GAL1) and 2 (ST3GAL2) [7]. The negatively charged sialic acid improves water binding of MUC2 and prevents degradation of the protein backbone [8, 9].

Apart from host *O*-glycans, pathogenic bacteria also have characteristic oligosaccharides on their surface that serve host-pathogen interactions and are due to co-evolution with their hosts [2, 10]. Here, *O*-glycans on mucins can act as ligands for bacterial adhesins and specific connections between bacterial and MUC2 glycans can enhance adherence and invasion of intestinal pathogens. Some gastrointestinal pathogens, such as *Campylobacter jejuni*, are able to bind host mucins mediated by glycan-glycan interactions and thereby penetrate the otherwise sterile inner mucus layer invading and infecting the underlaying epithelium [2]. In humans, *C. jejuni* is the leading cause of foodborne bacterial gastroenteritis (campylobacteriosis) worldwide (http://www.who.int). In pigs and poultry though, the zoonotic bacteria can colonise the intestinal tract asymptomatically without causing disease [11]. Even though *C. jejuni* infections in humans are highly prevalent, only little is known about the pathomechanisms, and further research is needed to understand the molecular and regulatory backgrounds with special emphasis on host glycans and their modifications.

Previous work has already assessed that microRNAs (miRNAs) play an important role in the mammalian immune response after bacterial or viral infections [10, 12–14]. miRNAs are short, non-coding RNAs that are involved in regulating gene expression and silencing [15]. After binding their target sites, they initiate degradation or translational repression of the mRNA [5]. While one miRNA can mediate the activity of different genes, a single gene could also be regulated by several miRNAs, resulting in complex regulatory networks that control cellular processes such as differentiation, proliferation or immune response [15]. For instance, it has been shown that *Mycobacterium tuberculosis* induces the overexpression of miR-125b to block tumour necrosis factor (TNF) biosynthesis for a suppressed immune response [16]. Also, decreased expression of miR-125a-5p was associated with the presence of *Helicobacter pylori* in human gastritis [17]. Our recent study in a mouse model of human campylobacteriosis based on secondary abiotic IL10$^{-/-}$ mice [18] has shown that the mammalian conserved miRNAs miR-615-3p and miR-125a-5p are dysregulated upon *C. jejuni* infection [10]. The study revealed that the identified miRNAs are mutually involved in regulation of several glycosyl- and sialyltransferases participating in mucin-type *O*-glycosylation in the murine colon. In the mentioned study, we mainly focused on the interaction between miR-615-3p and *St3gal2* and were able to demonstrate their molecular interaction in an infection-dependent context [19]. However, advanced knowledge about the role of these two miRNAs in gastrointestinal bacterial infections is still scarce.

Here, we investigated the *C. jejuni* infection dependent interaction between miR-125a-5p and the sialyltransferase ST3GAL1, a conserved target in both human and mouse. We identified target sites of miR-125a-5p in the 3' untranslated region (UTR) of *St3gal1* and validated them in vitro. By applying the above-mentioned in vivo mouse model of human campylobacteriosis [18], we demonstrated that *St3gal1* and *B4galt1* possess anti-correlated gene expression compared to miR-125a-5p during *C. jejuni* infection. This was supported by increased ST3GAL1 protein levels in colon samples of infected mice.

Results

The sialyltransferase ST3GAL1 is a predicted target of miR-125a-5p

We have recently shown that the two miRNAs, miR-125a-5p and miR-615-3p, are dysregulated after intestinal *C. jejuni* infections [10]. For deciphering regulatory

mechanisms of these miRNAs on mucin-type *O*-glycan biosynthesis, relevant human and murine target genes of the miRNAs were identified followed by KEGG pathway enrichment analysis [20] as described earlier [10, 12]. While only focussing on murine targets in the previous study, we have now expanded the enrichment analysis for both murine and human target genes. As shown in Fig. 1A, potential targets of both miRNAs within the mucin-type *O*-glycosylation pathway being conserved in both species were *St3gal1* and β1,4-galactosyltransferase *B4galt1*. However, *St3gal2, Gcnt4* and *Gcnt1* were only targeted by both miRNAs in mice, whereas the glucuronyltransferase *B3gnt1* was only a target in humans. In Additional file 1, all overlapping potential targets of miR-125a-5p and miR-615-3p in human and mouse are listed, including their pathways as determined by KEGG pathway enrichment analysis. As shown in Fig. 1B, the analysis pointed out specific sites of mucin-type *O*-glycan biosynthesis by the targeted transferases in mice and humans. While ST3GAL1 and 2 terminate the extension of the glycan chain by sialylation, B4GALT1 extends the core 2 structure by adding galactose residues. In Fig. 1B the intermediate steps in mucin-type *O*-glycosylation catalysed by ST3GAL1, ST3GAL2 and B4GALT1 were indicated (red asterisks), thereby forming potential interfaces with miR-125a-5p and miR-615-3p during *C. jejuni* infection. In previously published results, *St3gal2* was shown to be a target of miR-615-3p [10]. Furthermore, a clear anticorrelation between the expression of *St3gal1* and miR-125a-5p in the context of *C. jejuni* infection in vivo was observed. Therefore, we have mainly focused on this interaction in the analyses carried out here. Through RNAhybrid analysis [21], we have been able to identify two target sites of miR-125a-5p within the 3' UTR of murine *St3gal1* (Fig. 1C). Both target sites possessed canonical interaction characteristics with minimal free energies ≤ -22.7 kcal/mol.

miR-125a-5p targets *St3gal1* in the murine intestinal cell line CMT 93

We employed the murine intestinal cell line CMT 93 (ECACC 89111413) to examine the predicted interaction between miR-125a-5p and *St3gal1* in vitro. The efficiency of miR-125a-5p transfection was determined by measuring its cellular levels by RT-qPCR. After transfection, CMT 93 showed approximately tenfold increased and significant ($P \leq 0.01$) miR-125a-5p concentrations compared to non-target transfected controls (Fig. 2A). Since miRNAs are involved in gene silencing, anti-correlated expression of the target is

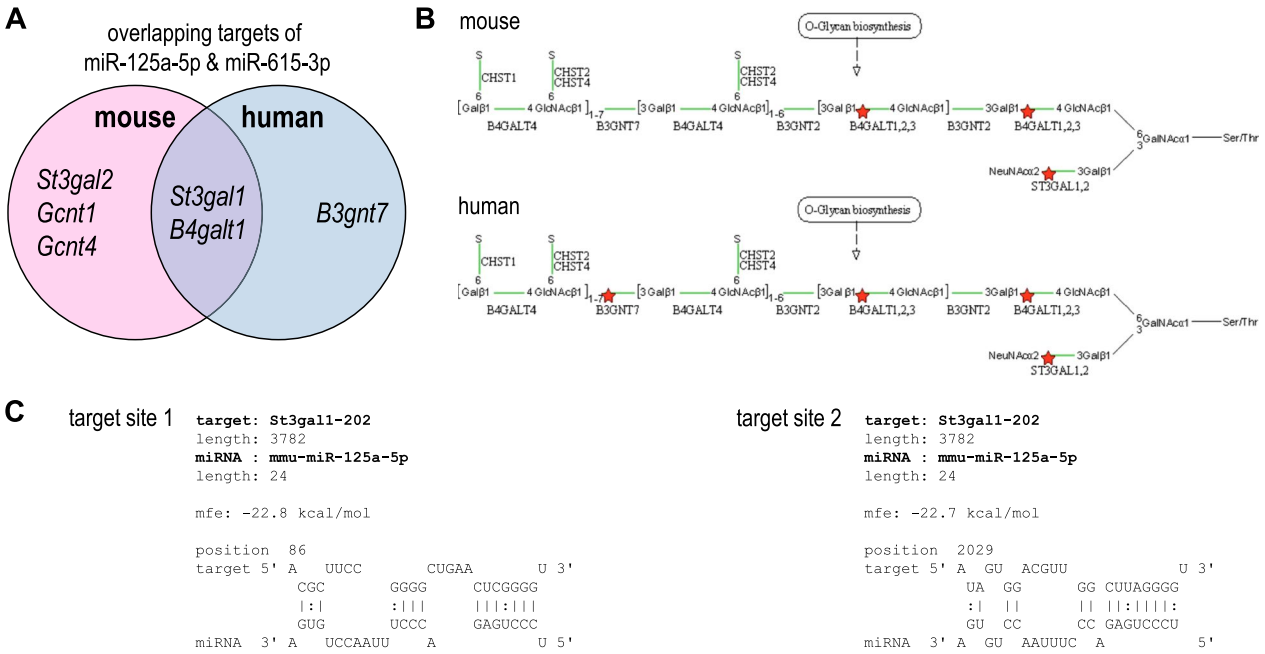

Fig. 1 In silico predicted conserved murine and human targets of miR-125a-5p and miR-615-3p. **A** The Venn diagram presents interfaces of overlapping targets of miR-125a-5p and miR-615-3p within the mucin-type *O*-glycosylation pathway of which the glycosyltransferases *St3gal1* and *B4galt1* are conserved in human and mouse, respectively. **B** Excerpt of the KEGG signalling pathway enrichment analysis of mucin-type *O*-glycosylation in mouse and human [20]. Marked by the red asterisks are the specific steps in the glycosylation that might be modified by miR-125a-5p and miR-615-3p interaction. **C** Two binding sites of miR-125a-5p were identified in the 3'UTR of the murine *St3gal1* using RNAhybrid [21]

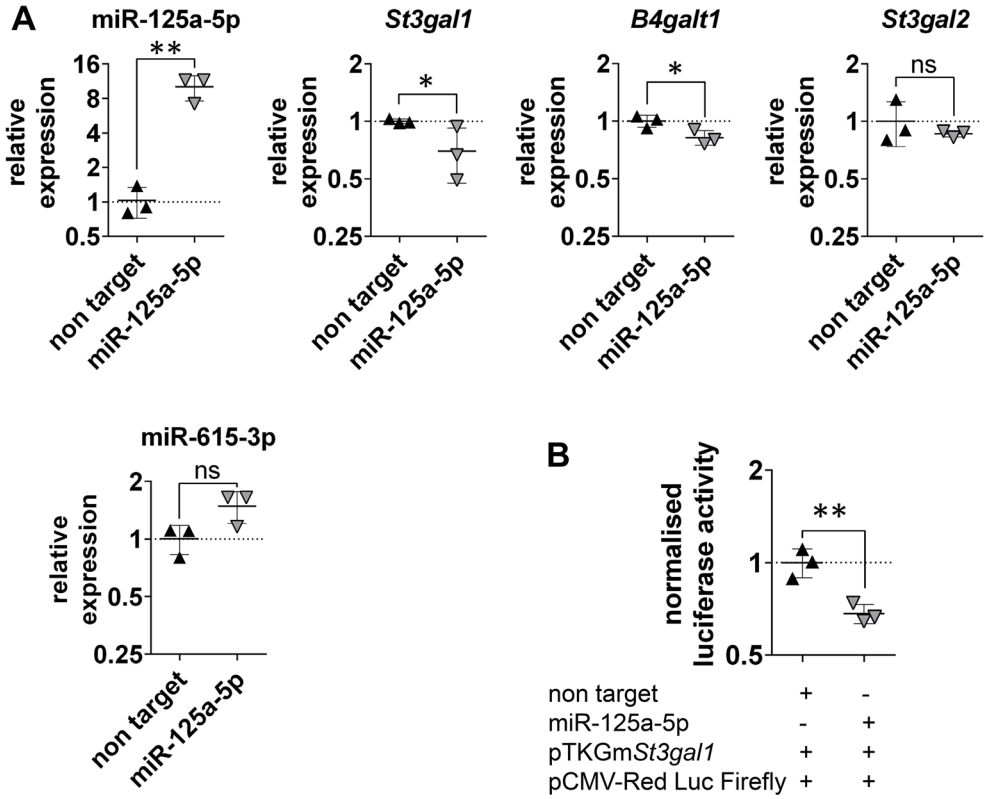

Fig. 2 Specific interaction between miR-125a-5p and *St3gal1* was verified by RNAi and dual luciferase reporter assay. **A** Transfection efficiency of the murine intestinal cell line CMT 93 with miR-125a-5p mimics as well as expression of potential targets was evaluated by means of RT-qPCR. Most pronounced and significant decrease of the target *St3gal1* was detected after miR-125a-5p transfection. *B4galt1* showed significantly reduced levels. *St3gal2* showed no significant difference. miR-615-3p showed upregulated but not significant expression. Non-target miRNA was used as a control, fold changes were calculated relatively to the non-target control and normalised with HPRT and SDHA or SNORD44 and SNORD 47, respectively. Charts indicate means ± standard deviations (SD) of three biological samples with triple measurements. **B** Relative luciferase activity was determined in comparison to control non-target miRNA mimic. miR-125a-5p caused clear and significant activity of the reporter gene fused to the target sites compared with non-target transfected controls. Charts indicate means ± SD of three biological replicates with technical triplicates. Statistical significance is presented by asterisks compared to negative controls at each time point. *P ≤ 0.05, **P ≤ 0.01, unpaired t-test

anticipated after RNAi and indicates an interaction. We found that RNAi with miR-125a-5p mimics caused significantly decreased expression of *St3gal1* by 0.7-fold ($P \leq 0.05$) in CMT 93 compared to non-target transfected controls (Fig. 2A). This confirmed our in silico analysis and pointed to *St3gal1* as a target of miR-125a-5p in mice.

Furthermore, we tested whether increased cellular miR-125a-5p levels had an effect on the transcripts of the potential targets *St3gal2* and *B4galt1* as well as the associated miR-615-3p. Although *B4galt1* was significantly downregulated 0.82-fold ($P \leq 0.05$), no significant differences in *St3gal2* expression levels were observed between mimics and controls, though a trend towards decreased mRNA levels was found (Fig. 2A). Hence, these results point to *B4galt1* as a further target of miR-125a-5p. Interestingly, miR-615-3p also exhibited a trend towards increased expression (not significant) after miR-125a-5p transfection, suggesting synergistic effects of both miRNAs (Fig. 2A).

Luciferase reporter assays prove specific interaction of miR-125a-5p with *St3gal1*

After screening the 3′ UTR of murine *St3gal1* for miR-125a-5p interaction sites by means of RNAhybrid [21], two binding sites were determined. The calculated minimal free energies for the interactions with miR-125a-5p were −22.7 kcal/mol and −22.8 kcal/mol, respectively (Fig. 1C). Dual reporter gene assays considering both identified *St3gal1* binding sites were performed as previously described [12]. After co-transfection of miR-125a-5p mimic together with the reporter plasmid (pTKGmSt3gal1) and the normalisation plasmid (pCMV-Red Firefly Luc), a significant 0.68-fold decrease ($P < 0.01$) in normalised luciferase activity ($Luc_{Gaussia}$: $Luc_{Red\ Firefly}$) was measured compared to non-target controls (Fig. 2B).

The downregulated magnitude of the reporter gene fused to *St3gal1* binding sites was comparable to the reduction of *St3gal1* transcript levels in transfected CMT 93 cells by miR-125a-5p mimics. This experiment thus proved that the interaction between *St3gal1* binding sites and miR-125a-5p is specific.

Murine *C. jejuni* infection model proves miR-125a-5p mediated *St3gal1* regulation

To investigate the physiological relevance of the above determined interaction between miR-125a-5p and the sialyltransferase *St3gal1* in vivo, tissue samples of secondary abiotic IL10 $^{-/-}$ mice that had been infected with *C. jej ni* and naïve controls were compared.

As shown in Fig. 3A, anticorrelated expression of miR-125a-5p and its target *St3gal1* was detected after *C. jejuni* infection. While miR-125a-5p was significantly downregulated by 0.6-fold ($P \leq 0.0001$), a pronounced upregulation of *St3gal1* gene expression was observed after infection (> 4-fold; $P \leq 0.0001$). Also, the expression of *B4galt1* was 1.6-fold upregulated ($P \leq 0.001$) in the infected samples (Fig. 3A). Although the RNAi experiments performed above indicated that *St3gal2* is not a target of miR-125a-5p, we tested its expression in vivo. As shown in Fig. 3B, *St3gal2* was significantly downregulated by 0.4-fold ($P \leq 0.0001$), while miR-615-3p was 2.1-fold increased ($P \leq 0.05$) confirming our previously published data [10].

The marked and contrasting expression of *St3gal1* compared to miR-125a-5p confirmed our in vitro experiments and pointed out the specific role of the identified interaction in the context of intestinal *C. jejuni* infection in the applied murine model.

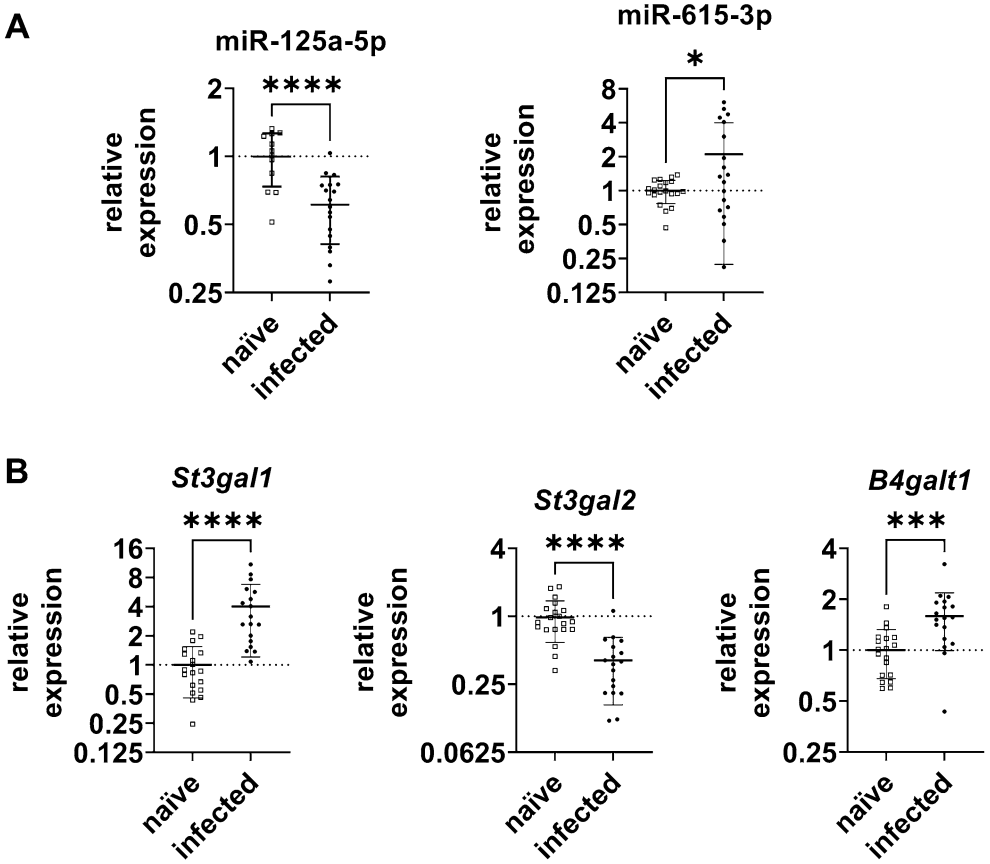

Fig. 3 Relative gene expression of relevant miRNAs and their target mRNAs in secondary abiotic IL10 $^{-/-}$ mice colonic tissue sections six days post *C. jejuni* infection. 19 *C. jejuni* infected and 20 naïve control mice were included in the study. Each data point in the diagram represents an animal that showed confirmed expression in the respective analysis. **A** Upon *C. jejuni* infection, expression of miR-125a-5p was significantly decreased, whereas transcriptional levels of *St3gal1* and *B4galt1* were significantly enhanced. **B** miR-615-3p levels were significantly increased, while *St3gal2* was significantly downregulated. Expressions were relatively calculated to naïve controls and normalised with SNORD44 and SNORD47 or with HPRT and SDHA, respectively. For each individual, the mean was calculated based on triplicate measurements. Charts show mean ± SD of all individuals. Statistical significance is presented by asterisks compared to naïve controls. *P ≤ 0.05, ***P ≤ 0.001, ****P ≤ 0.0001, unpaired t-test

The protein ST3GAL1 in the murine colon shows increased and corresponding levels after infection

Following the interaction and gene expression analysis, the aim was to verify whether the infection-dependent downregulation of miR-125a-5p exerts an effect on the protein concentration and distribution of ST3GAL1 in colonic tissue. For this purpose, both western blots and immunofluorescence staining (IF) were performed with colonic tissue derived from infected and naïve mice, corresponding to the samples used for RT-qPCR analysis. As determined by western blots in pooled samples, ST3GAL1 protein levels were increased in infected tissue compared to respective naïve controls, while the levels of the reference protein GAPDH were similar in both groups (Fig. 4A). To statistically evaluate the magnitude of ST3GAL1 upregulation, individual western blots were performed from eight naïve and eight infected mice that were randomly selected and analysed using densitometry. The 1.7-fold significant increase in relative ST3GAL1 protein levels ($P \leq 0.01$) in infected colonic tissue confirmed the transcriptional data (Fig. 4B). Western blot images of individual and pooled mice samples are shown in the Additional file 3.

Besides western blots, IF of ST3GAL1 in the corresponding colonic tissue sections was performed to assess protein abundance as well as localisation confirming the western blot data. An enhanced fluorescent signal of ST3GAL1 was detected in the *C. jejuni* infected group compared to naïve counterparts (Fig. 4C and Additional file 3), with an abundant cytosolic detection of ST3GAL1 in the enterocytes lining the entire length of the crypts of infected sections. In contrast, ST3GAL1 was more abundant in the upper part of the crypts towards the intestinal lumen in the control tissue. Additionally, ST3GAL1 was mainly localised on the apical side of the cell membrane in the naïve samples, whereas the fluorescence signal in the infected samples was more intense and evenly distributed over the entire cytosol of the cell (Fig. 4C). Images of individual sections from both groups and negative controls of the tissue sections, to ensure the specificity of the detected ST3GAL1 signal, are shown in the Additional file 5.

Discussion

Some pathogenic bacteria such as the zoonotic *C. jejuni* can infiltrate and penetrate the protective mucus layer in the colon and infect the mucosa. Even though *C. jejuni* is such a relevant human pathogen, the mechanisms underlying the infection have not been entirely unravelled yet and questions regarding colonisation and infection as well as the role of the host intestinal immune response remain unanswered to date. One major aspect within these processes forms the mucus. However, the role of the highly glycosylated MUC2, the main component of both colonic mucus layers, is not fully understood. In this study, we aimed to gain a more detailed insight into the regulatory mechanisms of mucin-type *O*-glycosylation in *C. jejuni* infections using a mouse model of human campylobacteriosis.

The importance of well-functioning MUC2 layers as a first line of defence against pathogens in the colon was revealed in previous studies [22–24]. As a response to *C. jejuni* infection, we have shown here that enzymes involved in the mucin-type *O*-glycosylation exhibit altered intestinal expression, which may lead to differential MUC2 glycosylation and consequently affect the protective properties of the glycoprotein. This was also reported upon infections with other pathogenic species. For example, *H. pylori* can modulate *O*-glycosylation, leading to changes in mucosal glycans and enhanced mucin sialylation due to dysregulations of sialyltransferases [25–28]. In the first line of *H. pylori* infection, the adhesion of the pathogen is mediated by antigen binding adhesin (BabA) binding at H-type 1 and Lewis b structures present on mucin (28]. The increase of sialylated mucin structures during the infection process promotes a closer membrane attachment of *H. pylori* mediated by the interaction of the sialic acid binding adhesin (SabA) with sialylated mucin structures, facilitating the infection [28]. This might also be the mechanism how *C. jejuni* penetrates the inner mucus layer and enables infection of the epithelium.

In the colon, ST3GAL1 primarily adds sialic acid to the core 1 *O*-glycans, a dominant core structure in mucin glycosylation, while ST3GAL2 transfers sialic acid to the terminal galactose residues found in glycoconjugates. B4GALT1, in contrast, catalyses the transfer of galactose to non-reducing ends of the sugar chain [29–31]. *C. jejuni* dependent dysregulation of miR-125a-5p and the previously reported miR-615-3p as well as the targeted glycosyltransferases in the applied mouse model suggest that a miRNA-dependent modification of mucin-type *O*-glycosylation takes place in the colon upon infection. It is still to be determined whether this is caused by *C. jejuni* directly or triggered by host immune responses. On the one hand, it was shown that modification of mucins and the increased mucus secretion is controlled by the epithelial cells responding to signals from the innate and adaptive immune system [26]. Pathogens have developed numerous mechanisms to penetrate the sterile inner mucus layer, thus, an altered mucin structure could serve as a host response preventing infection. This was seen in *H. pylori* infections and could also be assumed in infections with *C. jejuni* [32]. However, the altered *O*-glycosylation could also be pathogen-derived and may result in diminished mucin barrier function facilitating

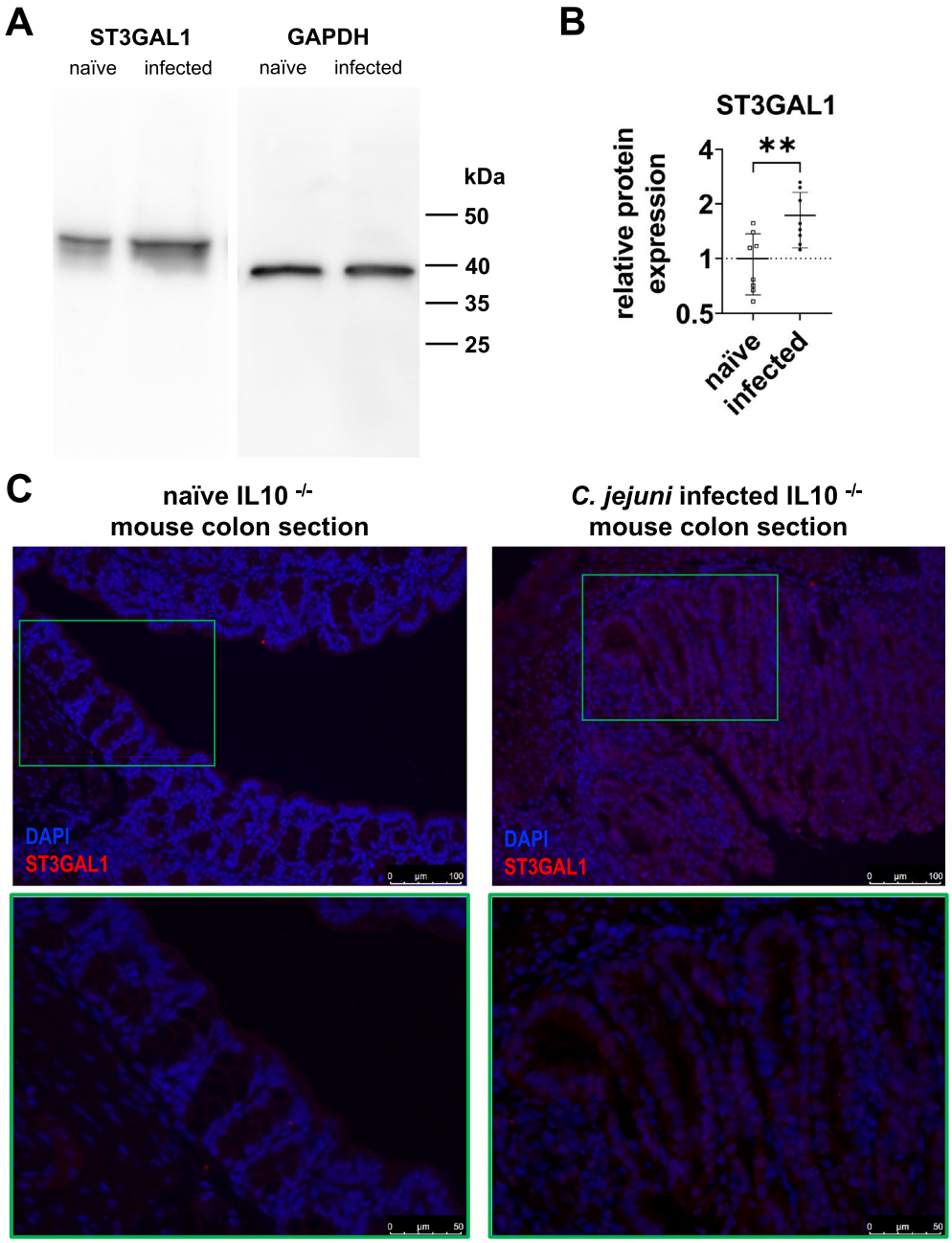

Fig. 4 Increased colonic ST3GAL1 protein levels in secondary abiotic IL10 $^{-/-}$ mice six days post *C. jejuni* infection compared to naïve controls. **A** Increased ST3GAL1 protein levels were detected by western blots in pooled protein samples of infected mice. GAPDH is presented as the respective loading reference. **B** ST3GAL1 detection of eight *C. jejuni* infected and eight naïve mice colon samples were quantified by means of western blotting followed by densitometric analysis relative to the respective GAPDH signals as controls. Protein levels of ST3GAL1 in the infected group were significantly and 1.7-fold increased, compared to naïve controls. Charts show normalised mean ± SD in each group. Statistical significance is presented by asterisks. **P ≤ 0.01, unpaired t-test. **C** Localisation and enhanced ST3GAL1 expression in the colon of *C. jejuni* infected mice determined in representative immunofluorescent staining compared to naïve controls. ST3GAL1 was detected by immunofluorescent staining and shown in red using DyLight 594 whereas the nuclei were stained blue using DAPI. Enhanced red signal intensity and pronounced cytosolic distribution was detected in infected controls. The top row shows the overview, with the area outlined in green in the bottom row shown enlarged. Scale bars indicate 100 µm and 50 µm. Exposure time was identical for all colon sections and presented images are representative for three biological replicates tested

the infection. These alterations could affect colonisation and infection by the pathogen.

In humans, *Campylobacter* causes symptoms such as severe diarrhoea and abdominal cramping [11]. During infection, *Campylobacter* trigger a range of immune responses and studies have shown that miRNAs are involved in regulating immune responses in several ways. The mechanisms known so far range from regulation of inflammation-dependent genes to control of apoptosis of infected host cells [10, 13, 33]. Understanding miRNA function can provide new insights into the pathogenesis of microorganisms. Here, the role of miR-125a-5p in infections with bacterial pathogens is of particular interest. In *Mycobacterium avium* infections, miR-125a-5p was overexpressed in human macrophages as part of the innate immune response to the bacterial infection [34]. On the other hand, upregulated miR-125a in *Mycobacterium tuberculosis* infections was associated with enhanced bacterial survival in human and murine macrophages [35]. Furthermore, *H. pylori* infections in humans were accompanied by decreased miR-125a-5p expression [17] and downregulation of miR-125a in mesenteric lymph nodes of piglets after *Salmonella* Typhimurium infection was identified, triggering diverse immune responses [36]. Finally, *C. jejuni* infections in mice have been recently found to be associated with reduced miR-125a-5p and enhanced miR-613-3p expression in the colon [10]. Interestingly, all studies that have focussed on infections with intestinal pathogens revealed decreased expression of miR-125a-5p. In the present study, we focused on the interaction of miRNA-125a-5p with putative targets conserved in human and mice to emphasise its relevance in *C. jejuni* infections. In silico analysis determined two overlapping targets of both dysregulated miRNAs involved in mucin-type *O*-glycosylation being conserved in human and mice, *St3gal1* and *B4galt1*. Here, miR-125a-5p was selected because of its known involvement in several bacterial infections, including *C. jejuni* infections [10, 17].

Decreased gene expression of *St3gal1* and *B4galt1* was observed after RNAi with miR-125a-5p mimics in our in vitro transfection experiments. Similar counter-regulated expression profiles of miR-125a-5p with *St3gal1* and *B4galt1* mRNAs were also observed in colonic tissue of the infected mice. Therefore, it is likely that expressions of both genes are negatively regulated by miR-125a-5p. In contrast, expression of *St3gal2* was not significantly regulated after RNAi with miR-125a-5p mimics and therefore does not seem to be a target of miR-125a-5p. The fact that miR-615-3p tends to be upregulated after miR-125a-5p transfection suggests a synergistic mode of action of both miRNAs. However, the underlying regulatory mechanisms still need to be investigated. Overall, miRNAs can play an important role in regulating the expression of glycosyltransferases during infection, and understanding these interactions can not only provide new insights into the pathogenesis of infectious diseases but also help to develop novel therapeutics.

Apart from matching mRNA and protein levels of ST3GAL1 after intestinal infection of mice, we determined the localisation of ST3GAL1 in the infected tissue and furthermore, at the cellular level. Mucin-type *O*-glycosylation takes place in the Golgi apparatus, and sialylated glycoproteins are stored in granules before being exported to the cell membrane or secreted [1, 37]. IF staining showed cytoplasmic ST3GAL1 signal, suggesting concordant localisation of ST3GAL1 in the Golgi apparatus. As adhesins of various pathogens can bind to sialic acids on mucins, abundance of ST3GAL1 could lead to increased integration of sialic acids in MUC2 glycans enhancing pathogen binding [26, 38]. The observation that the glycosyltransferases are dysregulated after interacting with the miRNAs during infection with *C. jejuni* supports our hypothesis that a miRNA-dependent modification of the *O*-glycosylation of MUC2 or other signalling proteins might take place here. Further research will focus on altered glycosylation pattern of mucin after *C. jejuni* infection.

Conventional laboratory mice with a complex commensal gut microbiota are not susceptible to *C. jejuni* infection, whereas secondary abiotic IL10 $^{-/-}$ mice generated upon antibiotic pre-treatment can not only be infected by the enteropathogens, but also display key features of human campylobacteriosis including acute enterocolitis within 6 days post-infection [18]. Although the model simulates the course of the disease in humans well, there are limitations, as in any translational model. Thus, the results cannot be completely transferred to human conditions and differences between mice and humans need to be considered. There are clear species differences in the extent of intestinal colonisation by *C. jejuni*. In contrast to humans and secondary abiotic mice, the enteropathogens colonise the intestinal tract of poultry and pigs asymptomatically without causing clear clinical signs of infection. Here, comparative studies of the interactions investigated may reveal possible differences between the animal species and humans to understand why the aforementioned animals are less susceptible to *C. jej ni*. This would even have applied effects on food safety, because a better understanding of the factors that contribute to colonisation can be used to reduce the load of zoonotic agents in the food chain.

The two miRNAs studied here and previously, miR-125a-5p and miR-615-3p, could be involved in the colonisation and infection process of the gut by *C. jejuni*. Through their targets, they could be part of the mucosal

and cellular host responses upon bacterial infection. Modified mucin-type *O*-glycosylation could be a direct mucosal response to hinder pathogenic colonisation and infection. On the contrary, *C. jejuni* could actively induce dysregulation of miRNAs facilitating host cell adhesion and invasion.

Conclusion

The aim of our study was to elucidate the regulatory effects of miR-125a-5p during *C. jejuni* infection. We determined mutually conserved targets of miR-125a-5p and miR-615-3p in humans and mice, namely the sialyltransferase *St3gal1* and the glycosyltransferase *B4galt1*, both known to be involved in mucin-type *O*-glycosylation. Here, we focussed on *St3gal1* and confirmed it as a bona fide target of miR-125a-5p. Moreover, our in vivo analysis showed that miR-125a-5p as well as *St3gal1* are dysregulated upon *C. jejuni* infection in susceptible mice. The interactions studied here may not only be involved in the modification of mucus glycosylation but could also target cellular signalling proteins. This study therefore provides a basis for better understanding molecular factors that are important for colonisation and infection of *C. jej ni*.

Methods

Animal experiment

In vivo experiments were carried out by the Forschungseinrichtungen für Experimentelle Medizin (FEM, Charité-Universitätsmedizin Berlin) and according to the European Guidelines for animal welfare (2010/63/EU) following agreement by the commission for animal experiments headed by the "Landesamt für Gesundheit und Soziales" (LaGeSo, Berlin, registration number G0104/19). Animal welfare was monitored twice a day. For the experiment, 39 secondary abiotic IL10$^{-/-}$ mice (C57BL/B10 background) were divided into two groups, *C. jej ni* infected and naïve, matched by age and sex [18]. In total, 19 animals were infected with 10^9 colony forming units (CFU) of *C. jejuni* strain 81–176 in 0.3 ml sterile phosphate-buffered saline (PBS, Thermo Fisher Scientific, Waltham, MA, USA) on days 0 and 1 by oral gavage while 20 animals were not infected as controls. The mice were sacrificed six days post infection and ex vivo biopsies of the colon were collected under aseptic conditions. For the gene expression and protein analysis, the colon tissue samples were stored in Allprotect Tissue Reagent (Qiagen, Venlo, Netherlands) or liquid nitrogen, respectively and stored at −80 °C. For the histopathological analysis, the biopsies were immediately fixed in 5% formalin and embedded in paraffin.

Cell line and culture conditions

The murine rectal carcinoma cell line CMT 93 (ECACC 89111413) was cultured in a humidified atmosphere at 37 °C and 5% CO_2 in Dulbeccco's Modified Eagle's Medium (DMEM) with 4.5 g/l Glucose and L-Glutamine (Gibco, Grand Island, NY, USA). The medium was supplemented with 100 µg/ml Gentamicin and 10% (v/v) fetal calf serum superior (Sigma-Aldrich, Darmstadt, Germany). The cells were grown in 75 cm^2 tissue culture flasks (Sarstedt, Nümbrecht, Germany) until approximately 80% confluence was reached.

RNA-isolation and RT-qPCR

Total RNA was isolated from the murine colonic tissue stored in Allprotect and CMT 93 cells using the miRVana Isolation Kit (Life Technologies, Carlsbad, CA, USA). Then, cDNA was synthesised from individual tissue samples or cell lysates. For this, the isolated total RNA was firstly treated with RNase-free DNase I (NEB GmbH, Frankfurt a/M, Germany) to remove residual genomic DNA. Then, 1 µg total RNA was applied for reverse transcription using 200 U M-MuLV Reverse Transcriptase (Thermo Fisher Scientific), 0.2 µg random hexamer primer (Thermo Fisher Scientific), 200 µM of each deoxynucleotide triphosphate (dNTP) (Thermo Fisher Scientific) and 1 × supplied RT buffer (Thermo Fisher Scientific). To verify the absence of genomic DNA, control samples were treated as just mentioned but without M-MuLV Reverse Transcriptase. Then, RT-qPCRs were carried out. The qPCR of the mRNAs was performed with the Blue S'Green qPCR Kit (Biozym Scientific GmbH, Hessisch Oldendorf, Germany) under following cycling conditions: amplification was conducted at 95 °C for 2 min, followed by 40 cycles with 15 s at 95 °C, 20 s at 60 °C and 30 s at 70 °C. For quality control, subsequent melting curve analysis was assessed by 95 °C for 15 s, 65 °C for 1 min, ramping from 65 to 95 °C at 5 °C/min. For the miRNA qPCR, the SensiFAST SYBR® Hi-ROX Kit (Bioline, Meridian Bioscience International Limited, Cincinnati, OH, USA) was used and cycling conditions comprised real-time analysis at 95 °C for 2 min, followed by 40 cycles with 15 s at 95 °C, 20 s at 60 °C and 30 s at 72 °C. Subsequent melting curve analysis was assessed by 95 °C for 15 s, 60 °C for 1 min, ramping from 60 to 95 °C at 5 °C/min. For RT-qPCR of the miRNAs, the miR-Q method [39] was used with specific RT-6-primer and corresponding reverse PCR primer (Additional file 2). All relative gene expression was calculated using the ΔΔCt method [40] as described before [10]. Stability of the reference was tested using geNorm [41]. The HPRT and SDHA genes served as references for mRNA expression and

the small RNAs SNORD44 and SNORD47 for miRNA expression. The mean Ct values of the target as well as the geometric mean of all Ct-values of the two respective references were calculated for each sample from three technical replicates. The ΔCt is equal to the difference between the Ct of the target and the geometric mean of both references. The ΔΔCt were calculated relative to controls.

All oligonucleotides in this study were synthesised by Sigma-Aldrich. Sequences, amplification efficiencies and primer concentrations and can be found in Additional file 2.

Western blot

Colonic tissue samples derived from the animal experiment were lysed in cold RIPA buffer (Cell Signaling Technology (CST), Danvers, MA, USA), supplemented with protease inhibitor cocktail (CST) and protein was isolated. Protein concentration was quantified by using the 2D Quant Kit (Qiagen). 30 µg of protein was loaded onto a 12% sodium dodecyl sulfate-polyacrylamide (SDS) gel for electrophoresis. Then, they were transferred onto a polyvinylidene fluoride membrane (PVDF) (GE Healthcare, Buckinghamshire, UK) by means of semi-dry blotting. To prevent unspecific binding of the antibody, the membrane was blocked in 5% (w/v) bovine serum albumin (Sigma-Aldrich) in TBST (Tris–HCl-buffer with 0.1% (v/v) Tween-20) for 1.5 h at room temperature. The membrane was incubated with the primary antibody Rabbit anti-ST3GAL1 (Novus Biologicals, biotechne, Minneapolis, MN, USA, NBP1-62540) 1:500 or Rabbit anti-GAPDH (CST, #5174) 1:2000 in 5% BSA in TBST at 4 °C overnight. After three washes in TBST for 15 min each, the membrane was probed with the secondary horseradish peroxidase (HRP)-linked anti-rabbit IgG antibody (1:2500 in 5% BSA in TBST, CST, #7074) for 2 h at room temperature. After three additional washes with TBST (Tris–HCl-buffer with 0.1% (v/v) Tween-20) for 15 min, immuno-reactive proteins were detected with the Amersham™ ECL Select™ Western Blotting Detection Reagent (GE Healthcare). Exposure conditions were identical for every blot. Protein quantification was performed by densitometry using the software BIO-1D (Vilber, Collégien, France). Here, a defined area was selected to be used on all lanes in each blot for 8 *C. jejuni* infected and 8 naïve mice colon samples and densitometry was measured. The optical density was determined by the software and the background was subtracted. The pixel density values of the ST3GAL1 signals were then normalised to the respective GAPDH signals and the fold change calculated on the mean of the controls. The raw pixel density values can be found in the Additional file 4.

Histopathology and immunofluorescence

Murine colon tissue sections from the animal experiment were immediately fixed in 5% formalin and embedded in paraffin. 5 µm serial sections were cut using the Epredia™ HM 340E Electronic Rotary Microtome (Thermo Fisher Scientific). The paraffin was melted at 60 °C for 45 min and the tissue sections deparaffinated in Roticlear (Carl Roth, Karlsruhe, Germany). Rehydration of the tissue was reached through a graded series of ethanol followed by rinsing with distilled water and PBS (pH 7.4, Sigma-Aldrich). For IF, antigen retrieval was carried out by incubating the sections in boiling citrate buffer for 15 min followed by 20 min of cooling down. Non-specific binding was blocked with 1% (v/v) BSA (Sigma-Aldrich) in PBST (0.1% (v/v) Tween-20 in PBS) for 1 h at room temperature. Then, the sections were incubated with a 1:50 dilution of the Rabbit anti-ST3GAL1 primary antibody (Novus Biologicals, NBP1-62540), in 1% (v/v) BSA in PBST overnight at 4 °C. Negative controls were treated with 1% (v/v) BSA in PBST without the primary antibody. After three washes with PBS for 10 min, the primary antibody was detected with goat anti-rabbit IgG DyLight 594 secondary antibody (1:400, diluted in 1% (v/v) BSA in PBST, Thermo Fisher Scientific, #35561) for 1 h at room temperature. Following three washes with PBS, the nuclei were counterstained with 200 ng/ml 4′, 6-diamidin-2-phenylindol (DAPI, Sigma-Aldrich) in PBS for 5 min at room temperature. Subsequently, slides were washed in PBS and mounted with Prolong™ Diamond Anti-fade Mountant (Life Technology). For IF, the Leica DMI6000B inverted microscope with the compatible Leica LAS-X software (Leica, Wetzlar, Germany) was used. All images were taken under identical microscope- and camera-settings. Experiments were carried out with three randomly selected biological replicates per group. Images were taken at least from three random areas per section and more than ten images per area were selected. The background was subtracted in each image.

RNAi and luciferase reporter assay

For both assays, CMT 93 cells were cultured as mentioned above. RNAi transfections of three biological replicates were performed using electroporation with the Nucleofector Technology (Lonza AG, Köln, Germany) as previously described with few modifications [41]. 1×10^6 cells were mixed with 50 pmol of miR-125a-5p miRNA mimic (Qiagen, MSY0000443) or 50 pmol non-target siRNA (Dharmacon Lafayette, CO, USA, D-001810-03-05) s a control. After 24 h, the cells were washed with PBS and lysed for RNA isolation.

The dual luciferase reporter assays were carried out as previously mentioned [10, 41]. For the generation

of the reporter plasmids, the in silico identified target sites of murine *St3gal1* were assembled using the hybridised oligonucleotides NotI-mmuSt3gal1ts-sense and XbaI-mmuSt3gal1ts-antisense from Sigma-Aldrich (Additional file 2). These target sites were cloned in pTK-Gluc (NEB GmbH) plasmid using the appropriate restriction enzymes *Not*I and *Xba*I (both NEB GmbH). For endotoxin-free reporter plasmids of the resulting derivative pTKGmSt3gal1, NucleoBond Xtra Midi Plus EF (Macherey–Nagel GmbH & Co. KG, Düren, Germany) was used. For the luciferase assay, 3.8×10^5 CMT 93 cells were inversely transfected with 3.25 µg of endotoxin-free pTKGmSt3gal1 and for normalisation, 350 ng pCMV-Red Firefly Luc (Thermo Fisher Scientific, 16156) together with 200 pmol miR-125a-5p miRNA mimic (Qiagen) on a 6-Well Plate (Sarstedt) using 7.5 µl Lipofectamin 3000 (Thermo Fisher Scientific) and 2.5 µl P3000 Reagent (Thermo Fisher Scientific). The transfected cells were cultured for 48 h. As a negative control, 200 pmol non-target siRNA (Dharmacon Lafayette) was transfected. Gaussia-Firefly Luciferase activity was detected in three biological and three technical replicates with the Pierce Gaussia-Firefly Luciferase Dual Assay Kit (Thermo Fisher Scientific). For the dual luciferase reporter assays, the CLARIOstarPlus plate reader (BMG Labtech, Ortenberg, Germany) was used under following conditions: top optic, number of multichromatics: 2, number of kinetic widows: 1, number of cycles: 1, measurement interval time: 1.27, emission Luciferase-Red Firefly: 623 nm, emission Luciferase-Gaussia: 485 nm.

In silico and statistical analysis

Mutual targets of miR-125a-5p and miR-615-3p in human and mouse were identified as well as data and pathway analysis performed as described earlier [10, 12]. Briefly, overlapping targets of both miRNAs were determined for mouse and human by miRmap followed by KEGG based pathway enrichment analysis. Conserved mutual targets involved in 'Glycosaminoglycan biosynthesis—keratan sulfate' (hsa00533 and mmu00533) and mucin type *O*-glycan biosynthesis (mmu00512) were determined. RNAhybrid was used to predict target sites of miRNA [21]. Normal distribution of data was assessed by the Anderson–Darling test. The unpaired t-test was used in this study to compare each treatment with control. All tests were conducted applying GraphPad Prism version 8.00 (GraphPad Software, La Jolla California USA, www.graphpad.com). Asterisks in figures summarize P values ($^*P \leq 0.05$; $^{**}P \leq 0.01$; $^{***}P \leq 0.001$; $^{****}P \leq 0.0001$).

Supplementary Information

The online version contains supplementary material available at https://doi.org/10.1186/s13099-023-00577-6.

Additional file 1. Raw data of the in silico analysis using KEGG pathway enrichment analysis. Sheet 1 shows overlapping targets of miR-125a-5p and miR-615-3p as well as their pathways in humans. Sheet 2 shows overlapping targets of miR-125a-5p and miR-615-3p and their pathways in mice. Overlapping targets conserved in both species are highlighted in bold.

Additional file 2. All oligonucleotides used in this study. Shown are the primer sequences, amplification efficiencies, primer concentrations and the determined region of ST3GAL1 where miR-125a-5p possibly binds cloned in the plasmid used for Luciferase-Assay.

Additional file 3. Randomly selected tissue samples in pooled and individual blots. (a,b) Western blot detection of ST3GAL1 in eight naïve (n1-8) and eight *C. jejuni* infected (i1-8) secondary abiotic IL-$10^{-/-}$ mouse colon sections. GAPDH is shown as the respective loading reference in the same samples. (c) Western blot detection of ST3GAL1 of pooled protein samples of four naïve (n1-4 and n5-8) and four *C. jejuni* infected (i1-4 and i5-8) secondary abiotic IL-$10^{-/-}$ mouse colon sections and pooled protein samples of all eight naïve (n1-8) and eight infected (i1-8) sections. GAPDH is shown as the respective loading reference in the same pooled samples.

Additional file 4. Pixel density values of individual and pooled western blots as well as the selected area used for the determination of ST3GAL1 expression in colonic tissue samples of naïve and *C. jejuni* infected mice. Sheet 1 shows the pixel density values of the first four individual naïve (n1-4) and *C. jejuni* infected (i1-4) samples, sheet 2 of the second four individual naïve (n5-8) and *C. jejuni* infected (i5-8) samples. In sheet 3 values of all pooled samples (n1-4, i1-4, n5-8, i5-8, n1-8 and i1-8) are shown.

Additional file 5. Detection of immunofluorescently stained ST3GAL1 in secondary abiotic IL-$10^{-/-}$mice upon *C. jejuni* 81–176 infection. ST3GAL1 is shown in red and nuclei were stained blue using DAPI. (a + b) Immunofluorescent staining of ST3GAL1 in two individual experiments of naïve mouse colon sections. (c + d) Two individual *C. jejuni* infected mouse colon sections immunostained with ST3GAL1. (e) Negative controls of naïve colonic tissue sections. (f) Negative controls of colon tissue sections infected with *C. jejuni*. Scale bars indicate 100 µm and 50 µm (magnification).

Acknowledgements
We would like to express our sincere thanks to Mrs. Kutz-Lohroff for professional support in conducting the experiments.

Author contributions
AK: Performed experiments, analysed data, wrote paper. SM: Designed and performed animal experiment, co-edited paper. MMH: Designed and performed animal experiment, co-edited paper. SB: Provided advice in study design, co-edited paper. RE: Provided advice in study design, co-edited paper. TA: Provided advice in study design, co-edited paper. GG: Designed study, performed experiments, co-wrote paper. SS: Designed study, performed experiments, analysed data, wrote paper.

Funding
Open Access funding enabled and organized by Projekt DEAL. This work was supported by the Research Committee of the Freie Universität Berlin. The funders had no role in study design, data collection and analysis, decision to publish or preparation of the manuscript.

Availability of data and materials
All data generated or analysed during this study are included in this published article and its supplementary information files.

Declarations

Ethics approval and consent to participate
Mouse experiments were carried out in compliance with the European Guidelines for animal welfare (2010/63/EU). The protocol was approved by the commission for animal experiments headed by the "Landesamt für Gesundheit und Soziales" (LaGeSo, Berlin, registration numbers G0172/16 and G0247/16). Animal welfare was monitored twice daily by assessment of clinical conditions.

Consent for publication
Not applicable.

Competing interests
The authors declare that they have no competing interests.

Author details
[1]Institute of Veterinary Biochemistry, Freie Universität Berlin, Berlin, Germany. [2]Institute of Microbiology, Infectious Diseases and Immunology, Humboldt-Universität zu Berlin, and Berlin Institute of Health, Charité-Universitätsmedizin Berlin, Corporate Member of Freie Universität Berlin, Berlin, Germany. [3]Institute of Food Safety and Food Hygiene, Freie Universität Berlin, Berlin, Germany.

Received: 10 July 2023 Accepted: 8 October 2023
Published online: 17 October 2023

References

1. Johansson MEV, Sjövall H, Hansson GC. The gastrointestinal mucus system in health and disease. Nat Rev Gastroenterol Hepatol. 2013;10(6):352–61.
2. Poole J, Day CJ, von Itzstein M, Paton JC, Jennings MP. Glycointeractions in bacterial pathogenesis. Nat Rev Microbiol. 2018;16(7):440–52.
3. Hansson GC. Role of mucus layers in gut infection and inflammation. Curr Opin Microbiol. 2012;15(1):57–62.
4. Johansson MEV, Larsson JMH, Hansson GC. The two mucus layers of colon are organized by the MUC2 mucin, whereas the outer layer is a legislator of host–microbial interactions. Proc Natl Acad Sci. 2011;108(supplement_1):4659–65.
5. Brockhausen I, Schachter H, Stanley P. O-GalNAc Glycans. In: Varki A, Cummings RD, Esko JD, Freeze HH, Stanley P, Bertozzi CR, et al., editors. Essentials of Glycobiology. Cold Spring Harbor (NY): Cold Spring Harbor Laboratory Press. Copyright © 2009, The Consortium of Glycobiology Editors, La Jolla, California; 2009.
6. Grondin JA, Kwon YH, Far PM, Haq S, Khan WI. Mucins in intestinal mucosal defense and inflammation: learning from clinical and experimental studies. Front Immunol. 2020;11:2054.
7. Chandrasekaran EV, Xue J, Xia J, Locke RD, Patil SA, Neelamegham S, et al. Mammalian sialyltransferase ST3Gal-II: its exchange sialylation catalytic properties allow labeling of sialyl residues in mucin-type sialylated glycoproteins and specific gangliosides. Biochemistry. 2011;50(44):9475–87.
8. Baos SC, Phillips DB, Wildling L, McMaster TJ, Berry M. Distribution of sialic acids on mucins and gels: a defense mechanism. Biophys J. 2012;102(1):176–84.
9. Lewis AL, et al. Essentials of glycobiology [Internet] (Chapter 15), 4th edn. Cold Spring Harbor (NY): Cold Spring Harbor Laboratory Press; 2022.
10. Xi D, Hofmann L, Alter T, Einspanier R, Bereswill S, Heimesaat MM, et al. The glycosyltransferase ST3GAL2 is regulated by miR-615-3p in the intestinal tract of *Campylobacter jejuni* infected mice. Gut Pathog. 2021;13(1):42.
11. Alter T, Bereswill S, Backert S. Campylobacteriose—eine zoonotische Infektionskrankheit. BIOspektrum. 2021;27(6):591–3.
12. Pawar K, Sharbati J, Einspanier R, Sharbati S. *Mycobacterium bovis* BCG Interferes with miR-3619-5p control of Cathepsin S in the process of autophagy. Front Cell Infect Microbiol. 2016;6:27.
13. Sharbati J, Lewin A, Kutz-Lohroff B, Kamal E, Einspanier R, Sharbati S. Integrated microRNA-mRNA-analysis of human monocyte derived macrophages upon *Mycobacterium avium* subsp. hominissuis Infection. PLoS ONE. 2011;6(5): e20258.
14. Eulalio A, Schulte L, Vogel J. The mammalian microRNA response to bacterial infections. RNA Biol. 2012;9(6):742–50.
15. Gebert LFR, MacRae IJ. Regulation of microRNA function in animals. Nat Rev Mol Cell Biol. 2019;20(1):21–37.
16. Sun Y-M, Lin K-Y, Chen Y-Q. Diverse functions of miR-125 family in different cell contexts. J Hematol Oncol. 2013;6(1):6.
17. Dos Santos MP, Pereira JN, De Labio RW, Carneiro LC, Pontes JC, Barbosa MS, et al. Decrease of miR-125a-5p in gastritis and gastric cancer and its possible association with *H. pylori*. J Gastrointest Cancer. 2021;52(2):569–74.
18. Haag LM, Fischer A, Otto B, Plickert R, Kühl AA, Göbel UB, et al. *Campylobacter jejuni* induces acute enterocolitis in gnotobiotic IL-10$^{-/-}$ mice via Toll-like-receptor-2 and -4 signaling. PLoS ONE. 2012;7(7): e40761.
19. Xi D, Alter T, Einspanier R, Sharbati S, Gölz G. *Campylobacter jejuni* genes Cj1492c and Cj1507c are involved in host cell adhesion and invasion. Gut Pathog. 2020;12(1):8.
20. Kanehisa M, Furumichi M, Sato Y, Kawashima M, Ishiguro-Watanabe M. KEGG for taxonomy-based analysis of pathways and genomes. Nucleic Acids Res. 2022;51(D1):D587–92.
21. Rehmsmeier M, Steffen P, Hochsmann M, Giegerich R. Fast and effective prediction of microRNA/target duplexes. RNA. 2004;10(10):1507–17.
22. Johansson MEV, Phillipson M, Petersson J, Velcich A, Holm L, Hansson GC. The inner of the two Muc2 mucin-dependent mucus layers in colon is devoid of bacteria. Proc Natl Acad Sci. 2008;105(39):15064–9.
23. Wenzel UA, Magnusson MK, Rydström A, Jonstrand C, Hengst J, Johansson MEV, et al. Spontaneous colitis in Muc2-deficient mice reflects clinical and cellular features of active ulcerative colitis. PLoS ONE. 2014;9(6): e100217-e.
24. Bergstrom KSB, Kissoon-Singh V, Gibson DL, Ma C, Montero M, Sham HP, et al. Muc2 protects against lethal infectious colitis by disassociating pathogenic and commensal bacteria from the colonic mucosa. PLoS Pathog. 2010;6(5): e1000902-e.
25. Arike L, Hansson GC. The densely O-glycosylated MUC2 mucin protects the intestine and provides food for the commensal bacteria. J Mol Biol. 2016;428(16):3221–9.
26. Linden SK, Sutton P, Karlsson NG, Korolik V, McGuckin MA. Mucins in the mucosal barrier to infection. Mucosal Immunol. 2008;1(3):183–97.
27. Radziejewska I, Leszczyńska K, Borzym-Kluczyk M. Influence of monoclonal anti-Lewis b, anti-H type 1, and anti-sialyl Lewis x antibodies on binding of *Helicobacter pylori* to MUC1 mucin. Mol Cell Biochem. 2014;385(1–2):249–55.
28. Magalhães A, Marcos-Pinto R, Nairn AV, Dela Rosa M, Ferreira RM, Junqueira-Neto S, et al. Helicobacter pylori chronic infection and mucosal inflammation switches the human gastric glycosylation pathways. Biochim Biophys Acta. 2015;1852(9):1928–39.
29. Angata K, Fukuda M. ST3 beta-galactoside alpha-2,3-sialyltransferase 1 (ST3GAL1). In: Taniguchi N, Honke K, Fukuda M, Narimatsu H, Yamaguchi Y, Angata T, editors. Handbook of glycosyltransferases and related genes. Tokyo: Springer Japan; 2014. p. 637–44.
30. Tsuji S, Takashima S. ST3 beta-galactoside alpha-2,3-sialyltransferase 2 (ST3GAL2). In: Taniguchi N, Honke K, Fukuda M, Narimatsu H, Yamaguchi Y, Angata T, editors. Handbook of glycosyltransferases and related genes. Tokyo: Springer Japan; 2014. p. 645–56.
31. Ramakrishnan B, Qasba PK. UDP-Gal: betaGlcNAc Beta 1,4-galactosyltransferase, polypeptide 1 (B4GALT1). In: Taniguchi N, Honke K, Fukuda M, Narimatsu H, Yamaguchi Y, Angata T, editors. Handbook of glycosyltransferases and related genes. Tokyo: Springer Japan; 2014. p. 51–62.
32. McGuckin MA, Lindén SK, Sutton P, Florin TH. Mucin dynamics and enteric pathogens. Nat Rev Microbiol. 2011;9(4):265–78.
33. Kaakoush NO, Deshpande NP, Man SM, Burgos-Portugal JA, Khattak FA, Raftery MJ, et al. Transcriptomic and proteomic analyses reveal key innate immune signatures in the host response to the gastrointestinal pathogen *Campylobacter concisus*. Infect Immun. 2015;83(2):832–45.
34. Wang Y, Chen C, Xu X-D, Li H, Cheng M-H, Liu J, et al. Levels of miR-125a-5p are altered in Mycobacterium avium-infected macrophages and associate with the triggering of an autophagic response. Microbes Infect. 2020;22(1):31–9.
35. Niu W, Sun B, Li M, Cui J, Huang J, Zhang L. TLR-4/microRNA-125a/NF-κB signaling modulates the immune response to *Mycobacterium tuberculosis* infection. Cell Cycle. 2018;17(15):1931–45.

36. Herrera-Uribe J, Zaldívar-López S, Aguilar C, Luque C, Bautista R, Carvajal A, et al. Regulatory role of microRNA in mesenteric lymph nodes after *Salmonella* Typhimurium infection. Vet Res. 2018;49(1):9.
37. Hugonnet M, Singh P, Haas Q, von Gunten S. The distinct roles of sialyltransferases in cancer biology and onco-immunology. Front Immunol. 2021;12: 799861.
38. Burzyńska P, Sobala ŁF, Mikołajczyk K, Jodłowska M, Jaśkiewicz E. Sialic acids as receptors for pathogens. Biomolecules. 2021;11(6):831.
39. Sharbati-Tehrani S, Kutz-Lohroff B, Bergbauer R, Scholven J, Einspanier R. miR-Q: a novel quantitative RT-PCR approach for the expression profiling of small RNA molecules such as miRNAs in a complex sample. BMC Mol Biol. 2008;9(1):34.
40. Livak KJ, Schmittgen TD. Analysis of relative gene expression data using real-time quantitative PCR and the $2^{(-\Delta\Delta C(_T))}$ Method. Methods. 2001;25(4):402–8.
41. Vandesompele J, De Preter K, Pattyn F, Poppe B, Van Roy N, De Paepe A, et al. Accurate normalization of real-time quantitative RT-PCR data by geometric averaging of multiple internal control genes. Genome Biol. 2002;3(7):RESEARCH0034.

Publisher's Note

5.2 Publication 2: Structured multicellular intestinal spheroids (SMIS) as a standardized model for infection biology

Kraski, A., Migdał, P., Klopfleisch, R. *et al.* Structured multicellular intestinal spheroids (SMIS) as a standardized model for infection biology. *Gut Pathog* **16**, 47 (2024).

DOI: https://doi.org/10.1186/s13099-024-00644-6

Gut Pathogens

RESEARCH

Open Access

Structured multicellular intestinal spheroids (SMIS) as a standardized model for infection biology

Angelina Kraski[1], Paweł Migdał[2], Robert Klopfleisch[3], Clara Räckel[1], Jutta Sharbati[4], Markus M. Heimesaat[5], Thomas Alter[6], Carlos Hanisch[7], Greta Gölz[6], Ralf Einspanier[1] and Soroush Sharbati[1*]

Abstract

Background 3D cell culture models have recently garnered increasing attention for replicating organ microarchitecture and eliciting in vivo-like responses, holding significant promise across various biological disciplines. Broadly, 3D cell culture encompasses organoids as well as single- and multicellular spheroids. While the latter have found successful applications in tumor research, there is a notable scarcity of standardized intestinal models for infection biology that mimic the microarchitecture of the intestine. Hence, this study aimed to develop structured multicellular intestinal spheroids (SMIS) specifically tailored for studying molecular basis of infection by intestinal pathogens.

Results We have successfully engineered human SMIS comprising four relevant cell types, featuring a fibroblast core enveloped by an outer monolayer of enterocytes and goblet cells along with monocytic cells. These SMIS effectively emulate the in vivo architecture of the intestinal mucosal surface and manifest differentiated morphological characteristics, including the presence of microvilli, within a mere two days of culture. Through analysis of various differentiation factors, we have illustrated that these spheroids attain heightened levels of differentiation compared to 2D monolayers. Moreover, SMIS serve as an optimized intestinal infection model, surpassing the capabilities of traditional 2D cultures, and exhibit a regulatory pattern of immunological markers similar to in vivo infections after *Campylobacter jejuni* infection. Notably, our protocol extends beyond human spheroids, demonstrating adaptability to other species such as mice and pigs.

Conclusion Based on the rapid attainment of enhanced differentiation states, coupled with the emergence of functional brush border features, increased cellular complexity, and replication of the intestinal mucosal microarchitecture, which allows for exposure studies via the medium, we are confident that our innovative SMIS model surpasses conventional cell culture methods as a superior model. Moreover, it offers advantages over stem cell-derived organoids due to scalability and standardization capabilities of the protocol. By showcasing differentiated morphological attributes, our model provides an optimal platform for diverse applications. Furthermore, the investigated differences of several immunological factors compared to monotypic monolayers after *Campylobacter jejuni* infection underline the refinement of our spheroid model, which closely mimics important features of in vivo infections.

Keywords Multilayered spheroid, 3D cell culture, Intestinal mucosa, Infection model

*Correspondence:
Soroush Sharbati
soroush.sharbati@fu-berlin.de
Full list of author information is available at the end of the article

Background

For many years, cell culture models have been a valuable tool for understanding complex molecular and cellular mechanisms in both basic and applied research. Using appropriate in vitro models, new and in-depth insights into cell biology for normal differentiation and pathogenesis have been gained [1, 2]. They also play a crucial role in investigating the pharmacokinetics and pharmacodynamics of drugs, conducting toxicity testing for various substances, and contributing to the emerging field of tissue engineering and regenerative medicine [3, 4]. The majority of in vitro experiments mentioned were originally performed as two-dimensional (2D) single cell or co-culture models, as they are inexpensive, easy to handle, reproducible and efficient [3, 5, 6]. Such models have clear limitations, as they can only reproduce complex tissue structures to a very limited extent and therefore often do not reflect the complexity of human or animal tissue physiology [6]. Especially concerning cell–cell interactions and extracellular microenvironments, 2D cell monolayers are inadequate for accurate representation [1]. While animal models offer a more comprehensive understanding of human physiology and pathophysiology they come with drawbacks. These include time-consuming nature of experiments, high costs, and limitations arising from species-specific differences. Additionally, significant inter-individual variability and ethical concerns regarding the welfare of animals utilized cannot be overlooked [7, 8].

Hence, three-dimensional (3D) cell culture models have gained increasing importance in recent decades. In these models, cells are cultured under conditions that allow them to grow and interact in all three spatial dimensions, closely resembling in vivo microstructures. As a result, 3D cell culture models bridge the gap between traditional 2D cultures and in vivo models, offering a promising path for overcoming the challenges previously mentioned. Moreover, these optimized models facilitate the development of cell–cell and cell-extracellular matrix interactions, resulting in tissue architectures that closely resemble the in vivo situation [9]. In line with the 3R principle (reduction, replacement and refinement of animal experiments), they not only reduce the number of animal experiments but also adequately reproduce in vivo data by more closely mimicking organ morphology and physiology.

3D cell culture can mainly be subdivided into organoids and spheroids. Organoids are derived either from (induced) pluripotent stem cells or from organ-specific adult stem cells obtained after tissue biopsies. As soon as they differentiate into tissue-specific and specialized cell types in culture, they organize themselves independently into organ-like structures [10, 11]. This includes, for example, the formation of typical tissue-specific protrusions such as crypts or villi in intestinal organoids [12, 13]. However, these mini-organs obtained from patients or individual donors have some disadvantages. They require human or animal biopsies, are relatively expensive to produce, time-consuming and the harmonization and standardization of the method is limited [14]. In this context, the accessibility of biopsies and the presence of inter-individual differences pose particular challenges, as organoids are derived from individual donors. On the other hand, this has advantages, as greater genetic diversity enables reliable and realistic results. The orientation of the mini-organ, which is usually embedded in a matrix, plays an important role. This applies in particular to the investigation of molecular aspects of infections. For instance, in intestinal organoids, the luminal surface is typically oriented towards the interior, posing challenges for exposing it to luminal factors like microbiota and pathogens. The reversal of orientation has rarely been performed, takes a long time and is a complex and labor-intensive procedure. Therefore, their use as standardized infection models or for high-throughput procedures is limited [15]. However, studies have been conducted utilizing apical-out orientated organoids as an advanced model, applied in infection research [15–18]. Spheroids, on the other hand, are formed from cell cultures or biopsy material in classic hanging drops or by using non-adhesive surfaces leading to aggregation of cells and the formation of 3D cell clusters [19–21]. Spheroids are spherical, self-organizing structures that can either be embedded in an extracellular matrix (e.g., Matrigel) or maintained without a matrix, floating freely in culture [22]. Spheroids facilitate 3D cell–cell interactions, closely resembling in vivo environments. They are cost-effective and straightforward to generate, offering reproducibility and ease of standardization and harmonization. They are distinguished in homotypic and multicellular (heterotypic) spheroid models. Homotypic spheroids consist of only one cell type, multicellular models of two or more cell types. However, the multicellular spheroid models have so far lacked a structured cellular composition and microarchitecture. They have been successfully used for many years for cell biology studies, preferably in preclinical oncology research [23–25]. While lung spheroids have been used in SARS-CoV-2 research, they have not yet been extensively studied as standardized bacterial infection models [26, 27]. Bacterial infections pose significant challenges to global health, yet suitable 3D models capable of replacing animal models and analyzing the molecular mechanisms underlying host cell invasion and dissemination remain limited. Particularly concerning the gastrointestinal tract, an ideal model would need to feature a surface composed of differentiated enterocytes

to be both functional and physiologically relevant while mimicking the 3D microarchitecture.

The mammalian intestinal epithelium is a rapidly self-renewing tissue. In homeostasis, $Lgr5^+$ stem cells located at the base of the crypts, produce precursor cells of secretory and enterocytes that terminally differentiate into goblet cells, enteroendocrine cells or nutrient-absorbing enterocytes migrating upwards [28]. Notably, during tissue repair after injury, enterocytes within the intestinal crypts can dedifferentiate to an undifferentiated state, replacing the $Lgr5^+$ stem cells and generating proliferative stem cells and Paneth-like secretory cells [28]. Various markers can be utilized, exhibiting altered expressions depending on the differentiation status of enterocytes along the crypt axis. The epidermal growth factor (EGF), a growth factor playing a crucial role in regulating cell proliferation and differentiation, is expressed in the microenvironment at the crypt basis [29, 30]. Further, ephrin receptors are predominantly expressed near the bottom of the crypts while Ephrin B1 and Ephrin B2 segregate differentiated from precursor cells in the villus and are dominantly prevalent there [29, 31, 32]. Ephrin receptors are the largest family of tyrosine kinase receptor. After ephrin binding, they facilitate contact-dependent communication between cells, whether of the same or different type, to regulate various cellular processes such as morphology, adhesion, movement, proliferation, survival, and differentiation [33]. Markers for fully differentiated and functional enterocytes are the transporters solute carrier family 5 member 1 (SLC5A1 or SGLT1) and peptide transporter 1 (SLC15A1 or PEPT1) [34]. While the sodium-dependent SGLT1 is primarily responsible for the absorption of dietary glucose and galactose from the intestinal lumen, PEPT1 facilitates the uptake of dipeptides and tripeptides into enterocytes. Both of these transporters are located in the brush border membrane of functional intestinal enterocytes [35, 36]. Ideally, intestinal 3D cell culture models should exhibit abundant expression of these markers to demonstrate their differentiation status and, consequently, their resemblance to the in vivo environment.

Here we have tackled the task of developing a suitable intestinal infection model that mimics the intestinal mucosal microarchitecture. In contrast to most previously reported intestinal spheroids, which are limited to only one type of cells [37, 38], the spheroids described here consist of up to four different cell types that self-assemble in an ordered fashion in a liquid medium. By integrating fibroblasts, enterocytes, goblet cells and monocytic cells, relevant players in bacterial infections were considered. In the loose connective tissue of the mucosa, fibroblasts are the predominant cell type, while enterocytes form the inner lining of the intestine. Goblet cells, responsible for producing protective mucus, further highlight the relevance of SMIS for studying intestinal infections. Monocytes are chosen as exemplary intestinal immune cells. The interactions between epithelial and immune cells constitute a crucial aspect of the immune response to infection, which are not replicated in conventional single-cell spheroids [39, 40]. We characterized the formed spheroids and compared them with conventional 2D cell cultures and an in vivo model in an infection-dependent context. In this study, spheroids were infected with *Campylobacter jejuni*, a significant zoonotic bacterium utilized in our previous research and selected as an exemplary pathogen. Various infection markers were tested and compared to those of 2D monolayers and in vivo infections. To demonstrate the versatility of the developed protocol, we have extended SMIS to the species mouse (*Mus musculus*) and pig (*Sus scrofa*).

Results

Assembly and characterization of human structured multicellular intestinal spheroids (SMIS)

The objective of this study was to design and characterize novel structured multicellular spheroids resembling the mammalian luminal intestinal surface. Given that most available spheroid models are either homotypic or lack specific structure, we initially experimented with creating a basic version of human SMIS using only primary fibroblasts (NHDF neo) and absorptive enterocytes (Caco-2). In mimicking the intestinal mucosa, fibroblasts first formed a spheric mesenchymal core, which was subsequently colonized with epithelial cells as a monocellular layer and incubated for two days. After only 24 h of culture, the core remained partially uncovered whereas slight structural instability was observed in the spheroids after five days in culture. This led to the decision to focus on the two-day colonization time for further analysis. After successfully generating the basic version, we further enhanced the model by incorporating a colonic goblet cell model (HT-29-MTX-E12) into the outer cell layer using the same protocol. This resulted in the formation of multicellular spheroids.

To characterize and ensure accurate formation of SMIS, immunofluorescent staining (IF) was conducted. Each staining procedure was replicated, with a minimum of 10 spheroids examined in each instance, yielding consistent results to ensure reproducibility. Here, fibroblasts were stained using vimentin, a mesenchymal marker expressed in the fibroblasts core, while adherens junctions between intestinal epithelial and goblet cells were identified by CTNNB1 (β-Catenin) immunostaining. Z-stack microscopy yielded images of different focal layers that revealed significant findings. Predominantly, a monolayer of isoprismatic enterocytes and goblet

cells was observed, arranged around and covering the entire spheric fibroblast core. This configuration facilitated direct contact between the epithelial cell layer and the underlying fibroblasts (Fig. 1A). The successful generation of structured multicellular spheroids facilitated interactions between enterocytes and mesenchymal cells as well as between enterocytes and goblet cells. However, some green-positive cells were visible at the edge of the SMIS. For additional observations, single staining images for each channel are provided in Additional Fig. 1. Finally, we expanded the model to include four relevant intestinal cell types by integrating the monocytic cell line A-THP-1. Immunostaining with Cluster of Differentiation 68 (CD68), a surface protein expressed in monocytes and macrophages, allowed us to visualize the localization of the immune cells (Fig. 1B). The surface areas of the spheroids were completely lined with epithelial cells, goblet cells and monocytes. This arrangement facilitated the development of immune-enterocyte and immune-mesenchymal interactions, in addition to those mentioned earlier. To distinguish between proliferating and non-proliferating cells, SMIS were stained with the proliferation marker Proliferating-Cell-Nuclear-Antigen (PCNA). As depicted, the majority of proliferating cells

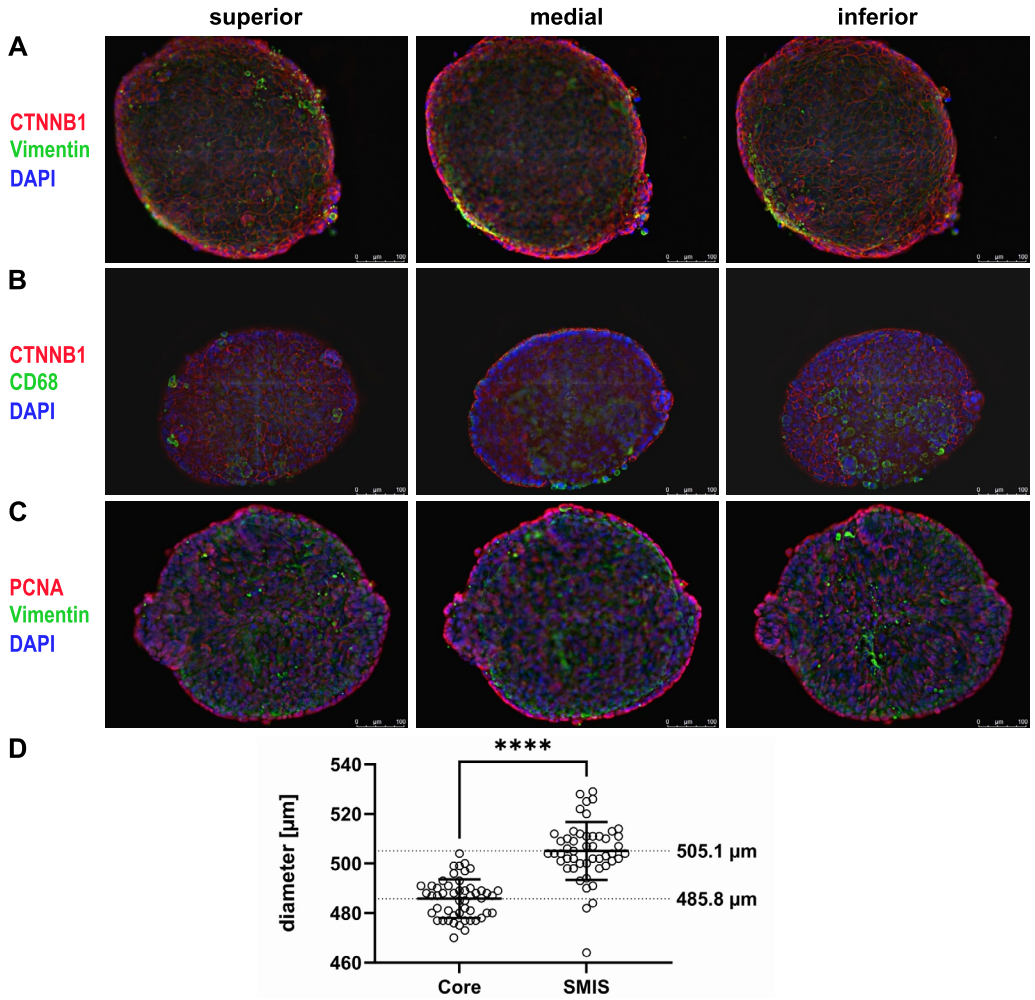

Fig. 1 Structural architecture of human SMIS detected by Immunofluorescence staining and Z-stack projections. **A** Representative images of the localization of vimentin (green), adherens junctions between epithelial and goblet cells (CTNNB1, red) and nuclei (blue). **B** Staining of human SMIS after the implementation immune cells (THP-1) to the model. CD68 is stained green, CTNNB1 red and nuclei blue. **C** To identify active proliferation in the human spheroids, the proliferation marker PCNA was stained red. For a better overview, vimentin was stained green and nuclei blue. For green immunostaining DyLight 488 and for red staining DyLight 594 was used, whereas nuclei were stained blue by DAPI. Scale bars indicate 100 µm (magnification). Exposure time was identical for all spheroids and presented images are representative for 10 biological replicates tested. **D** Diameter distribution of 50 human fibroblast cores and 50 human SMIS. The charts display each individual measurement with mean ± SD (bars)

was detected on the external side facing the environment (Fig. 1C). No proliferation was detected in the fibroblast core.

To evaluate the scalability and of the spheroids as well as standardization of the protocol, we measured the diameter of 50 fibroblast cores and subsequently 50 multicellular spheroids. The fibroblast cores exhibited an average diameter of 485.8 µm (± 7.8 µm), while the multicellular spheroids, featuring an epithelial monolayer, measured 505.1 µm (± 11.7 µm). Data sets of the diameter distribution including standard deviation within the measured population can be found in Fig. 1D. Standardization of SMIS was ensured by utilizing cells from similar passages across all experiments. Our capacity allowed for the formation of up to 180 spheroids simultaneously, with the limiting factor being the availability of cells rather than the spheroid formation process.

Characterization of SMIS by electron microscopy

Next, we conducted a more detailed examination of the surface of the spheroids and their degree of differentiation, exemplified by scanning electron microscopy (SEM) and transmission electron microscopy (TEM). As shown in Fig. 2, the surface of SMIS including goblet cells (Fig. 2A, B) and without goblet cells (Fig. 2C, D) as covered by small, outgrowth structures, potentially identified as microvilli. Microvilli are miniature, uniform, finger-like protrusions of the cell membrane in enterocytes, facing the intestinal lumen. They are regularly ordered to form brush borders, which serve to enhance absorption [41]. In the SEMs of our human model, we observed finger-like protrusions, although they were irregularly arranged and varied in length. These SEM observations suggested that the spheroids exhibited dysplastic (not fully developed) microvilli produced by the Caco-2 cells. Individual cellular membrane protrusions were visible in the TEM images of the SMIS with goblet cells, confirming our observation regarding microvilli and verifying the nature of the finger-like structures as microvilli (Fig. 2E, F). Furthermore, the observed lengths of the microvilli presented here are consistent with the lengths found in vivo, typically ranging from 1 to 3 µm [41]. While the microvilli may not appear densely packed and aligned as they do in vivo, SMIS seem to form a brush border to some extent within 2 days after assembly.

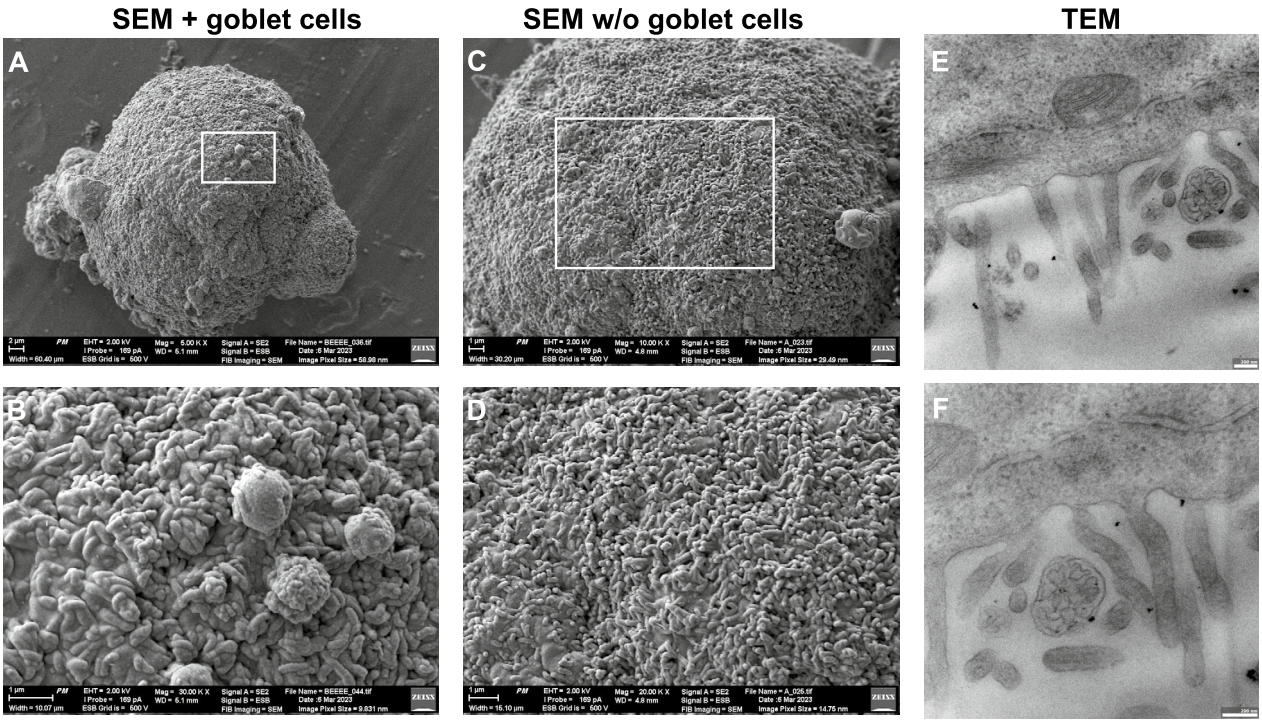

Fig. 2 Scanning and transmission electron microscopy of human SMIS. **A** SEMs display the surface of the spheroids consisting of a fibroblast core, covered by epithelial and goblet cells. Scale bars indicate 2 µM. **B** Higher magnification of the SEMs, scale bars indicate 1 µM. **C** Analysis of the surface of human SMIS with only fibroblasts and epithelial cells by SEM. Scale bars indicate 1 µM. **D** SEMs in higher magnification, scale bars indicate 1 µM. **E** Transmission electron microscopy of the spheroids consisting of fibroblasts, epithelial and goblet cells to identify membrane protrusions proving microvilli formation. Scale bars indicate 200 nm. **F** Higher magnification of the TEMs, scale bars indicate 200 nm

Intestinal epithelial layer in SMIS shows significantly earlier differentiation than conventional 2D cell cultures

The intestinal epithelium of mammals forms a constantly renewing system with proliferating cells at the bottom of the crypts, migrating upward, differentiating into absorbing enterocytes with microvilli that form a brush border [41, 42]. After electron microscopy revealed the formation of microvilli on the surface of the spheroids, we hypothesized that the epithelial cells incorporated into SMIS show earlier differentiation compared to Caco-2 monolayers cultured under the same conditions for two days. To validate this assumption and assess the physiological relevance of the spheroids, we examined the expression of several markers associated with proliferating and fully differentiated epithelial cells in both SMIS and conventional 2D Caco-2 cultures. Epidermal growth factor (EGF) and ephrin B receptor 2 (EPHB2) were chosen as markers for proliferating enterocytes [43–45]. In the 3D model, both markers exhibited a significant approximately five-fold increase in expression compared to the Caco-2 monolayer (Fig. 3A, B). EphrinB1 (EFNB1) and EphrinB2 (EFNB2) were also examined as markers present in differentiated enterocytes. Similarly, mRNA levels of both genes exhibited a significant increase in the spheroids, with *EFNB1* increasing by 3.5-fold ($P \leq 0.01$) and *EFNB2* by 2.7-fold ($P \leq 0.0001$) (Fig. 3C, D). Additionally, to assess the absorptive capacities of Caco-2 cells in both 3D and 2D cultures, we analyzed the expression of sodium-dependent glucose cotransporter 1 (SGLT1) and peptide transporter 1 (PEPT1), solute carrier proteins localized in the brush border of differentiated enterocytes. Our analyses revealed that *SGLT1* was significantly upregulated by 3.9-fold in the spheroids ($P \leq 0.0001$), while surprisingly, *PEPT1* was significantly reduced by 0.64-fold ($P \leq 0.05$) compared to the 2D culture (Fig. 3E, F).

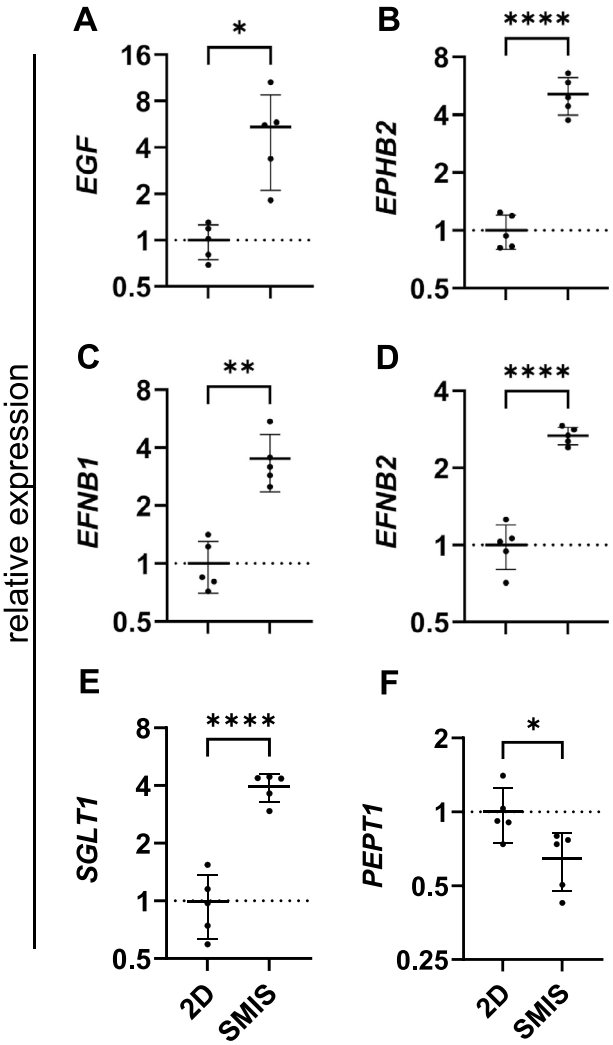

Fig. 3 Relative gene expression of relevant differentiation and proliferation factors of human SMIS compared to Caco-2 monolayers. **A** Expression of the proliferation factor *EGF* is upregulated in the spheroids. **B** mRNA levels of the proliferation marker *EPHB2* are increased in SMIS. **C** Gene expression analysis revealed elevated levels of the differentiation marker *EFNB1* in the 3D model. **D** Intracellular *EFNB2* is upregulated in the spheroids. **E** Absorptive capacities of the SMIS were assessed by increased *SGLT1* expression. **F** As the only downregulated factor, *PEPT1* levels were decreased in the 3D intestinal model. All expressions were relatively calculated to 2D Caco-2 monolayers and normalized with HPRT, PPIB and B2M. Charts show mean ± SD (bars) of each sample in triplicate measurements with five biological replicates. For each SMIS sample, 15 spheroids were pooled. Statistical significance is presented by asterisks compared to 2D monolayers. *$P \leq 0.05$, **$P \leq 0.01$, ****$P \leq 0.0001$, unpaired t-test

Application of human SMIS for infection biology compared to 2D monolayers

While there are several suitable 3D intestinal infection models available, they are labor-intensive and have limited scalability. In vivo animal models are still widely used but raise ethical concerns and are complex in nature. Following the 3R principles, we investigated whether SMIS could serve as a suitable infection model for intestinal campylobacteriosis, aiming to reduce and replace the use of animal models. Therefore, we have implemented infection assays as a functional assay in this study. Moreover, we compared our results with those obtained from conventional Caco-2 monolayers. To achieve this, we selected various immunological and infection-related markers based on our previous studies [46, 47]—categorized into subgroups: 'Regulation of the Immune Response' (NFKB1, NFKB2, HLA-G, HLA-DMA, EGFR, TLR2, TLR5), 'Cytokine Response' (CCL2, IL1a, IL1b, IL6, IL8, IL10, IL12a, IL18, IFI6, IFNGR1, TNFA), 'Apoptosis'

(TP53, BAX, BCL2, CASP3, CASP7), and '*C. jejuni*-related' (ST3GAL1, B4GALT1)—and analyzed them using gene expression analysis. The markers related to *C. jej ni* infections were identified and published in our previous studies [48, 49]. To determine underlying differences between the models, we first investigated these infection markers in the conventionally cultured Caco-2 monolayers (Fig. 4A). In infected Caco-2 monolayers, only six factors were significantly regulated possessing a foldchange below 0.5- or higher than twofold compared to their naïve counterpart. Most significantly regulated were *IL12a* (19-fold increase, $P \leq 0.0001$), *IFI6* (0.25-fold decrease, $P \leq 0.0001$) and *ST3GAL1* (2.5-fold increase $P \leq 0.001$). We then compared the infection markers in SMIS infected with *C. jejuni* compared to naïve SMIS. Gene expression analysis revealed 11 significantly regulated targets possessing a foldchange below 0.5- or higher than twofold compared to non-infected controls (Fig. 4B). Interleukins *IL6* (59-fold, $P \leq 0.0001$), *IL8* (53-fold, $P \leq 0.0001$), *IL1*a (42-fold, $P \leq 0.0001$) and *IL1b* (25-fold, $P \leq 0.0001$) showed the most strikingly increased foldchanges. In addition, mRNA levels of *ST3GAL1*

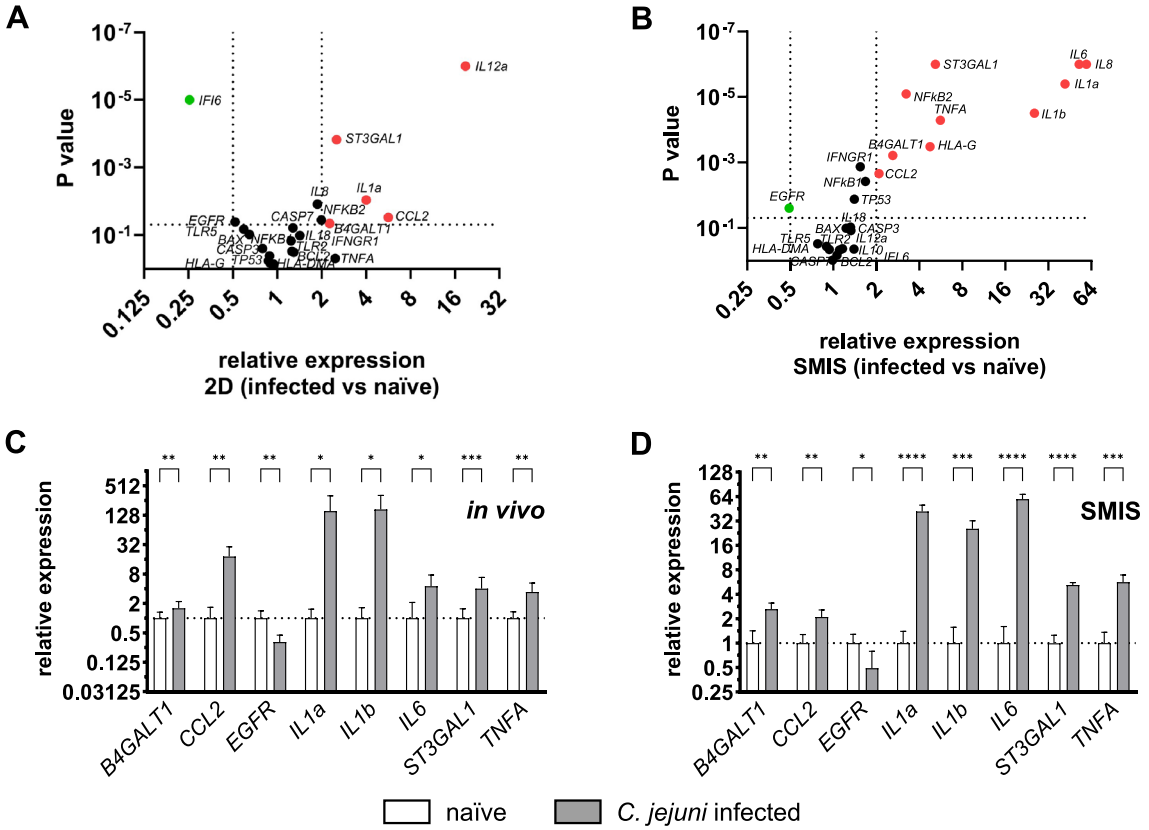

Fig. 4 Gene expression analysis of immunological markers in human SMIS compared to single Caco-2 monolayers and to murine in vivo samples. **A** Volcano Plot of differently expressed immunological genes in *C. jejuni* infected compared to naïve Caco-2 cells. Only six factors are significantly regulated in infected monolayers, highest upregulation can be detected in *IL12a* whereas downregulation in *IFI6*. Expressions were relatively calculated to naive 2D controls. **B** Gene expression analysis of the immunological factors in *C. jejuni* infected SMIS, relatively calculated to naïve SMIS and presented in a Volcano Plot. Intracellular mRNA levels of eleven factors are significantly regulated in the infected samples. Most dominantly upregulation can be detected in the interleukins *IL8*, *IL6*, *IL1b* and *IL1a* whereas only levels of *EGFR* are significantly decreased. The infection experiments were conducted once, consisting of five independent biological replicates. Expressions of all targets shown in the volcano plots are normalized by HPRT, PPIB and B2M. Marked in red are all significantly regulated factors that are upregulated by two or more and in green all factors that are downregulated by 0.5 or less. Dots in the plots show the mean of all samples (n = 5) in triplicate measurements for five biological replicates. For each 3D sample, 15 SMIS were pooled. For statistical significance, unpaired t-tests were performed. **C** Relative gene expression of the significantly regulated immunological factors murine *C. jejuni* infected colonic tissue samples. All factors that are significantly upregulated in 3D are also significantly increased in the in vivo samples whereas mRNA levels of *EGFR* are significantly decreased in both. **D** Gene expression analysis of significantly regulated immunological factors in infected 3D SMIS. Bars show mean + SD of all samples (n = 5 for the spheroids and n = 19 in the colonic tissue samples) in triplicate measurements. For each 3D sample, 15 SMIS were pooled. Statistical significance is presented by asterisks. *P ≤ 0.05, **P ≤ 0.01, ***P ≤ 0.001, ****P ≤ 0.0001, unpaired t-test

(fivefold, $P \leq 0.0001$), *NFKB2* (threefold, $P \leq 0.0001$) and *TNFA* (sixfold, $P \leq 0.0001$) were strongly increased. Only *EGFR* was significantly downregulated by a factor of 0.5 ($P \leq 0.05$). We also analyzed differences in the expression of the targets in SMIS compared to 2D under naïve conditions as well as after *C. jejuni* infection. Numerous genes from all categories exhibited differential regulation in the spheroids compared to their 2D counterparts (Additional Fig. 2). Immunological markers were more prominently expressed in SMIS than in 2D. Nevertheless, the regulation of *IL18* (0.45-fold, $P \leq 0.001$) was significantly reduced in the spheroids.

Overall, the amplitude of regulations was notably more pronounced in SMIS for most factors than for the naïve counterparts. Additionally, a greater number of infection-relevant markers were regulated in 3D compared to 2D, highlighting the advantage of utilizing SMIS as suitable infection models over 2D monolayers.

The infection data obtained from human SMIS closely resemble those observed in the murine in vivo model of human campylobacteriosis

To evaluate the potential of the human SMIS to reduce and replace animal studies as infection models, we compared the SMIS infection results to those obtained from *C. jej ni* infected murine colonic tissue samples. These murine samples were derived from a specific mouse model of human campylobacteriosis, as described in our previous study [49]. Naïve colonic tissue samples were utilized as controls. We focused on significantly regulated genes with a foldchange below 0.5 or higher than two from the previously mentioned infected versus naïve SMIS analysis. Consistent with the 3D results, *B4GALT1*, *CCL2*, *IL1a*, *IL1b*, *IL6*, *ST3GAL1* and *TNFA* were also significantly upregulated in the infected murine samples compared to their naïve counterparts except of *EGFR*, which was also downregulated (Fig. 4C). Highly upregulated expression was observed in both models in *IL1a* and *IL1b* (Fig. 4C, D). *IL8*, *NFKB2* and *HLA-G* were excluded from the analysis: *IL8* was below the detection limit in the in vivo samples, *NFKB2* showed no regulation, and *HLA-G* was not expressed in mice.

The SMIS model can be adapted to the mouse and pig species

To evaluate reproducibility, we expanded the application of SMIS to mouse and pig species, demonstrating that a basic version of the human spheroid protocol can be universally applied across other species as well. Here, we assembled a fibroblast core and lined it solely with intestinal epithelial cells. For the murine model, we initially utilized NIH-3T3 embryonic fibroblasts to form the fibroblast core and employed the murine intestinal epithelial cell line CMT-93 to line the core. To characterize the spheroids, we stained them using IF with vimentin and CTNNB1 (Additional Fig. 3). In the nearly round spheroids, a prominent CTNNB1 signal was observed, indicating the fast formation of adherens junctions between CMT-93 cells that coated the entire surface of the murine SMIS. However, there was a weak vimentin signal detected in the core. For a more detailed examination, we further analyzed the spheroids using scanning and transmission electron microscopy (Fig. 5A). Similar to human electron micrographs, the murine spheroids with the NIH-3T3 core exhibited small, uneven microvilli-like membrane protrusions on the surface. However, in the murine spheroids, these finger-like protrusions appeared less irregular and displayed a more structured arrangement. Upon imaging at higher magnification, it became evident that these finger-like protrusions were composed of bundles of filaments, resembling the structure of microvilli. After successfully generating murine SMIS, we enhanced the model by substituting NIH-3T3 with primary intestinal myofibroblasts (pMF) isolated from murine colon tissue. Immunofluorescence staining revealed perfectly round-shaped spheroids. A strong vimentin signal in the pMF-core and CTNNB1 signal in the surrounding epithelial cells uncovered a monolayer of prismatic CMT-93 cells attached to the myofibroblasts (Fig. 5B). TEM images of the mouse SMIS with the pMF core showed regular membrane protrusions from the epithelial cells, identified as microvilli (Fig. 5C).

To extend the model for comparative studies related to zoonotic pathogens, porcine spheroids were generated using primary porcine colonic myofibroblasts [50] and the widely used porcine enterocyte cell line IPEC-J2. Characterization was performed using immunostaining of vimentin and CTNNB1. In the round-shaped spheroids, the adherens junctions revealed a complete enterocyte layer lining the myofibroblast core (Fig. 5D). However, only weak vimentin signal was detected, and it did not appear to be present evenly. Additionally, some epithelial cells seemed to be only partially connected to the core; vimentin artefacts due to spheroid fixation were visible.

Discussion

In recent years, 3D cell culture has rapidly advanced and is now widely used in various biological research areas, showing promising outcomes. These models closely mimic animal and human tissue, aiding in reducing animal model usage. In our study, we developed advanced 3D cell cultures (SMIS) for human, mouse, and pig species. We characterized these spheroids using various microscopy techniques and compared them to traditional intestinal 2D cell cultures (Caco-2 cells). We also tested

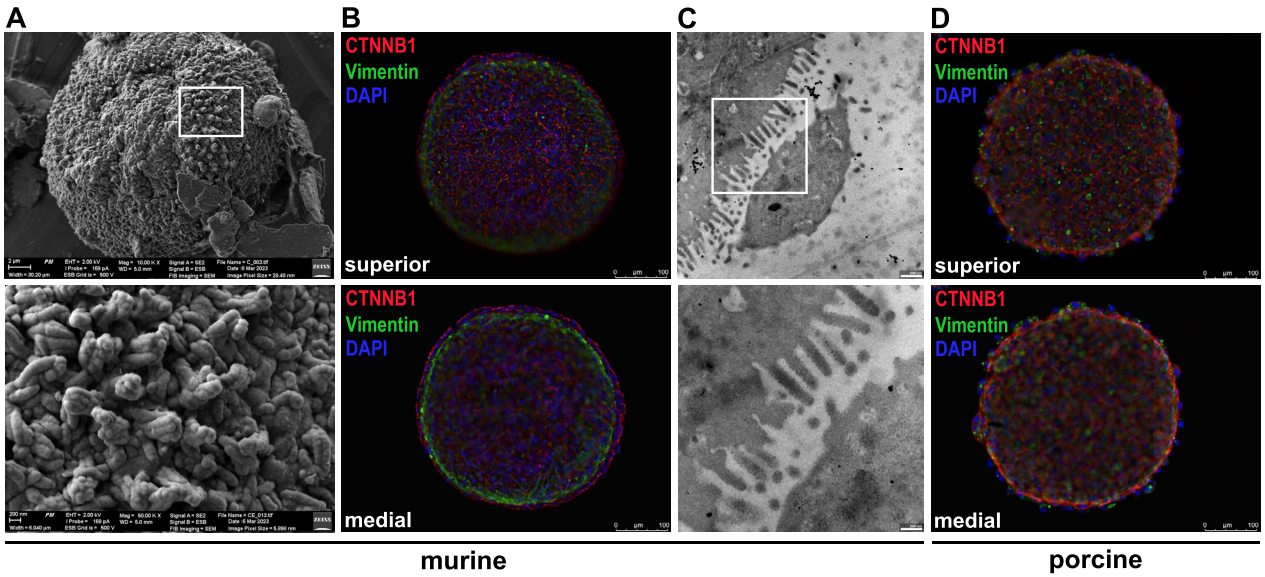

Fig. 5 Characterization of murine and porcine SMIS. **A** Analysis of the surface of the murine SMIS, implementing embryonic fibroblasts (3T3) and epithelial cells (CMT-93) by scanning electron microscopy at two different magnifications. Higher magnification images identify membrane protrusions. Scale bar of the upper image indicates 2 µm while the lower displays 200 nm. **B** Immunostaining of superior and medial z-stack projections of murine spheroids consisting of a primary colonic myofibroblast (pMF) core (vimentin, green) and intestinal epithelial cells (CMT-93, CTNNB1, red). Nuclei are stained blue. **C** TEMs display the surface of the spheroids consisting of murine primary intestinal myofibroblasts (pMF) and epithelial cells (CMT-93) to identify membrane protrusions proving ordered microvilli formation. Scale bars of the upper image indicate 500 nm and of the lower image 200 nm. **D** Representative images of superior and medial z-stack projections of porcine SMIS. Localization of primary colonic fibroblasts is shown by immunostaining using vimentin (green) whereas epithelial cells by adherens junctions (IPEC-J2, CTNNB1, red). Scale bars indicate 100 µm. For green immunostaining DyLight 488 and for red staining DyLight 594 was used, whereas cell-nuclei were stained blue by DAPI in all IFs. Exposure time was identical for all spheroids and presented images are representative for three biological replicates tested

the spheroids' response to *C. jejuni* infection, comparing them to infected 2D cultures and in vivo data. This analysis aims to determine if 3D cultures could replace 2D models and serve as effective alternatives to animal testing.

Numerous methods exist for generating spheroids, including liquid overlay, hanging drops, microfluidics, or utilizing ultra-low attachment (ULA) plates [51–53]. Additionally, spheroids can be embedded in an extracellular matrix or cultured free-floating. Following an evaluation of various methods for forming the SMIS and considering factors such as cell seeding, spheroid formation, morphology, and reproducibility, we decided to utilize ULA plates with free-floating and modular self-assembling cellular aggregates in culture, which we were able to structure in a given order. This approach enabled the development of human SMIS, comprising a fibroblast core (NHDF neo) surrounded by a monolayer of enterocytes (Caco-2), goblet cells (HT-29/MTX-E12), and activated monocytes (A-THP-1), which completely lined the core. Nearly every cell on the outer layer made direct contact with the underlying fibroblasts. This achievement is noteworthy and has not been reported previously. In other studies involving multicellular spheroids, formation is achieved by simply mixing different cell types together without any directed organization [54, 55]. Further, in Kapałczyńska et al., for instance, the authors noted that, in their experience, cells of different phenotypes, such as fibroblasts and epithelial cells (as well as monocytes), did not integrate and form 3D structures together [1]. Moreover, the direct contact between enterocytes and other surrounding cell types facilitates not only epithelial-mesenchymal but also epithelial-immune cell interactions. Our intestinal model successfully integrates four important cell types to mimic the microarchitecture of the luminal intestinal surface as in the intestine, both epithelial cells and monocytes interact directly with mesenchymal cells of the Lamina propria. Simultaneously, relevant functional features such as microvilli formation are incorporated in SMIS. Caco-2 cells, in particular, exhibit a high degree of morphological and physiological similarity to the human intestinal epithelium. They are capable of forming a brush border, expressing typical metabolic enzymes, and efflux transporters [56, 57]. In 2D monolayers, these cells begin differentiation after seven days in culture and complete the process within 21 days [56, 58]. Notably, in our model, Caco-2 cells in contact with the mesenchymal core formed microvilli within

just two days, as observed through scanning and transmission electron microscopy, rendering the spheroids a valuable model. Additionally, in contrast to our results, other studies have shown, that homotypic Caco-2 spheroids cultured for two to five days form round structures with a continuous smooth surface without microvilli [38]. This leads us to conclude that these mesenchymal-epithelial and mesenchymal-monocyte interactions are crucial factors driving the accelerated differentiation of enterocytes and the development of essential intestinal features, such as microvilli, within just two days of culture. In contrast, achieving full differentiation of Caco-2 cells for example requires up to 14 days when cultured in 2D [59].Apart from that, it's worth noting that intestinal organoids typically require 5–7 days to differentiate, emphasizing the time-efficiency of our model compared to both 2D and other 3D cell culture models [11]. We made the decision to culture the spheroids for only two days following the addition of enterocytes, goblet cells, and monocytes to minimize the occurrence of necrosis in the core caused by nutrient and oxygen deprivation. We observed slight structural instability in the spheroids after five days, likely due to necrotic processes within the spheroid [60, 61]. Unlike 2D monolayers, where cells receive uniform access to oxygen and nutrients, 3D spheroid models more accurately replicate the limited supply of these resources found in living tissues, particularly in the core. This constrained environment provides a more realistic simulation of physiological conditions, making the 3D model a more representative in vitro system [62].

The mammalian intestinal epithelium comprises various specialized types of proliferating and differentiated cells essential for maintaining intestinal functions. Proliferating cells located at the bottom of the crypts migrate upwards and undergo progressive differentiation into mature absorptive enterocytes. Genes such as *EGF* or *EPHB2* are predominantly expressed in undifferentiated, proliferative cells at the crypt base. EGF stimulates proliferation through growth factor signaling, while EPHB2, as a target of the Wnt-signaling pathway, regulates cell migration and proliferation upon activation by ligands [63–65]. Conversely, an opposing gradient in the expression of EPHB2 ligands, EFNB1, and EFNB2, can be observed. They exhibit high expression in differentiated cells of the upper parts of the crypt, particularly at the crypt-villus junction, which decreases towards the crypt base [64, 66]. We analyzed these four markers in SMIS and compared them with Caco-2 monolayers cultured for two days. *EFNB1* and *B2* exhibited significantly increased expression in the spheroids, suggesting a higher degree of differentiation in the intestinal cells of our spheroid model. However, *EGF* and *EPHB2* were also upregulated, indicating typical cell proliferative properties. This conclusion is further supported by the confirmed formation of microvilli, which are characteristic features of differentiated enterocytes. Thus, the enterocytes in the SMIS model achieve a higher degree of differentiation while simultaneously promoting proliferation, a combination that is typically challenging to attain within the same in vitro culture system. This underscores the advancement of the spheroids over 2D monolayers. The elevated proliferation of *EGF* and *EPHB2* found in SMIS may suggest that longer culture periods could be supported. However, as noted above, the structural instability after five days indicates that factors such as limited nutrient and oxygen diffusion might limit prolonged viability, despite active proliferation of the outer layer. A more detailed investigation into how SMIS simultaneously facilitates enhanced differentiation and increased proliferation will be addressed by our future studies.

To assess the absorptive capacities of the enterocytes in SMIS, we analyzed the expression of two transporters, the monosaccharide transporter *SGLT1* and the peptide transporter *PEPT1*. Both transporters are typically localized at the brush border of differentiated and absorptive enterocytes. [67, 68]. As expected, *SGLT1* expression was significantly upregulated in the spheroids compared to Caco-2 monolayers. However, *PEPT1* was significantly downregulated. This regulation might be attributed to increased EGF levels, as studies have shown that EGF can influence the expression of *PEPT1* [69, 70]. Although EGF treatment was not administered to Caco-2 cells in our study, considerable increase in *EGF* levels potentially provided by the fibroblast core could yield a similar effect. In the crypts, proliferation relies on various stimuli from the neighboring microenvironment, known as the niche. Studies have demonstrated that in the colon, intestinal mesenchymal cells establish an extra-epithelial niche by sustaining stimuli, including signals from EGF, Notch, and Wnt [71]. This may account for the increased expression of *EGF* and the subsequent reduction of *PEPT1* in SMIS. Nevertheless, we assert that the 3D co-culture model presented here exceeds conventional 2D models in sophistication, not solely in terms of the degree of differentiation. Taken together, the spheroids could serve as a novel and standardized research model not only for infection biology but also for other exposure studies. In addition to differentiation, the polarity of epithelial cells also plays a crucial role and directly impacts their physiology. The epithelial tissue of the mammalian intestinal mucosa is characterized by a simple, highly prismatic, columnar epithelium with a brush border containing microvilli on the apical side. We consistently observed a single layer of epithelial cells surrounding the spheroid core. Additionally, we observed cell–cell interactions between epithelial cells and the formation of

microvilli exclusively at the apical side of the spheroids, highlighting the similarity to the luminal intestinal surface. However, given that SMIS are cultured for only two days, we were unable to detect columnar enterocytes as seen in vivo; instead, they exhibited a more isoprismatic shape. Investigating whether the morphology of enterocytes transitions to a more columnar shape with longer culture durations would be a stimulating point to explore in future studies. Moreover, the green-positive cells observed at the edge of the SMIS indicating vimentin expression, may suggest epithelial-to-mesenchymal transition (EMT). This could be attributed to a not fully differentiated status of the epithelial layer.

To assess SMIS as a suitable 3D infection model, we have implemented infection assays as a functional assay and infected the spheroids to investigate pathogen-epithelial interactions that were compared to our earlier in vivo studies [48, 49]. In intestinal infections, the initial tissue layers affected are the luminal layers of the mucosa, including the *Lamina epithelialis mucosae* and *Lamina propria mucosae*. Given that our model mimics these intestinal layers, the spheroids provide optimal conditions for an intestinal infection model. Moreover, the four cell types utilized have been demonstrated to be relevant for infection processes [72–75]. Our research and previous work [48, 49] has focused on the regulation of the molecular host cell response to infection, for which we initially developed a simpler 2D model. While conventional experiments on pathogen adhesion, invasion, and replication can still be effectively conducted using standard 2D cultures, the microarchitecture of SMIS, including the mesenchymal core, offers a unique opportunity to investigate cellular communication, transmigration and dissemination through subepithelial tissue. In this study, we focused on *C. jejuni* as an exemplary model pathogen. This choice is based on our prior studies involving this zoonotic pathogen, as well as the availability of in vivo infection samples for evaluation of SMIS and quality control [48, 49, 76]. Nonetheless, we are confident that the developed model will also be applicable to other bacterial pathogens.

We compared *C. jejuni*-infected SMIS to the naïve SMIS. In total, 10 immunological markers showed significant upregulation in the infected SMIS, with the highest levels observed in pro-inflammatory cytokines such as *IL1a*, *1b*, *6*, *8*, *TNFA* and *CCL2*. These cytokines play crucial roles in modulating cell-mediated immune responses following infection [77]. They orchestrate immune cell recruitment to the infection site, facilitating the control and elimination of intracellular pathogens such as *C. jejuni* through inflammation [78]. The upregulation of the investigated cytokines can thus be considered a representative defense mechanism of the SMIS against infection, a finding that has been investigated and published in numerous studies [79–82]. However, when comparing infected and uninfected Caco-2 monolayers, these findings may not be directly applicable. Among the six cytokines mentioned earlier, only *IL1a, IL12a* and *CCL2* show significant upregulation, albeit with a lower overall expression amplitude. The broader range of immunologically regulated factors with their intricate molecular mechanisms underscores the superiority of SMIS as an infection model over conventional 2D monolayers. Furthermore, all factors that are significantly upregulated in infected 2D model are also significantly increased in infected 3D models, but the reverse is not observed. The only exception is *IL12a* which is upregulated in the 2D but not in the spheroids. IL12a is predominantly expressed by macrophages and induces the cytolytic activity of immune cells. Yet, no studies have shown regulation of the cytokine in Caco-2 cells though an upregulation after *C. jejuni* infection was assessed before in human dendritic cells [82]. Increase of intracellular ST3GAL1 and B4GALT1 were detected in both infected 2D and 3D and supports our previously published data [49]. Only mRNA levels of *EGFR* are significantly downregulated in infected spheroids. The EGFR signaling pathway may play an important role in *C. jejuni* infection. Fibronectin-binding proteins from *C. jejuni* have been shown to activate the EGFR signaling pathway in host cells [83]. This activation leads to the Rho-GTPase CDC42-dependent formation of host cell membrane protrusions and is associated with increased invasion of *C. jejuni* [84]. Therefore, we hypothesize that the observed downregulation serves as a defense mechanism employed by the cells to impede pathogen invasion. We also compared non-infected human SMIS with Caco-2 monolayers and found upregulation of interleukins, TNFA, and ST3GAL1 in SMIS. This enhanced abundance of immunological markers suggests advantages from monocytic cell integration and intercellular interactions, underscoring the benefits of utilizing structured multicellular spheroids as a model system. We selected Caco-2 monolayers as a control for our SMIS model because they represent the traditional and widely used in vitro approach in intestinal infection biology. The added complexity of spheroids response to infection underscores the advantages of our model.

To evaluate how closely the molecular SMIS response mirrors in vivo infection and its potential to replace animal experiments, we compared our data with those from a murine model of human campylobacteriosis. This model was selected due to the limited availability of in vivo human samples, its extensive use in prior studies, and its suitability for comparing the immunopathological features of acute campylobacteriosis in humans

with those observed in SMIS. For this analysis, we utilized cDNA from murine colon samples infected with *C. jejuni*, obtained from a previous study [49]. All immunological markers in the infected spheroids that were expressed in mice and had a significant upregulation more than two-fold (B4GALT1, CCL2, IL1a, IL1b, IL6, ST3GAL1, TNFA) were tested in *C. jejuni* infected colon samples and compared to naïve counterparts. All representative factors exhibited significant upregulation in the infected in vivo samples, indicating a close resemblance between the reported 3D infection model and the in vivo model. The gene expression patterns of numerous important immune factors mirror those observed in the animal experiment, highlighting the disparity with 2D monolayers. Additionally, we analyzed *EGFR*, the sole downregulated factor in the spheroids, which also showed downregulation in the colonic samples of infected mice. Based on these findings, we conclude that SMIS serve as an excellent model for studying intestinal infection biology, can be produced in a standardized and scalable manner, and are evidently superior to conventional monolayers. Furthermore, the comparable results from SMIS and the murine model of human campylobacteriosis suggest that SMIS not only represents gene expression patterns but also accurately reflects the functional aspects of the infection.

The core concept of our approach was to utilize readily accessible and expandable components, thus, we mainly used immortalized cell lines. Additionally, SMIS offer the advantage of growing in suspension, facilitating collection and fixation for downstream analyses such as IF, SEM or TEM. This offers a distinct advantage over other models, which e.g. involve feeder layers adhering to the culture flask, or two-compartment cultures that prevent direct physical contact between mesenchymal and epithelial cells. In our human model, we employed NHDF neo cells to establish the fibroblast core. However, previous research has pointed out genetic disparities between gastrointestinal and non-gastrointestinal fibroblasts. As NHDF neo cells are a human dermal fibroblast cell line, they might not precisely represent intestinal myofibroblasts [85]. Given the limited accessibility of human intestinal myofibroblasts, we optimized and adapted our model by incorporating murine and porcine primary myofibroblasts instead. Notably, the murine SMIS with a pMF core exhibited significantly enhanced differentiation of the epithelial layer with the same culture conditions as shown in the TEM images and immunofluorescence analyses. While the enterocytes in the human SMIS rapidly developed partly ordered microvilli, the murine SMIS with the pMF core exhibited more regular and ordered microvilli, making them more comparable to in vivo structures. Consequently, future studies should consider employing primary intestinal myofibroblasts also for human SMIS to enhance the model's physiological relevance. Moreover, we plan to incorporate monocytes into the spheroid core to better resemble intestinal microarchitecture. It's important to note that while the production of spheroids may be more labor-intensive compared to conventional 2D cell culture, they offer a unique level of complexity. Despite this, they are easy to reproduce, require less time, and are more cost-effective than organoids, other 3D models, or in vivo models, while still yielding comparable readouts.

As a versatile model, mammalian SMIS are not restricted solely to the study of bacterial infections; they hold potential for a wide range of scientific investigations. Particularly in the realm of nutrient absorption studies, this model offers practical utility due to its structural similarity to the luminal surface of mammalian intestinal organs, optimized cell differentiation, and the formation of microvilli. It is presumed that these characteristics contribute to improved absorptive properties of SMIS compared to traditional 2D cell cultures. Additionally, SMIS can prove beneficial in the examination of intestinal viral infections, pharmacological drug permeability and development, as well as toxicity testing. Certainly, the model holds the potential for expansion to mimic other organs by adjusting the cell types used to reflect the specific characteristics of the organ of interest. This adaptability opens doors for exploring various organ systems and their functions in a more physiologically relevant context. Indeed, our findings indicate the feasibility of extending the model to other species such as mice and pigs, thereby presenting numerous opportunities for its application. The reproducibility of the protocol for different species was successfully validated using different cell lines, providing consistent and reproducible results. Furthermore, our results also show the scalability of the protocol, which makes the use of the model suitable for medium-throughput.

Adhering to the principles of Reduction and Replacement outlined in the 3Rs framework, our mouse model can serve as a valuable tool for studying various pathological processes. Moreover, the mouse model offers the possibility of employing cell manipulation techniques to modify cellular responses, thereby enhancing its relevance and comparability for basic human and animal science. Pigs represent a promising model for investigations into nutrition and absorption, given the ecological and economic significance of these aspects in animal husbandry. Extensively studied for their physiological similarity to the human intestine and various analogous disease mechanisms [86], pig models offer valuable insights. However, differences in susceptibility to zoonotic pathogens present numerous molecular bases

that we can explore using this model to translate preventive measures to humans. These attributes render them invaluable tools for advancing research and developing new therapeutic strategies.

In summary, we have successfully created structured multicellular intestinal spheroids for humans, mice, and pigs, that are fully standardized and scalable mimicking the luminal surface of the intestine in mammals. These spheroids exhibit typical intestinal traits observed in both differentiated and proliferating enterocytes. Among their diverse applications, SMIS represent an advanced model for investigating infection biology, yielding superior outcomes compared to conventional monolayers and demonstrating similarity to in vivo models.

Conclusion

The aim of the study was to develop structured multicellular intestinal spheroids (SMIS) tailored for studying molecular basis of intestinal pathogenic infections. These innovative spheroids mimic the microarchitecture of the human intestinal mucosa by comprising four relevant cell types. For that, a fibroblast core is enveloped by an outer monolayer of enterocytes and goblet cells together with monocytic cells. These SMIS effectively emulate the in vivo architecture of the intestinal mucosal surface and manifest differentiated morphological characteristics within a mere two days of culture. By analyzing various aspects, we have shown that these spheroids attain heightened levels of differentiation compared to 2D monolayers. Moreover, SMIS serve as an optimized infection model to study intestinal pathogens like *Campylobacter jejuni*, surpassing the capabilities of traditional 2D cultures, and exhibit a regulatory pattern of immunological markers similar to in vivo infections. Remarkably, our protocol extends beyond human spheroids, demonstrating adaptability to other species such as mice and pigs.

Materials and methods

Cell lines and culture conditions

All cell lines were cultured in a humidified atmosphere at 37°C and 5% CO_2. The human intestinal epithelial cells Caco-2 (DSMZ ACC 169) as well as the human colonic goblet cell model HT-29/MTX-E12 (ECACC 12040401), the murine intestinal cell line CMT-93 (ECACC 89111413), the murine primary colonic myofibroblasts (pMF), the murine embryonic fibroblast cell line NIH-3T3 (DSMZ ACC 59) and the porcine primary colonic myofibroblasts [50] were maintained in Dulbecco's Modified Eagle's Medium (DMEM) with 4.5 g/l Glucose and L-Glutamine (Gibco, Grand Island, NY, USA). The human dermal fibroblasts from the neonatal foreskin NHDF neo (Lonza, CC-2509) and porcine intestinal enterocytes IPEC-J2 (DSMZ ACC 701) were cultured in Gibco Dulbecco's Modified Eagle Medium: Nutrient Mixture F12 (DMEM: F12) with GlutaMAX supplement (Gibco) and an adherent subclone of the human monocyte-like cell line A-THP-1 [87] in RPMI Medium 1640 (Gibco) with 100×HEPES (Carl Roth GmbH+Co. KG, Karlsruhe, Germany) and 10×Sodium pyruvate (Sigma-Aldrich, Darmstadt, Germany). All media were supplemented with 10 µg/ml Gentamicin (Sigma-Aldrich) and 10% (v/v) fetal calf serum superior (Sigma-Aldrich). The cells were grown in 75 cm^2 tissue culture flasks (Sarstedt, Nümbrecht, Germany) until approximately 80% confluence was reached. All cell lines were authenticated and recently tested for contaminations.

Isolation of murine and porcine primary colonic myofibroblasts

The porcine intestinal myofibroblasts (clone #163) used in this study were isolated and described earlier [50]. Murine intestinal myofibroblasts (pMF) were isolated from wild-type NMRI mice by outgrowth culture using the porcine protocol [50] adjusted to the murine model. The murine colon tissue used for the isolation of pMF in this study was provided as excess material obtained from dissections conducted for teaching purposes at the OSZ Lise Meitner according to the European Guidelines for animal welfare (2010/63/ EU) following agreement by the commission for animal experiments headed by the "Landesamt für Gesundheit und Soziales" (LaGeSo, Berlin, registration number E0073/22). Colonic tissue was washed with warm medium (DMEM with 4.5 g/l Glucose and L-Glutamine, Gibco), supplemented with 10 µg/ml Gentamicin, 0.25 µg/ml Amphotericin B, 100 U/ml Penicillin and 100 µg/ml Streptomycin (Sigma-Aldrich). The lumen was cut open and the mucosa gently scraped off with a scalpel. The tissue was cut into small pieces (2×2 mm) and ead on a petri dish (Sarstedt). The dish was then filled with medium until the tissue was covered. The sections were then incubated at 37°C and 5% CO_2. Medium was changed every 2–3 days. After approximately 4–5 days, first cells that morphologically looked like fibroblasts grew out of the tissue onto the plate. After the cells reached 80% confluence, they were transferred in a 75 cm^2 tissue culture flasks (Sarstedt) and cultivated further.

Characterization of murine primary colonic myofibroblasts

To identify whether the outgrown cells are in fact myofibroblasts, they were characterized by immunofluorescent staining of vimentin, a structural protein in mesenchymal cells, as well as alpha smooth muscle actin (α-SMA), a multifunctional protein of smooth muscle cells as described earlier [50]. Briefly, 5×10^4 cells were seeded in each well of an 8-well cell culture chamber

slide (Sarstedt) and incubated for two days. They were then fixed for 15 min at room temperature with Roti-Histofix (4% formaldehyde, Carl Roth). After blocking for 2 h at room temperature using 5% goat serum (v/v, Cell Signaling Technology (CST), Danvers, MA, USA) in phosphate-buffered saline (PBS, ROTIFair PBS 7.4, Carl Roth), the primary antibodies vimentin (Dako, Agilent Technologies, Waldbronn, Germany) and α-SMA (PROGEN Biotechnik GmbH, Heidelberg, Germany), were applied and incubated overnight. The next day, the cells were incubated with the matching secondary antibodies for 2 h at room temperature. Dilutions of all primary and secondary antibodies can be found in Additional Table 4 and 5. After three washes with PBS, the myofibroblasts were mounted on the glass microscope slide of the chamber slide in 50% glycerol in ddH_2O. Immunostainings of the pMF can be found in the Additional Fig. 6.

Assembly of SMIS

In order to generate ultra-low attachment surfaces for spheroid formation, suspension round-bottom 96-well cell culture plates (Sarstedt) were coated with Anti-Adherence Rinsing Solution (AARS, STEMCELL Technologies, Cologne, Germany, #07010) overnight at room temperature and washed with PBS the next day. For human SMIS, a core of fibroblasts was formed by using 5×10^3 NHDF neo seeded on the coated wells and incubated for one day at 37°C and 5% CO_2. The next day, 8×10^2 Caco-2, 1×10^2 HT-29/MTX-E12 and 1×10^2 A-THP-1 were added to each well and observed under the microscope after two, four and six hours. When the cells were not arranged uniformly around the core, the cells were stirred up again using a pipette. The spheroids were then incubated for two days. For the murine intestinal spheroids 5×10^3 pMF or 5×10^3 NIH-3T3 were seeded on the AARS coated wells and incubated overnight. The next day, 1×10^3 CMT-93 were added and multicellular spheroids formed after two days. For the porcine intestinal spheroids, 5×10^3 porcine primary colonic myofibroblasts were firstly incubated for one day for the core and then 1×10^3 IPEC-J2 were added and incubated for two days.

Immunofluorescent staining of SMIS

Spheroids were fixed for 45 min at room temperature using Roti-Histofix (4% formaldehyde, Carl Roth). After three washes with PBS, antigen retrieval was carried out using a citrate buffer (10 mM sodium citrate dihydrate, 0.05% (v/v) TWEEN 20, pH 6) for 20 min at 97°C on a heating block. After switching off the heating block, the spheroids remained in the cooling block for a further 20 min. Subsequent steps were carried out at room temperature. The spheroids were then blocked for 3 h on a roller mixer using a blocking buffer (PBS with Triton-X-100 (1% v/v) and 5% goat serum (v/v) (CST)). They were then stained with the primary antibodies vimentin (Dako), CTNNB1 (Cell Signaling), CD68 (Novus Biologicals, bio-techne, Minneapolis, MN, USA) and PCNA (Abcam, Cambridge, UK) overnight. After the aspiration of the primary antibody solution and three washes with PBS, incubation of the secondary antibody solution (Thermo Fisher Scientific, Waltham, MA, USA, DyLight 488 goat-anti mouse; DyLight 594 goat anti rabbit) for three hours followed with three additional washes using PBS. Dilutions of all primary and secondary antibodies can be found in Additional Table 4 and 5. The nuclei were counterstained with 200 ng/ml 4′, 6-diamidin-2-phenylindol (DAPI, Sigma-Aldrich) diluted in PBS for 45 min. After three washes with PBS, the spheroids were mounted on a glass microscope slide in 50% glycerol in ddH_2O. For microscopy, a Leica DMI6000B along with the Leica LAS-X-software (Leica, Wetzlar, Germany) was used. All images were taken under identical settings from at least 10 biological replicates. For the generation of 3D data, Z Stacks were used. Deconvolution was carried out by the LAS-X-integrated module.

Scanning electron microscopy

Single human and murine spheroids were fixed in Eppendorf tubes using 2 ml of a 2.5% solution of glutaraldehyde (Sigma-Aldrich). Samples were washed two times in 0.1 M cacodylate buffer (Sigma-Aldrich). For dehydration, samples were passed through an increasing ethanol concentration gradient (30%, 50%, 70%, 90% and 99.8%). The obtained samples were sputtered with a carbon layer (Leica, EM ACE600) and observed with the Scanning Electron Microscope Auriga 60 (Carl Zeiss Microscopy, Oberkochen, Germany) as described earlier [88].

Transmission electron microscopy

For thin section electron microscopy, the human and murine spheroids were individually fixed and stored in 2.5% glutaraldehyde. Prior to dehydration, samples were rinsed in 0.2 M sodium cacodylate (pH 7.2) and fixed in 2% aqueous osmium tetroxide for 2 h. After that, samples were washed in distilled water, dehydrated through a series of ethanol and impregnated, embedded and polymerized for 24 h at 60°C in Agar 100 epoxy resin. Ultra-thin (60–80 nm) sections were cut with diamond knives on a Leica ultramicrotome. For electron microscopy, sections were stained with 2% uranyl acetate and examined in a

JEOL 1200EX transmission electron microscope operated at 80 kV as described earlier [88].

Infection with *C. jejuni* 81–176

Human SMIS were generated as described above. 75 spheroids were then infected as previously described with *C. jejuni* strain 81–176 for six hours in a humidified atmosphere at 37°C and 5% CO_2 using a multiplicity of infection (MOI) of 500 [49]. As controls, 75 non-infected spheroids only treated with PBS were considered. 15 spheroids from each group were randomly pooled to provide enough RNA for gene expression analysis and thus represented one biological replicate. Spheroids were washed in an Eppendorf tube five times using PBS, letting them sink to the bottom after every wash. To investigate differences between 3 and 2D cell culture, monolayers were infected as described earlier [49] with following adaptions: 3×10^5 Caco-2 cells were seeded on 6 Well Plates (Sarstedt) and incubated for two days. The wells were then infected with *C. jejuni* strain 81–176 for six hours (also MOI of 500). As controls, non-infected monolayers were treated with PBS. After the infection time, wells were washed five times with PBS.

RNA-isolation and RT-qPCR

For gene expression analysis, infected and non-infected spheroids and monolayers were lysed and RNA was isolated. For the spheroids, the *Quick*-RNA Micro Prep Kit (Zymo Research Europe GmbH, Freiburg, Germany) was used, for the Caco-2 cells the *Quick*-RNA Mini Prep Kit (Zymo Research Europe GmbH). 15 spheroids were pooled for one biological sample. RT-qPCR was performed as described earlier [48, 49]. As reference genes, *HPRT*, *B2M* and *PPIB* were selected and stability tested with geNorm [89]. For comparing SMIS with in vivo samples, murine cDNA generated from colon samples (LaGeSo, Berlin, registration number G0104/19) from our published study was used [49]. All oligonucleotides in this study were synthesized by Sigma-Aldrich. Sequences and primer concentrations can be found in Additional Table 7 and 8.

Statistical analysis

Normal distribution of data was assessed by the Anderson–Darling test. The two-tailed unpaired t-test was used in this study to compare infected with non-infected control samples. All tests were conducted applying GraphPad Prism version 10.0.2 (GraphPad Software, La Jolla California USA, http://www.graphpad.com). Asterisks in figures summarize P values ($^*P\leq0.05$; $^{**}P\leq0.01$; $^{***}P\leq0.001$; $^{****}P\leq0.0001$).

Supplementary Information

The online version contains supplementary material available at https://doi.org/10.1186/s13099-024-00644-6.

Supplementary Material 1

Acknowledgements
We extend our special thanks to Dr. Lena Hoeke for her assistance in providing excess intestinal material from the mice, which were sacrificed for teaching purposes. Additionally, we would like to express our gratitude to Dr. Kamlesh Pawar for critically reviewing the manuscript. Our sincere appreciation also goes to Mrs. Kutz-Lohroff for her professional support in conducting the experiments.

Author contributions
AK: Performed experiments, analyzed and interpreted data, wrote paper PM: Performed experiments, co-edited paper RK: Analyzed and interpreted data CR: Performed experiments JS: Provided material, co-edited paper MMH: Provided material, co-edited paper TA: Provided material CH: Provided material, co-edited paper GG: Provided material, co-edited paper RE: Provided material and advice SS: Designed study, analyzed and interpreted data, wrote paper.

Funding
Open Access funding enabled and organized by Projekt DEAL. Open access funding enabled and organized by Projekt DEAL. This work was supported by the Research Committee of the Freie Universität Berlin. Clara Raeckel's work was supported by the H. Wilhelm Schaumann Foundation, Hamburg, Germany. The funders had no role in study design, data collection and analysis, decision to publish or preparation of the manuscript.

Data availability
No datasets were generated or analysed during the current study.

Declarations

Ethics approval and consent to participate
Mouse experiments were carried out in compliance with the European Guidelines for animal welfare (2010/63/EU). The protocol was approved by the commission for animal experiments headed by the "Landesamt für Gesundheit und Soziales". Animal welfare was monitored twice daily by assessment of clinical conditions. Registration numbers are given in Materials and Methods.

Consent for publication
Not applicable.

Competing interests
The authors declare no competing interests.

Author details
[1]Institute of Veterinary Biochemistry, Freie Universität Berlin, Berlin, Germany. [2]Institute of Animal Husbandry and Breeding, Wrocław University of Environmental and Life Sciences, Wrocław, Poland. [3]Institute of Veterinary Pathology, Freie Universität Berlin, Berlin, Germany. [4]School of Science, OSZ Lise Meitner, Berlin, Germany. [5]Institute of Microbiology, Infectious Diseases and Immunology, Charité, Universitätsmedizin Berlin, Corporate Member of Freie Universität Berlin, Humboldt-Universität Zu Berlin, and Berlin Institute of Health, Berlin, Germany. [6]Institute of Food Safety and Food Hygiene, Freie Universität Berlin, Berlin, Germany. [7]SGS INSTITUT FRESENIUS GmbH, Berlin, Germany.

Received: 21 June 2024 Accepted: 12 September 2024
Published online: 17 September 2024

References

1. Kapałczyńska M, Kolenda T, Przybyła W, Zajączkowska M, Teresiak A, Filas V, Ibbs M, Bliźniak R, Łuczewski Ł, Lamperska K. 2D and 3D cell

cultures—a comparison of different types of cancer cell cultures. AMS. 2018;14(4):910–9.
2. Preksha G, Yesheswini R, Srikanth CV. Cell culture techniques in gastrointestinal research: methods, possibilities and challenges. Indian J Pathol Microbiol. 2021;64(Supplement):S52-s57.
3. Biju TS, Priya VV, Francis AP. Role of three-dimensional cell culture in therapeutics and diagnostics: an updated review. Drug Deliv Transl Res. 2023;13(9):2239–53.
4. Achilli TM, Meyer J, Morgan JR. Advances in the formation, use and understanding of multi-cellular spheroids. Expert Opin Biol Ther. 2012;12(10):1347–60.
5. Ryan S-L, Baird A-M, Vaz G, Urquhart AJ, et al. Drug discovery approaches utilizing three-dimensional cell culture. Assay Drug Dev Technol. 2016;14(1):19–28.
6. Jensen C, Teng Y. Is it time to start transitioning from 2D to 3D cell culture? Front Mol Biosci. 2020. https://doi.org/10.3389/fmolb.2020.00033.
7. Klingelhutz AJ, Gourronc FA, Chaly A, Wadkins DA, Burand AJ, Markan KR, Idiga SO, Wu M, Potthoff MJ, Ankrum JA. Scaffold-free generation of uniform adipose spheroids for metabolism research and drug discovery. Sci Rep. 2018;8(1):523.
8. Shanks N, Greek R, Greek J. Are animal models predictive for humans? Philos Ethics Humanit Med. 2009;4:2.
9. Koledova Z. 3D cell culture: an introduction. Methods Mol Biol. 2017;1612:1–11.
10. Clevers H. Modeling development and disease with organoids. Cell. 2016;165(7):1586–97.
11. Pleguezuelos-Manzano C, Puschhof J, van den Brink S, Geurts V, Beumer J, Clevers H. Establishment and culture of human intestinal organoids derived from adult stem cells. Curr Protoc Immunol. 2020;130(1): e106.
12. Serra D, Mayr U, Boni A, Lukonin I, Rempfler M, Challet Meylan L, Stadler MB, Strnad P, Papasaikas P, Vischi D, et al. Self-organization and symmetry breaking in intestinal organoid development. Nature. 2019;569(7754):66–72.
13. Almeqdadi M, Mana MD, Roper J, Yilmaz ÖH. Gut organoids: mini-tissues in culture to study intestinal physiology and disease. Am J Physiol Cell Physiol. 2019;317(3):C405-c419.
14. Kim J, Koo B-K, Knoblich JA. Human organoids: model systems for human biology and medicine. Nat Rev Mol Cell Biol. 2020;21(10):571–84.
15. Co JY, Margalef-Català M, Li X, Mah AT, Kuo CJ, Monack DM, Amieva MR. Controlling epithelial polarity: a human enteroid model for host-pathogen interactions. Cell Rep. 2019;26(9):2509-2520.e2504.
16. Kakni P, López-Iglesias C, Truckenmüller R, Habibović P, Giselbrecht S. PSC-derived intestinal organoids with apical-out orientation as a tool to study nutrient uptake, drug absorption and metabolism. Front Mol Biosci. 2023. https://doi.org/10.3389/fmolb.2023.1102209.
17. Li L, Jiao L, Feng D, Yuan Y, Yang X, Li J, Jiang D, Chen H, Meng Q, Chen R, et al. Human apical-out nasal organoids reveal an essential role of matrix metalloproteinases in airway epithelial differentiation. Nat Commun. 2024;15(1):143.
18. Stroulios G, Brown T, Moreni G, Kondro D, Dei A, Eaves A, Louis S, Hou J, Chang W, Pajkrt D, et al. Apical-out airway organoids as a platform for studying viral infections and screening for antiviral drugs. Sci Rep. 2022;12(1):7673.
19. Hofmann S, Cohen-Harazi R, Maizels Y, Koman I. Patient-derived tumor spheroid cultures as a promising tool to assist personalized therapeutic decisions in breast cancer. Transl Cancer Res. 2021;11(1):134–47.
20. Białkowska K, Komorowski P, Bryszewska M, Miłowska K. Spheroids as a type of three-dimensional cell cultures-examples of methods of preparation and the most important application. Int J Mol Sci. 2020;21(17):6225.
21. Luo L, Zhang W, Wang J, Zhao M, Shen K, Jia Y, Li Y, Zhang J, Cai W, Xiao D, et al. A novel 3D culture model of human ascs reduces cell death in spheroid cores and maintains inner cell proliferation compared with a nonadherent 3D culture. Front Cell Dev Biol. 2021. https://doi.org/10.3389/fcell.2021.737275.
22. Gunti S, Hoke ATK, Vu KP, London NR. Organoid and spheroid tumor models: techniques and applications. Cancers. 2021;13(4):874.
23. Weiswald L-B, Bellet D, Dangles-Marie V. Spherical cancer models in tumor biology. Neoplasia. 2015;17(1):1–15.
24. Shield K, Ackland ML, Ahmed N, Rice GE. Multicellular spheroids in ovarian cancer metastases: biology and pathology. Gynecol Oncol. 2009;113(1):143–8.
25. Tutty MA, Prina-Mello A. Three-dimensional spheroids for cancer research. Methods Mol Biol. 2023;2645:65–103.
26. Rosa RB, Dantas WM, do Nascimento JCF, da Silva MV, de Oliveira RN, Pena LJ. In vitro and in vivo models for studying sars-cov-2, the etiological agent responsible for COVID-19 pandemic. Viruses 2021;13(3):379
27. da Silva da Costa FA, Soares MR, Malagutti-Ferreira MJ, da Silva GR, Lívero F, Ribeiro-Paes JT. Three-dimensional cell cultures as a research platform in lung diseases and COVID-19. Tissue Eng Regen Med 2021, 18(5):735-745.
28. Tetteh PW, Basak O, Farin HF, Wiebrands K, Kretzschmar K, Begthel H, van den Born M, Korving J, de Sauvage F, van Es JH, et al. Replacement of lost Lgr5-positive stem cells through plasticity of their enterocyte-lineage daughters. Cell Stem Cell. 2016;18(2):203–13.
29. Krug SM. Von 3D zu 2D: organoid-basierte monolayer als modell der Darmbarriere. BIOspektrum. 2023;29(7):745–8.
30. Abud HE, Chan WH, Jardé T. Source and impact of the EGF family of ligands on intestinal stem cells. Front Cell Dev Biol. 2021;9: 685665.
31. Perez White BE, Getsios S. Eph receptor and ephrin function in breast, gut, and skin epithelia. Cell Adh Migr. 2014;8(4):327–38.
32. Holmberg J, Genander M, Halford MM, Annerén C, Sondell M, Chumley MJ, Silvany RE, Henkemeyer M, Frisén J. EphB receptors coordinate migration and proliferation in the intestinal stem cell niche. Cell. 2006;125(6):1151–63.
33. Lisabeth EM, Falivelli G, Pasquale EB. Eph receptor signaling and ephrins. Cold Spring Harb Perspect Biol. 2013. https://doi.org/10.1101/cshperspect.a009159.
34. Weiß F, Holthaus D, Kraft M, Klotz C, Schneemann M, Schulzke JD, Krug SM. Human duodenal organoid-derived monolayers serve as a suitable barrier model for duodenal tissue. Ann N Y Acad Sci. 2022;1515(1):155–67.
35. Lehmann A, Hornby PJ. Intestinal SGLT1 in metabolic health and disease. Am J Physiol Gastrointest Liver Physiol. 2016;310(11):G887-898.
36. Spanier B, Rohm F. Proton coupled oligopeptide transporter 1 (PepT1) function, regulation, and influence on the intestinal homeostasis. Compr Physiol. 2018;8(2):843–69.
37. El Harane S, Zidi B, El Harane N, Krause KH, Matthes T, Preynat-Seauve O. Cancer spheroids and organoids as novel tools for research and therapy: state of the art and challenges to guide precision medicine. Cells. 2023;12(7):1001.
38. Gheytanchi E, Naseri M, Karimi-Busheri F, Atyabi F, Mirsharif ES, Bozorgmehr M, Ghods R, Madjd Z. Morphological and molecular characteristics of spheroid formation in HT-29 and Caco-2 colorectal cancer cell lines. Cancer Cell Int. 2021;21(1):204.
39. Xue Y, Wang M, Han H. Interaction between alveolar macrophages and epithelial cells during *Mycoplasma pneumoniae* infection. Front Cell Infect Microbiol. 2023;13:1052020.
40. Philpott DJ, Girardin SE, Sansonetti PJ. Innate immune responses of epithelial cells following infection with bacterial pathogens. Curr Opin Immunol. 2001;13(4):410–6.
41. Crawley SW, Mooseker MS, Tyska MJ. Shaping the intestinal brush border. J Cell Biol. 2014;207(4):441–51.
42. Kaunitz JD, Akiba Y. Control of intestinal epithelial proliferation and differentiation: the microbiome, enteroendocrine L cells, telocytes, enteric nerves, and GLP. Too Dig Dis Sci. 2019;64(10):2709–16.
43. Suzuki A, Sekiya S, Gunshima E, Fujii S, Taniguchi H. EGF signaling activates proliferation and blocks apoptosis of mouse and human intestinal stem/progenitor cells in long-term monolayer cell culture. Lab Invest. 2010;90(10):1425–36.
44. Duckworth CA. Identifying key regulators of the intestinal stem cell niche. Biochem Soc Trans. 2021;49(5):2163–76.
45. Genander M, Halford MM, Xu NJ, Eriksson M, Yu Z, Qiu Z, Martling A, Greicius G, Thakar S, Catchpole T, et al. Dissociation of EphB2 signaling pathways mediating progenitor cell proliferation and tumor suppression. Cell. 2009;139(4):679–92.
46. Hanisch C, Sharbati J, Kutz-Lohroff B, Huber O, Einspanier R, Sharbati S. Trefoil factor 3 mediates resistance to apoptosis in colon carcinoma cells by a regulatory RNA axis. Cell Death Dis. 2017;8(3): e2660.
47. Sharbati J, Lewin A, Kutz-Lohroff B, Kamal E, Einspanier R, Sharbati S. Integrated microRNA-mRNA-analysis of human monocyte derived macrophages upon *Mycobacterium avium* subsp. hominissuis infection. PLoS ONE. 2011;6(5):e20258.

48. Xi D, Hofmann L, Alter T, Einspanier R, Bereswill S, Heimesaat MM, Gölz G, Sharbati S. The glycosyltransferase ST3GAL2 is regulated by miR-615-3p in the intestinal tract of *Campylobacter jejuni* infected mice. Gut Pathogens. 2021;13(1):42.
49. Kraski A, Mousavi S, Heimesaat MM, Bereswill S, Einspanier R, Alter T, Gölz G, Sharbati S. miR-125a-5p regulates the sialyltransferase ST3GAL1 in murine model of human intestinal campylobacteriosis. Gut Pathogens. 2023;15(1):48.
50. Sharbati J, Hanisch C, Pieper R, Einspanier R, Sharbati S. Small molecule and RNAi induced phenotype transition of expanded and primary colonic epithelial cells. Sci Rep. 2015;5:12681.
51. Tevlek A, Keçili S, Ozcelik O, Kulah H, Tekin H: Spheroid Engineering in Microfluidic Devices. ACS Omega 2023, 8.
52. Sant S, Johnston PA. The production of 3D tumor spheroids for cancer drug discovery. Drug Discov Today Technol. 2017;23:27–36.
53. Pinto B, Henriques AC, Silva PMA, Bousbaa H. Three-dimensional spheroids as in vitro preclinical models for cancer research. Pharmaceutics. 2020;12(12):1186.
54. Dolznig H, Walzl A, Kramer N, Rosner M, Garin-Chesa P, Hengstschläger M. Organotypic spheroid cultures to study tumor–stroma interaction during cancer development. Drug Discov Today Dis Model. 2011;8(2):113–9.
55. Herter S, Morra L, Schlenker R, Sulcova J, Fahrni L, Waldhauer I, Lehmann S, Reisländer T, Agarkova I, Kelm J, et al. A novel three-dimensional heterotypic spheroid model for the assessment of the activity of cancer immunotherapy agents. Cancer Immunol Immunother. 2017. https://doi.org/10.1007/s00262-016-1927-1.
56. Schimpel C, Passegger C, Egger S, Tam-Amersdorfer C, Strobl H. A novel 3D cell culture model to study the human small intestinal immune landscape. Eur J Immunol. 2023;53(3):2250131.
57. Sambuy Y, De Angelis I, Ranaldi G, Scarino ML, Stammati A, Zucco F. The Caco-2 cell line as a model of the intestinal barrier: influence of cell and culture-related factors on Caco-2 cell functional characteristics. Cell Biol Toxicol. 2005;21(1):1–26.
58. Ding X, Hu X, Chen Y, Xie J, Ying M, Wang Y, Yu Q. Differentiated Caco-2 cell models in food-intestine interaction study: current applications and future trends. Trends Food Sci Technol. 2021;107:455–65.
59. Lea T. Caco-2 Cell Line. In: Verhoeckx K, Cotter P, López-Expósito I, Kleiveland C, Lea T, Mackie A, Requena T, Swiatecka D, Wichers H, editors. The Impact of food bioactives on health: in vitro and ex vivo models. Cham: Springer International Publishing; 2015. p. 103–11.
60. Däster S, Amatruda N, Calabrese D, Ivanek R, Turrini E, Droeser RA, Zajac P, Fimognari C, Spagnoli GC, Iezzi G, et al. Induction of hypoxia and necrosis in multicellular tumor spheroids is associated with resistance to chemotherapy treatment. Oncotarget. 2017;8(1):1725–36.
61. Barisam M, Saidi MS, Kashaninejad N, Nguyen NT. Prediction of necrotic core and hypoxic zone of multicellular spheroids in a microbioreactor with a U-shaped barrier. Micromachines (Basel). 2018;9(3):94.
62. Dini S, Binder BJ, Fischer SC, Mattheyer C, Schmitz A, Stelzer EH, Bean NG, Green JE. Identifying the necrotic zone boundary in tumour spheroids with pair-correlation functions. J R Soc Interface. 2016. https://doi.org/10.1098/rsif.2016.0649.
63. Antfolk M, Jensen KB. A bioengineering perspective on modelling the intestinal epithelial physiology in vitro. Nat Commun. 2020;11(1):6244.
64. Scoville D, Sato T, He XC, Li L. Current view: intestinal stem cells and signaling. Gastroenterology. 2008;134:849–64.
65. Papadakos S, Petrogiannopoulos L, Pergaris A, Theocharis S. The EPH/Ephrin system in colorectal cancer. Int J Mol Sci. 2022;23:2761.
66. Kania A, Klein R. Mechanisms of ephrin-Eph signalling in development, physiology and disease. Nat Rev Mol Cell Biol. 2016;17(4):240–56.
67. Wang Y, Wang J, Yang L, Qiu L, Hua Y, Wu S, Zeng S, Yu L, Zheng X. Epigenetic regulation of intestinal peptide transporter PEPT1 as a potential strategy for colorectal cancer sensitization. Cell Death Dis. 2021;12(6):532.
68. Merino B, Fernández-Díaz CM, Cózar-Castellano I, Perdomo G. Intestinal fructose and glucose metabolism in health and disease. Nutrients. 2020;12(1):94.
69. Wang CY, Liu S, Xie XN, Tan ZR. Regulation profile of the intestinal peptide transporter 1 (PepT1). Drug Des Devel Ther. 2017;11:3511–7.
70. Nielsen CU, Amstrup J, Steffansen B, Frokjaer S, Brodin B. Epidermal growth factor inhibits glycylsarcosine transport and hPepT1 expression in a human intestinal cell line. Am J Physiol Gastrointest Liver Physiol. 2001;281(1):G191-199.
71. Brugger MD, Valenta T, Fazilaty H, Hausmann G, Basler K. Distinct populations of crypt-associated fibroblasts act as signaling hubs to control colon homeostasis. PLoS Biol. 2020;18(12): e3001032.
72. Allaire JM, Crowley SM, Law HT, Chang S-Y, Ko H-J, Vallance BA. The intestinal epithelium: central coordinator of mucosal immunity. Trends Immunol. 2018;39(9):677–96.
73. Iftekhar A, Sigal M. Defence and adaptation mechanisms of the intestinal epithelium upon infection. Int J Med Microbiol. 2021;311(3): 151486.
74. Roulis M, Flavell RA. Fibroblasts and myofibroblasts of the intestinal lamina propria in physiology and disease. Differentiation. 2016;92(3):116–31.
75. Bain CC, Mowat AM. The monocyte-macrophage axis in the intestine. Cell Immunol. 2014;291(1–2):41–8.
76. Xi D, Alter T, Einspanier R, Sharbati S, Golz G. Campylobacter jejuni genes Cj1492c and Cj1507c are involved in host cell adhesion and invasion. Gut Pathog. 2020;12:8.
77. Zhang JM, An J. Cytokines, inflammation, and pain. Int Anesthesiol Clin. 2007;45(2):27–37.
78. Turner MD, Nedjai B, Hurst T, Pennington DJ. Cytokines and chemokines: at the crossroads of cell signalling and inflammatory disease. Biochim Biophys Acta Mol Cell Res. 2014;1843(11):2563–82.
79. Siegesmund AM, Konkel ME, Klena JD, Mixter PF. Campylobacter jejuni infection of differentiated THP-1 macrophages results in interleukin 1 beta release and caspase-1-independent apoptosis. Microbiology (Reading). 2004;150(Pt 3):561–9.
80. Al-Banna NA, Cyprian F, Albert MJ. Cytokine responses in campylobacteriosis: linking pathogenesis to immunity. Cytokine Growth Factor Rev. 2018;41:75–87.
81. Bücker R, Krug SM, Moos V, Bojarski C, Schweiger MR, Kerick M, Fromm A, Janßen S, Fromm M, Hering NA, et al. Campylobacter jejuni impairs sodium transport and epithelial barrier function via cytokine release in human colon. Mucosal Immunol. 2018;11(2):474–85.
82. Hu L, Bray MD, Osorio M, Kopecko DJ. *Campylobacter jejuni* induces maturation and cytokine production in human dendritic cells. Infect Immun. 2006;74(5):2697–705.
83. Larson CL, Samuelson DR, Eucker TP, O'Loughlin JL, Konkel ME. The fibronectin-binding motif within FlpA facilitates *Campylobacter jejuni* adherence to host cell and activation of host cell signaling. Emerg Microbes Infect. 2013;2(10): e65.
84. Krause-Gruszczynska M, Boehm M, Rohde M, Tegtmeyer N, Takahashi S, Buday L, Oyarzabal OA, Backert S. The signaling pathway of *Campylobacter jejuni*-induced Cdc42 activation: Role of fibronectin, integrin beta1, tyrosine kinases and guanine exchange factor Vav2. Cell Commun Signal. 2011;9:32.
85. Higuchi Y, Kojima M, Ishii G, Aoyagi K, Sasaki H, Ochiai A. Gastrointestinal fibroblasts have specialized, diverse transcriptional phenotypes: a comprehensive gene expression analysis of human fibroblasts. PLoS ONE. 2015;10(6): e0129241.
86. Gonzalez LM, Moeser AJ, Blikslager AT. Porcine models of digestive disease: the future of large animal translational research. Transl Res. 2015;166(1):12–27.
87. Tominaga T, Suzuki M, Saeki H, Matsuno S, Tachibana T, Kudo T. Establishment of an activated macrophage cell line, A-THP-1, and its properties. Tohoku J Exp Med. 1998;186(2):99–119.
88. Krzyżek P, Migdał P, Grande R, Gościniak G. Biofilm formation of helicobacter pylori in both static and microfluidic conditions is associated with resistance to clarithromycin. Front Cell Infect Microbiol. 2022;12:868905.
89. Vandesompele J, De Preter K, Pattyn F, Poppe B, Van Roy N, De Paepe A, Speleman F. Accurate normalization of real-time quantitative RT-PCR data by geometric averaging of multiple internal control genes. Genome Biol. 2002;3(7):Research0034.

Publisher's Note

6. Discussion

The pathogenesis of *C. jejuni* infections remains incompletely understood. Therefore, the first study presented (5.1) explored the molecular mechanisms underlying *C. jejuni* infections by identifying specific miRNA:mRNA interactions within the mucin-type *O*-glycosylation pathway. Here, a combination of *in silico*, *in vivo* and *in vitro* approaches were used. In the second study (5.2), a novel and advanced 3D cell culture model that closely mimics the *in vivo* intestinal mucosal surface microarchitecture was designed. Due to limitations in current *in vitro* infection models, it is possible to study *C. jejuni* infections more realistically with this model.

The German Federal Ministry for Economic Cooperation and Development (BMZ) has reported that seventy-five percent of all newly emerging infectious diseases originate from animals, posing considerable health risks to both humans and animals [90]. Especially the combination of the rise in zoonotic diseases on the one hand and the simultaneous increase in antimicrobial resistance on the other hand presents hazard. The food-borne microbial infections affecting the human gastrointestinal tract are specifically concerning since they lead to alarmingly high rates of morbidity worldwide. *Campylobacter* in particular is considered as the most common cause for foodborne enteric infections in humans in the EU and globally. Around 140.000 cases were confirmed in 2022 and reported in the EU, with nearly one-third (44.000) occurring from Germany alone ([27]). However, the European Food Safety Authority (EFSA) estimates that the actual number of cases could be as high as nine million annually, due to a high estimated number of cases that are unreported or undiagnosed. Moreover, the socioeconomic impact of *Campylobacter* infections is substantial, with estimated annual costs, including public health system burdens and productivity losses in the EU, reaching about 2.4 billion € per year (EFSA). Taking the severity of these numbers into account, it is essential to deepen the understanding of underlying mechanisms in *Campylobacter* infections to control the spread of the pathogen, develop novel treatment options or prevent infections altogether. Despite pressing need of understanding the pathogenesis of *Campylobacter* infections however, the mechanisms behind infections, particularly those involving *C. jejuni*, are yet only incompletely understood, highlighting the importance for continued research. Here comprehensive insight into the disease development and progression following *Campylobacter* infections is necessary.

Campylobacter infections have a high impact on individuals and economy. Therefore the "One World - One Health" approach has been established to reduce this burden. This initiative collaboratively brings together public health authorities, veterinarians, clinicians, researchers, and policymakers to focus on the interconnection between health of humans, domestic animals, livestock, wild animals, and the ecosystems they inhabit (BMZ). Following this approach, the studies presented in this thesis aim to enhance the understanding of the molecular and cellular mechanisms underlying *C. jejuni* infections, including the development of an advanced 3D cell culture model to study the infection in greater detail to optimize human health. Alarmingly, researchers have also revealed that certain *Campylobacter* subspecies exhibit antibiotic resistance, particularly to fluoroquinolones, and are classified by the WHO as high-priority targets for research and the development of new antibiotics [91]. This underlines the urgent need for improved research.

The complex double mucus layer serves as a physical barrier and first line of defense in the mammalian colon. Here, the viscoelastic mucus traps microorganisms which are then cleared through intestinal movements and mucus renewal. Under physiological conditions, the inner dense layer of the mucus remains sterile. Certain pathogens however, like *C. jejuni*, have adapted highly advanced mechanisms to penetrate this protecting mucus layer and infect the underlying epithelium. Not only has *C. jejuni* been shown to survive in the mucus by evading rapid mucosal clearance but also reproduce there *in vitro* [92]. As a result to the presence of invading bacteria such as the intestinal pathogens *Helicobacter pylori* (*H. pylori*), *Shigella flexneri* (*S. flexneri*) and *C. jejuni*, changes in mucin synthesis and mucin secretion occur. More specifically, *H. pylori* inhibited mucin synthesis by over eighty percent *in vitro*, while *S. flexneri* hindered mucin secretion through aggregating on the cellular surface and altered the mucin structure by changing the glycosylation profiles [93, 94]. Previous studies suggest that in case of *C. jejuni,* a downregulation in the transcription levels of MUC2 in intestinal goblet cells during *in vivo* and *in vitro* infections can be observed, along with the dysregulation of the co-secreted Trefoil factor 3 (TFF3) [50, 95].

The *O*-glycans on the protein backbone of MUC2 are synthesized and elongated in a stepwise process, catalyzed by specific enzymes, known as glycosyltransferases. These enzymes play an important role in the biosynthesis of *O*-glycans and the loss or alteration of specific glycosyltransferases leads to abnormal glycan structures that are characterized by reduced

extension or modified patterns. [12]. Differentiated glycosylation patterns in MUC2 were previously identified in the intestinal tract of *C. jejuni* infected mice [50]. Here, the sialyltransferase *St3gal2* was significantly decreased. In the first study presented, these results were able to be reproduced, observing a significant 0.4-fold decrease in *St3gal2* expression. Additional dysregulation in the sialyltransferase *St3gal1* and Galactosyltransferase *B4galt1* in the colon of a murine model of human campylobacteriosis six days post *C. jejuni* infection was identified. Notably, the two glycosyltransferases are conserved in the species human and mouse and are associated with mucin-type *O*-glycosylation. *St3gal1* was significantly upregulated by 4-fold and *B4galt1* by 1.6-fold, both compared to naïve control animals. Significantly elevated gene expression levels of *ST3GAL1* and *B4GALT1* were correspondingly observed in *C. jejuni* infected Caco-2 monolayers and human SMIS six hours post infection (both compared to naïve counterparts). Elevated protein expression levels of ST3GAL1 were additionally detected in the colon of infected mouse samples. Combining all these findings, the results suggest that *C. jejuni* infection significantly alters the expression of specific glycosyltransferase genes involved in mucin-type *O*-glycosylation in the species human and mouse. MUC2 is primarily defined by their *O*-glycans, therefore the observed dysregulations of these glycosyltransferases could hypothetically impact the glycosylation pattern of MUC2 and alter structure and function of the mucin. A study by Larsson et al. (2011) indicated that strong changes in the glycan pattern and a shift towards smaller and less complex glycans on MUC2 were associated with the development of inflammation and a more severe disease course in ulcerative colitis patients [96]. The upregulation of *St3gal1* as observed in the study could induce elevated sialylation and thus termination of the glycan chain extension, that potentially leads to the formation of smaller and less complex glycans on MUC2. This raises important questions about the role of sialylation in mucosal defense mechanisms. Sialic acids on MUC2 have been shown to play a role in both facilitating bacterial adhesion and covering bacterial attachment sites [8]. Therefore, it remains unclear whether these modifications are driven by the pathogen to enhance colonization and infection or are a response by the mucosal immune system to fight the infection. Further investigation is required to clarify this aspect.

Mucin-type *O*-glycosylation is not just limited to mucins. Recent findings have linked the above-mentioned sialyltransferase ST3GAL1 to differential glycosylation of the Epidermal Growth Factor Receptor (EGFR). This glycosylation modulates the corresponding EGFR

signaling pathway, which is important for various cellular processes [97]. More precisely, the ST3GAL1-mediated sialylation of the EGFR inhibits its phosphorylation, which then impacts the activation of downstream pathways such as the inhibition of phosphoinositide 3-kinase (PI3K)-Protein kinase B (AKT) pathway [97]. The PI3K-AKT pathway represents an important signaling pathway that regulates cell growth, differentiation, survival, proliferation and nutrient uptake. EGFR as an upstream activator of PI3K initiates this pathway when ligands like the Epidermal growth factor (EGF) bind to it. Upon activation, PI3K is recruited to the cell membrane and phosphorylates phosphatidylinositol-4,5-bisphosphate (PIP2) to generate phosphatidylinositol-3,4,5-trisphosphate (PIP3). PIP3 then recruits AKT which in turn is phosphorylated again and induces the phosphorylation of various substrates regulating numerous cellular processes [98]. Therefore, when ST3GAL1 inhibits EGFR phosphorylation, it suppressed the activation of the PI3K-AKT pathway.

The interactions between glycosylations and signaling pathways become particularly interesting in the context of *C. jejuni* infections. It was shown that specific fibronectin-binding proteins from *C. jejuni* activate the EGFR signaling pathway within host cells [99]. This activation triggers a cascade of intracellular mechanisms, resulting in the Rho-GTPase CDC42-dependent formation of membrane protrusions known as filopodia that facilitate enhanced bacterial invasion into host cells [100]. The ability of *C. jejuni* to manipulate and interfere with host signaling pathways, including the EGFR pathway, demonstrates the pathogen's ability to alter cellular mechanisms to their own benefit. The interaction between *C. jejuni* and EGFR and also ST3GAL1 represents an intriguing aspect of the bacterial infection process that needs to be further investigated, especially when considering the results discovered in this research. Understanding these complex interplays is crucial for gaining new insights into the pathogenesis of *C. jejuni* and developing potential new strategies to fight these infections.

miRNAs have gained increasing attention over the past decade as significant contributors to the interactions between bacterial pathogens and their host. Bacteria have evolved advanced mechanisms to manipulate host miRNAs and thereby alter host pathways for their own advantage. These small RNAs play a crucial role in coordinating an effective immune response to manage and eliminate infections [75]. As demonstrated by previous research, a dysregulation in the two miRNAs miR-125a-5p and miR-615-3p follows intestinal *C. jejuni* infections [101]. These findings were both confirmed and extended in Study 5.1, revealing a

significant reduction in miR-125a-5p by 0.6-fold and an increase in miR-615-3p by 2.1-fold in infected murine colonic tissue samples compared to naïve controls. Whether these dysregulations are directly caused by the pathogen or are a response of the immune system to the infection, remains uncertain. The studies additionally suggest that the two miRNAs are possibly involved in regulating mucins by modulating their expression and synthesis through their targets. This mechanism holds potential for therapeutic use as targeting mucins directly may offer benefits, since their aberrant expression is linked to diseases like cancer [102, 103]. Notably, an inverse correlation between miR-615-3p and the expression of *MUC2* and co-secreted *TFF3* during *C. jejuni* infections was detected, underlining a potential critical role of miR-615-3p in regulating mucin levels in the context of this infection [50].

miRNAs have been identified to critically regulate the glycome and glycosylation processes through the modulation of specific glycosyltransferases [104, 105]. Several glycosyltransferases involved in mucin-type *O*-glycosylations have been found to be controlled by miRNAs including the UDP-GalNAc:polypeptide *N*-acetylgalactosaminyltransferases (GalNAc-T) 1-5, initiating the mucin-type *O*-glycosylation process, as well as GCNT3 [106-111]. The aforementioned miRNAs miR-125a-5p and miR-615-3p have recently been linked to mucin-type *O*-glycosylation, too [50]. To further investigate these interactions, *in silico* analysis was conducted to identify relevant murine and human targets of these miRNAs (see Study 5.1). This analysis revealed *St3gal1* and *B4galt1* as potential overlapping targets of the two miRNAs. Both enzymes are involved in the mucin-type *O*-glycosylation pathway and conserved in human and mouse species. *St3gal2*, *Gcnt1* and *Gcnt4* were predicted to be targeted by the miRNAs exclusively in mice, while the glucuronyltransferase *B3GNT1* was identified as a target in humans. Although primary focus of the study was on *St3gal1* and *B4galt1*, further research is needed to fully explore the role of these miRNAs, glycosyltransferases, and other identified targets in mucin-type *O*-glycosylation. The relationship between miR-125a-5p and *St3gal1* and *B4galt1* was examined more closely in Study 5.1, particularly in the context of *C. jejuni* infections. Gene and protein expression analysis of the infected murine colonic tissue samples revealed an inverse correlation of miR-125a-5p and *St3gal1* and *B4galt1*, suggesting that *C. jejuni* infection may influence the expression of these glycosyltransferase genes in the murine colon, potentially through a miRNA-dependent mechanism. The transfection of the murine intestinal cell line CMT-93 with miR-125a-5p led to a significant reduction in the transcripts of *St3gal1* and *B4galt1*, indicating

a regulation by this miRNA. *St3gal2*, however, was not significantly affected. Luciferase reporter assays confirmed a specific binding of miR-125a-5p to sites on *St3gal1*, demonstrating a direct interaction between the miRNA and its target.

These findings collectively suggest a link between miR-125a-5p, *St3gal1*, *B4galt1* and *C. jejuni* infections. However, the exact underlying mechanism and whether the observed dysregulations impact MUC2 or are related to other mucin-type *O*-glycosylations remain unclear, necessitating further research. Here, the impact of the miRNAs on EGFR signaling through differential *O*-glycosylation during *C. jejuni* infection presents another interesting aspect for future investigations.

In response to the unanswered questions from Study 5.1 and to achieve a deeper understanding of the cellular processes involved in *C. jejuni* infections, it was necessary to develop an advanced cell culture model that does not rely on laboratory animals. Notably, current research in bacterial infection biology, particularly involving in *C. jejuni*, suffers from a significant lack of standardized, scalable and reproducible 3D models. Study 5.2 introduced a novel and innovative 3D cell culture model to address and overcome these deficiencies. This new model offers a new broad foundation for investigating the molecular mechanisms underlying *C. jejuni* infections and is versatile enough for application in a range of other research areas as well. Furthermore, the creation of this model aligns with the critical need for improved tools to study *C. jejuni* infections, as highlighted by Tacconelli et al. (2018) [91]. Thus, the advancement of effective models is crucial for addressing challenges and contributing to the broader field of infectious disease research.

Infection and virulence studies of intestinal pathogens are typically carried out using *in vivo* or *in vitro* models. *In vivo* studies often use small animal models, mice for example, due to their resemblance to human anatomy, physiology and pathophysiology. As complex organisms, mice express innate immune responses after infections that are comparable to those found in humans. However, while *in vivo* models are essential for understanding host-pathogen interactions, they also have strong limitations. These include ethical concerns about animal welfare, significant inter-individual variability, and high costs in terms of time and resources [112]. Moreover, mice do not always replicate human responses to pathogens accurately. For instance, *H. pylori*, a human specific gastric pathogen, can cause chronic infections that lead

to gastric ulcers and gastric cancer in humans [113]. In contrast, in mice result *H. pylori* infections usually only in mild gastritis, which does not progress to ulcerations or cancer [114]. Similarly, *C. jejuni* pathogenesis is only limitedly transferable from animal models to humans. While *C. jejuni* can colonize chickens as a commensal bacterium without causing a disease, it is also less susceptible to mice compared to humans, likely due to competition with the murine intestinal microbiota [46]. To overcome this problem, the murine intestinal microbiota is often depleted in *in vivo* models using antibiotics, which increases susceptibility to *C. jejuni* and facilitates its rapid growth to high concentrations in the intestine [46, 114]. Despite this, disease symptoms in mice are often minimal and are rarely observed. To address this issue, alternative models were invented. For instance, IL-10 deficiency models induce inflammation and colitis in mice and are used to simulate symptoms more closely to campylobacteriosis in humans [45, 115].

Alternatively, infection studies can be conducted using *in vitro* models. Initially, 2D cell culture were employed, where immortalized cell lines are grown as monolayers and subsequently infected with the pathogen of interest. These cell models are cost-effective, less labor-intensive, and easily accessible compared to *in vivo* studies. They offer reproducibility and efficiency in experimental setups. While 2D monolayers have significantly extended our understanding of basic host-pathogen interactions, they fall short in representing the complex tissue architecture and physiological conditions of living organisms. They are limited in their ability to replicate important cell-cell interactions and extracellular microenvironments [116]. Concluding, animal models cannot always accurately predict the disease development in humans and 2D cell culture systems lack important characteristics of the complex *in vivo* tissue architecture. To overcome these limitations, advanced 3D cell culture methods have been developed, providing more accurate models that mimic the complexities of human tissue physiology and pathophysiology while precisely project disease progression.

3D cell culture techniques bridge the gap between 2D and *in vivo* models by allowing cells to grow and interact within a three-dimensional environment. These cells are cultured under controlled conditions and aim to develop a microarchitecture that closely mimics those of living organisms. Cell-cell and cell-extracellular matrix interactions are enhanced and thereby *in vivo* conditions more accurately resembled [117]. 3D models offer the opportunity to reduce the reliance on animal studies while improving traditional 2D methods. Organoids

provide an advanced research model as for instance, intestinal organoids, replicate tissue-specific features such as crypts and villi, and consist of a fully polarized, multicellular epithelium including enterocytes, goblet cells, Paneth cells, and enteroendocrine cells [118, 119]. This is a major advantage when using organoids as infection models as it has been shown in *C. jejuni*, *Salmonella* and *S. flexneri* [58, 120, 121]. However, the limitations of organoids can pose challenges, especially for infection studies. A critical weakness of organoids is the fact that the luminal surface is typically oriented towards the interior which complicates exposure to luminal factors like microbiota and pathogens. Although labor-intensive techniques exist to reorient organoids to an apical-out configuration, this remains a challenging aspect of their use [122].

Spheroids, on the other hand, can bypass the majority of these limitations while still resembling *in vivo* microarchitecture and facilitating *in vivo*-like cell-cell interactions. Spheroids are cost-effective, easy to generate, and offer reproducibility and standardization. They can be classified into homotypic models, consisting of only a single cell type, and multicellular models, comprising two or more cell types. Multicellular spheroids are commonly used in tumor research and are typically formed by simply mixing different cell types without any directed organization [123, 124]. In the Study 5.2 however, structured multicellular intestinal spheroids (SMIS) for the species human, mouse and pig were developed using ULA-plates that were grown in a given order. The primary goal was to create self-assembling cellular structures featuring a fibroblast core (NHDF neo) surrounded by a monolayer of enterocytes (Caco-2), goblet cells (HT-29/MTX-E12), and activated monocytes (A-THP-1). This setup aimed to replicate the *in vivo* intestinal microarchitecture of the luminal surface. Moreover, in SMIS, nearly every cell on the outer layer was connected to the inner fibroblast core, ensuring important cell-cell connections. The direct contact between enterocytes and surrounding cell types facilitated not only epithelial-mesenchymal but also epithelial-immune cell cross-talks, which has been shown to be an essential factor for organ functionality and development [125-127]. Immunofluorescent staining and phenotype-specific markers confirmed the organized structure of the spheroids, revealing a central fibroblast core lined with epithelial cells, goblet cells, and monocytes. This study represents the first successful creation of multicellular intestinal spheroids with a structured organization.

In the electron microscopy analysis of human und murine spheroids, relevant intestinal functional histological features, such as microvilli formation, were observed. This is particularly noteworthy given that the SMIS were only cultured for two days after the addition of enterocytes, goblet cells, and immune cells to the fibroblast core. The rapid achievement of these features underscores the time efficiency of the SMIS compared to other models. For instance, intestinal organoids, especially those derived from induced pluripotent stem cells, require a prolonged period for differentiation and microvilli formation [119, 128]. Similarly, Caco-2 monolayers need 14-21 days post-confluence to differentiate fully [129]. The presence of microvilli in differentiated enterocytes within the SMIS suggests that these epithelial cells quickly attain functional enterocyte characteristics. An important feature of SMIS are the mesenchymal-epithelial and mesenchymal-monocyte interactions. These connections might also play a pivotal role in promoting the rapid differentiation of enterocytes and the formation of key intestinal structures, like microvilli, within just two days of culture. Notably, single type Caco-2 spheroids, in contrast, exhibited a smooth surface without microvilli formation, highlighting the significance of diverse cell-cell interactions between relevant cells even more [130].

For further validation, marker for intestinal differentiation (EphrinB1 (EFNB1) and EphrinB2 (EFNB2)) were investigated by gene expression analysis in human SMIS compared to Caco-2 monolayers cultured for the same amount of time. The mammalian intestinal epithelium constantly renews itself, with proliferating cells at the crypt base, that, migrating upwards, differentiate into absorptive enterocytes. Considering this, proliferation marker (EGF and ephrin B receptor 2 (EPHB2)) were also evaluated. Interestingly, all four markers were significantly elevated in SMIS compared to Caco-2 monolayers, indicating the presence of both proliferating and differentiated enterocytes in the SMIS. This is usually very challenging to achieve in cell culture models, emphasizing the advancement SMIS and the superiority of the spheroids over 2D monolayers. Moreover, the expression of sodium-dependent glucose cotransporter 1 (SGLT1) and peptide transporter 1 (PEPT1), key solute carrier proteins found in the brush border of differentiated enterocytes were identified to assess the absorption potential of Caco-2 cells in both 3D and 2D cultures. The significantly elevated *SGLT1* (3.9-fold) supports the differentiation findings, while reduced *PEPT1* (0.64-fold) require further investigation. As discussed in Study 5.2, elevated EGF levels might contribute to this outcome,

however additional research is needed to elucidate the reasons behind the downregulation of *PEPT1*.

SMIS were originally generated to investigate the molecular mechanisms underlying *C. jejuni* infections, given their ability to closely mimic the intestinal mucosa where initial infections occur. In Study 5.2 human SMIS were infected with *C. jejuni* and a comprehensive analysis on genes associated with categories 'Regulation of the Immune Response', 'Cytokine Response', 'Apoptosis', and '*C. jejuni*-related' conducted. These findings were compared with those from *C. jejuni*-infected Caco-2 monolayers, naïve SMIS, and *C. jejuni*-infected murine colonic tissue samples from Study 5.1. The comparison to 2D Caco-2 cells revealed fundamental differences between 2D and 3D models while the comparison to naïve SMIS highlighted pathogen-derived differences in gene expression. In particular, the infected SMIS showed a greater number of infection-relevant markers with more pronounced regulation compared to the 2D model. Ten immunological markers were significantly elevated in the infected SMIS relative to naïve spheroids, with the highest levels observed for *IL1a*, *1b*, *6*, *8*, *TNFA* and *CCL2*. These pro-inflammatory cytokines, primarily produced by activated macrophages, are critically involved in the immune and inflammatory response also regarding infections. The upregulation of these markers aligns with similar responses observed in other intestinal pathogen infections. Elevated levels of IL6 and TNFA for instance have been documented in *H. pylori* and *Salmonella* infections, highlighting their role in the physiological immune response to these pathogens [131, 132]. This underscores the relevance of the SMIS model in studying immune interactions during *C. jejuni* infections and its potential for broader applications in understanding other gastrointestinal infections.

A major advantage of the SMIS model is its close resemblance to *in vivo* conditions. When comparing *C. jejuni* infected SMIS with murine colonic tissue samples obtained from the Study 5.1, similar dysregulations in the representative cytokines, *EGFR*, *ST3GAL1* and *B4GALT1* were detectable. This similarity highlights the advanced nature of the SMIS model compared to conventional 2D Caco-2 cells, which did not show these correlations to the same extent. To explore whether the observed dysregulations in *ST3GAL1* and *B4GALT1* in infected SMIS might be influenced by the miRNA miR-125a-5p, as seen in the infected colon samples from Study 5.1., forms an intriguing point for future research connecting both Studies. This could provide valuable insights in the modulating role of miR-125a-5p on the glycosyltransferase activity

during *C. jejuni* infections and enhance the understanding of molecular mechanisms behind it.

Human intestinal cancer cell lines have recently shown an upregulation in MUC2, induced by proinflammatory cytokines such as IL-1, IL-8 and TNFA [133]. In Study 5.2, as mentioned above, significant upregulation of these proinflammatory cytokines following *C. jejuni* infection in murine *in vivo* samples and in 2D and 3D cell culture models was also observed. This raises compelling questions for future research including whether MUC2 expression is dysregulated in these models and whether this dysregulation is driven by *C. jejuni*, the proinflammatory cytokines, or a combination of both. Further exploring could provide deeper insights into the interplay between pathogen-driven inflammation and mucin regulation.

In both Studies presented, the infection studies were carried out using *C. jejuni* strain 81-176. Interestingly, *C. jejuni* exhibits significant genetic variability among different strains [134]. It possesses natural competence, allowing the uptake of macromolecular DNA from its environment and integrating it in their genomes, which facilitates the recombination between strains for an even greater diversity [135]. Therefore, selecting the specific *C. jejuni* strain is crucial for experimental outcomes, as different strains vary significantly in their adhesion, colonization, and infection capabilities. *C. jejuni* strain 81-176 was chosen in both studies due to its high invasiveness and strong colonization ability [33]. However, the choice of strain can profoundly impact the experimental results, including the pathogen's invasion and colonization efficiency. Other commonly used strains in *C. jejuni* research, such as NCTC 11168, 81116, and F38011, might yield different results in infection studies due to their varying characteristics. This highlights the importance of carefully selecting the strain based on the specific research goals and the biological questions being addressed.

The Study 5.2 demonstrated that SMIS constitute a highly accessible, standardized, scalable and reproducible model. It provides a higher level of tissue complexity compared to traditional 2D cell cultures by also being more time- and cost-efficient than *in vivo* or other 3D models like organoids, while still producing comparable results. In retrospective, there are aspects however, that can be improved in the future. Firstly, human SMIS were generated using NHDF neo cells for the core. These cells are dermal fibroblasts and therefore do not accurately replicate intestinal fibroblasts. To better mimic the *in vivo* architecture, future studies should

incorporate human intestinal fibroblasts. Due to difficulties in obtaining human intestinal fibroblasts, the murine and porcine models were improved by integrating primary intestinal myofibroblasts instead, with promising results. Murine SMIS generated with primary intestinal myofibroblasts to form the core displayed enhanced differentiation of the epithelial layer compared to the murine SMIS with an embryonic fibroblast core. The microvilli in the murine spheroids with the primary cells were more orderly and better structured in contrast to the only partially organized microvilli observed in human SMIS, making them more comparable with microvilli *in vivo*. This suggests that incorporating human primary intestinal fibroblasts could further improve the model's relevance to human physiology. Additionally, integrating activated monocytes into the core rather than the outer layer would more accurately replicate the Lamina propria. Other intestinal cell types like enteroendocrine cells of Tuft cells can increase the resemblance of the intestinal mucosa even further.

As a versatile model, SMIS are easily expandable to other intestinal pathogens. As shown in the Study 5.2, the model can also be successfully applied to the species mouse and pig, with murine SMIS exhibiting well-structured histological features like microvilli. Future research could explore the generation of spheroids to other species as well. Furthermore, to further connect Study 5.1 and 5.2, detailed investigations on molecular mechanisms in *C. jejuni* infections might uncover fundamental differences between murine and human models, potentially explaining why mice exhibit lower susceptibility to the pathogen. Here also other species are intriguing to study. Interestingly, research suggests that *C. jejuni* invades human intestinal cell lines more efficiently than non-human cell lines [136]. It was shown that *C. jejuni* has a higher capability to invade human versus chicken epithelial cells and a significantly higher invasion of *C. jejuni* was demonstrated in Caco-2 cells compared to porcine IPEC-1 cells [34, 137]. This aligns with the observation that humans are more susceptible to *C. jejuni* invasion and infections compared to most other wild and domestic animals. Here, avian spheroids could provide valuable insights into campylobacteriosis, helping to identify physiological variations between humans and birds and elucidate why *C. jejuni* does not cause illness in birds. Given the use of IL-10 deficient mice in the *in vivo* studies, incorporating IL-10 knockout in murine SMIS could offer new perspectives for refining and reducing animal models. SMIS can also be adapted for other tissues by using organ-specific cell lines. Beyond infection studies, SMIS have broad applications in areas such as nutrition uptake, regenerative

medicine, and drug screening. When using primary cells from specific donors, SMIS could also serve as personalized models.

In summary, dysregulation of the glycosyltransferases *ST3GAL1* and *B4GALT1*, both associated with mucin-type *O*-glycosylation, is evident following *C. jejuni* infection. These changes are likely driven by altered regulation of the miRNA miR-125a-5p, which targets these enzymes. However, unresolved questions remain regarding the interplay between miR-125a-5p, ST3GAL1, and B4GALT1 in the context of *C. jejuni* infections. Future research should focus on elucidating the impact of differential glycosylation of MUC2 and other mucin-type *O*-glycosylation enzymes. Additionally, a novel and advanced 3D cell culture model was developed to study *C. jejuni* infections in greater detail, minimizing reliance on animal studies. Structured multicellular intestinal spheroids (SMIS) were created for human, mouse, and pig species, incorporating a fibroblast core covered by a monolayer of relevant intestinal cell lines to mimic the microarchitecture and morphological characteristics of the intestinal mucosa. Human SMIS, featuring four relevant cell lines, surpassed traditional 2D cell models regarding differentiation and infection studies. The immunological marker patterns observed in SMIS are comparable to those found in *in vivo* infections.

7. Conclusion

The presented Studies 5.1 and 5.2 have significantly advanced our understanding of the molecular and cellular mechanisms underlying *C. jejuni* infections. The research revealed a complex interaction between miRNAs, glycosyltransferases and host cell responses during *C. jejuni* infections.

Study 5.1 demonstrated that miR-125a-5p and miR-615-3p play a role in the regulation of the glycosylation patterns of host cell response proteins during *C. jejuni* infections. The observed dysregulation of the sialyltransferases *St3gal1* and *St3gal2*, as well as the galactosyltransferase *B4galt1*, suggests a miRNA-mediated regulatory network that influences mucin glycosylation in the colon. This network may be part of the host's immune response to hinder pathogenic colonization or, conversely, a mechanism that is used by the pathogen to facilitate invasion.

The development of structured multicellular intestinal spheroids (SMIS) in Study 5.2 represents a significant advancement in infection biology research. SMIS offer a standardized, scalable and reproducible model that closely mimics the luminal layer of the mammalian intestinal mucosa. Their enhanced differentiation states, functional morphological characteristics and ability to exhibit regulatory patterns of immunological markers similar to *in vivo* infections make them a valuable tool for studying *C. jejuni* pathogenesis.

Looking ahead, these findings open up several fields for promising research. The role of altered mucin-type *O*-glycosylation in *C. jejuni* infections requires further investigations, particularly regarding potential modifications of MUC2 but also other signaling proteins. Glycan analysis could provide valuable insights into these modifications. Additionally, future studies should also explore the application of SMIS to other species and organs, expanding its utility beyond infection biology. Integrating primary intestinal fibroblasts and the monocytes into the SMIS core could further enhance its resemblance to the mammalian colon and the Lamina propria. Moreover, incorporating other immune cells could create a more complex immunological response, potentially leading to an even more accurate representation of the intestinal environment. Investigating the newly identified miRNAs by using the SMIS model could provide a more comprehensive understanding of the regulatory roles in *C. jejuni* infections.

In conclusion, these studies have enhanced the understanding of molecular and cellular mechanisms of *C. jejuni* infections better and have provided a promising new model for future research. The combination of molecular insights and advances *in vitro* models can lead the way for more targeted approaches in developing strategies to fight *C. jejuni* infections and potentially other gastrointestinal pathogens.

8. References

1. Grondin, J.A., et al., *Mucins in Intestinal Mucosal Defense and Inflammation: Learning From Clinical and Experimental Studies.* Front Immunol, 2020. **11**: p. 2054.
2. Sun, J., et al., *Therapeutic Potential to Modify the Mucus Barrier in Inflammatory Bowel Disease.* Nutrients, 2016. **8**(1).
3. Ramos, F.L., J.S. Krahnke, and V. Kim, *Clinical issues of mucus accumulation in COPD.* Int J Chron Obstruct Pulmon Dis, 2014. **9**: p. 139-50.
4. Lewis, W.G., et al., *Degradation, foraging, and depletion of mucus sialoglycans by the vagina-adapted Actinobacterium Gardnerella vaginalis.* J Biol Chem, 2013. **288**(17): p. 12067-79.
5. Gubatan, J., et al., *Antimicrobial peptides and the gut microbiome in inflammatory bowel disease.* World J Gastroenterol, 2021. **27**(43): p. 7402-7422.
6. Bergstrom, K. and L. Xia, *The barrier and beyond: Roles of intestinal mucus and mucin-type O-glycosylation in resistance and tolerance defense strategies guiding host-microbe symbiosis.* Gut Microbes, 2022. **14**(1): p. 2052699.
7. Kudelka, M.R., et al., *Intestinal epithelial glycosylation in homeostasis and gut microbiota interactions in IBD.* Nature Reviews Gastroenterology & Hepatology, 2020. **17**(10): p. 597-617.
8. Arike, L., J. Holmén-Larsson, and G.C. Hansson, *Intestinal Muc2 mucin O-glycosylation is affected by microbiota and regulated by differential expression of glycosyltranferases.* Glycobiology, 2017. **27**(4): p. 318-328.
9. Lindén, S.K., T.H.J. Florin, and M.A. McGuckin, *Mucin Dynamics in Intestinal Bacterial Infection.* PLOS ONE, 2008. **3**(12): p. e3952.
10. Bautista, M.V., et al., *IL-8 regulates mucin gene expression at the posttranscriptional level in lung epithelial cells.* J Immunol, 2009. **183**(3): p. 2159-66.
11. Kim, Y.S. and S.B. Ho, *Intestinal goblet cells and mucins in health and disease: recent insights and progress.* Curr Gastroenterol Rep, 2010. **12**(5): p. 319-30.
12. Corfield, A.P., *The Interaction of the Gut Microbiota with the Mucus Barrier in Health and Disease in Human.* Microorganisms, 2018. **6**(3).
13. Raev, S.A., et al., *Intestinal mucin-type O-glycans: the major players in the host-bacteria-rotavirus interactions.* Gut Microbes, 2023. **15**(1): p. 2197833.
14. Tran, D.T. and K.G. Ten Hagen, *Mucin-type O-glycosylation during development.* J Biol Chem, 2013. **288**(10): p. 6921-9.
15. Paone, P. and P.D. Cani, *Mucus barrier, mucins and gut microbiota: the expected slimy partners?* Gut, 2020. **69**(12): p. 2232.
16. Poole, J., et al., *Glycointeractions in bacterial pathogenesis.* Nature Reviews Microbiology, 2018. **16**(7): p. 440-452.
17. Naughton, J.A., et al., *Divergent mechanisms of interaction of Helicobacter pylori and Campylobacter jejuni with mucus and mucins.* Infect Immun, 2013. **81**(8): p. 2838-50.
18. Yao, Y., et al., *Mucus sialylation determines intestinal host-commensal homeostasis.* Cell, 2022. **185**(7): p. 1172-1188.e28.
19. Taniguchi, M., et al., *Sialylation shapes mucus architecture inhibiting bacterial invasion in the colon.* Mucosal Immunology, 2023. **16**(5): p. 624-641.
20. Duan, L.L., et al., *Regulation of metastasis-suppressive gene Nm23-H1 on glycosyl-transferases involved in the synthesis of sialyl Lewis antigens.* J Cell Biochem, 2005. **94**(6): p. 1248-57.

21. Angata, K. and M. Fukuda, *ST3 Beta-Galactoside Alpha-2,3-Sialyltransferase 1 (ST3GAL1)*, in *Handbook of Glycosyltransferases and Related Genes*, N. Taniguchi, et al., Editors. 2014, Springer Japan: Tokyo. p. 637-644.
22. Lopez, P.H., et al., *Mice lacking sialyltransferase ST3Gal-II develop late-onset obesity and insulin resistance.* Glycobiology, 2017. **27**(2): p. 129-139.
23. Regina Todeschini, A. and S.I. Hakomori, *Functional role of glycosphingolipids and gangliosides in control of cell adhesion, motility, and growth, through glycosynaptic microdomains.* Biochim Biophys Acta, 2008. **1780**(3): p. 421-33.
24. Huizinga, R., et al., *Sialylation of Campylobacter jejuni Lipo-Oligosaccharides: Impact on Phagocytosis and Cytokine Production in Mice.* PLOS ONE, 2012. **7**(3): p. e34416.
25. Lindahl, J.F. and D. Grace, *The consequences of human actions on risks for infectious diseases: a review.* Infect Ecol Epidemiol, 2015. **5**: p. 30048.
26. Rahman, M.T., et al., *Zoonotic Diseases: Etiology, Impact, and Control.* Microorganisms, 2020. **8**(9).
27. *Plain Language Summary on The European Union One Health 2022 Zoonoses Report.* EFSA Journal, 2023. **21**(12): p. p211202.
28. Corcionivoschi, N. and O. Gundogdu, *Foodborne Pathogen Campylobacter.* Microorganisms, 2021. **9**(6).
29. Gölz, G., et al., *Relevance of Campylobacter to public health—The need for a One Health approach.* International Journal of Medical Microbiology, 2014. **304**(7): p. 817-823.
30. Alemka, A., N. Corcionivoschi, and B. Bourke, *Defense and adaptation: the complex inter-relationship between Campylobacter jejuni and mucus.* Front Cell Infect Microbiol, 2012. **2**: p. 15.
31. Flanagan Rebecca, C., et al., *Examination of Campylobacter jejuni Putative Adhesins Leads to the Identification of a New Protein, Designated FlpA, Required for Chicken Colonization.* Infection and Immunity, 2009. **77**(6): p. 2399-2407.
32. Talukdar, P.K., et al., *Molecular Dissection of the Campylobacter jejuni CadF and FlpA Virulence Proteins in Binding to Host Cell Fibronectin.* Microorganisms, 2020. **8**(3).
33. Backert, S. and D. Hofreuter, *Molecular methods to investigate adhesion, transmigration, invasion and intracellular survival of the foodborne pathogen Campylobacter jejuni.* Journal of microbiological methods, 2013. **95**.
34. Tegtmeyer, N., et al., *Campylobacter Virulence Factors and Molecular Host-Pathogen Interactions.* Curr Top Microbiol Immunol, 2021. **431**: p. 169-202.
35. Campana, R. and W. Baffone, *Intracellular Survival and Translocation Ability of Human and Avian Campylobacter jejuni and Campylobacter coli Strains*, in *Advances in Microbiology, Infectious Diseases and Public Health: Volume 14*, G. Donelli, Editor. 2020, Springer International Publishing: Cham. p. 115-125.
36. Buelow, D.R., et al., *Campylobacter jejuni survival within human epithelial cells is enhanced by the secreted protein CiaI.* Mol Microbiol, 2011. **80**(5): p. 1296-312.
37. Louwen, R., et al., *Campylobacter jejuni translocation across intestinal epithelial cells is facilitated by ganglioside-like lipooligosaccharide structures.* Infect Immun, 2012. **80**(9): p. 3307-18.
38. Hameed, A., *Human Immunity Against Campylobacter Infection.* Immune Netw, 2019. **19**(6): p. e38.
39. Kløve, S., et al., *Toll-Like Receptor-4 Is Involved in Mediating Intestinal and Extra-Intestinal Inflammation in Campylobacter coli-Infected Secondary Abiotic IL-10(-/-) Mice.* Microorganisms, 2020. **8**(12).

40. Heimesaat, M.M., et al., *Human Campylobacteriosis—A Serious Infectious Threat in a One Health Perspective*, in *Fighting Campylobacter Infections: Towards a One Health Approach*, S. Backert, Editor. 2021, Springer International Publishing: Cham. p. 1-23.
41. Alter, T., S. Bereswill, and S. Backert, *Campylobacteriose — eine zoonotische Infektionskrankheit.* BIOspektrum, 2021. **27**(6): p. 591-593.
42. Kemper, L. and A. Hensel, *Campylobacter jejuni: targeting host cells, adhesion, invasion, and survival.* Applied Microbiology and Biotechnology, 2023. **107**(9): p. 2725-2754.
43. Yuki, N., et al., *Carbohydrate mimicry between human ganglioside GM1 and Campylobacter jejuni lipooligosaccharide causes Guillain–Barré syndrome.* Proceedings of the National Academy of Sciences, 2004. **101**(31): p. 11404-11409.
44. Yuki, N., *Ganglioside mimicry and peripheral nerve disease.* Muscle Nerve, 2007. **35**(6): p. 691-711.
45. Haag, L.M., et al., *Campylobacter jejuni induces acute enterocolitis in gnotobiotic IL-10-/- mice via Toll-like-receptor-2 and -4 signaling.* PLoS One, 2012. **7**(7): p. e40761.
46. Bereswill, S., et al., *Novel murine infection models provide deep insights into the "ménage à trois" of Campylobacter jejuni, microbiota and host innate immunity.* PLoS One, 2011. **6**(6): p. e20953.
47. Heimesaat, M.M., et al., *Gram-negative bacteria aggravate murine small intestinal Th1-type immunopathology following oral infection with Toxoplasma gondii.* J Immunol, 2006. **177**(12): p. 8785-95.
48. Mansfield, L.S., et al., *Genetic background of IL-10(-/-) mice alters host-pathogen interactions with Campylobacter jejuni and influences disease phenotype.* Microb Pathog, 2008. **45**(4): p. 241-57.
49. Bereswill, S., et al., *Campylobacter jejuni infection of conventionally colonized mice lacking nucleotide-oligomerization-domain-2.* Gut Pathog, 2017. **9**: p. 5.
50. Xi, D., et al., *The glycosyltransferase ST3GAL2 is regulated by miR-615-3p in the intestinal tract of Campylobacter jejuni infected mice.* Gut Pathog, 2021. **13**(1): p. 42.
51. Mousavi, S., et al., *Vitamin C alleviates acute enterocolitis in Campylobacter jejuni infected mice.* Scientific Reports, 2020. **10**(1): p. 2921.
52. Everest, P.H., et al., *Differentiated Caco-2 cells as a model for enteric invasion by Campylobacter jejuni and C. coli.* J Med Microbiol, 1992. **37**(5): p. 319-25.
53. Wine, E., V.L. Chan, and P.M. Sherman, *Campylobacter jejuni Mediated Disruption of Polarized Epithelial Monolayers is Cell-Type Specific, Time Dependent, and Correlates With Bacterial Invasion.* Pediatric Research, 2008. **64**(6): p. 599-604.
54. Konkel, M.E. and W. Cieplak, *Altered synthetic response of Campylobacter jejuni to cocultivation with human epithelial cells is associated with enhanced internalization.* Infection and Immunity, 1992. **60**(11): p. 4945-4949.
55. Šikić Pogačar, M., et al., *Effect of Lactobacillus spp. on adhesion, invasion, and translocation of Campylobacter jejuni in chicken and pig small-intestinal epithelial cell lines.* BMC Veterinary Research, 2020. **16**(1): p. 34.
56. Montanari, M., et al., *Extracellular Vesicles from Campylobacter jejuni CDT-Treated Caco-2 Cells Inhibit Proliferation of Tumour Intestinal Caco-2 Cells and Myeloid U937 Cells: Detailing the Global Cell Response for Potential Application in Anti-Tumour Strategies.* Int J Mol Sci, 2022. **24**(1).
57. Lobo de Sá, F.D., et al., *Curcumin Mitigates Immune-Induced Epithelial Barrier Dysfunction by Campylobacter jejuni.* Int J Mol Sci, 2019. **20**(19).

58. Aguirre Garcia, M., et al., *Intestinal Organoids: New Tools to Comprehend the Virulence of Bacterial Foodborne Pathogens.* Foods, 2022. **11**(1).
59. Si, W., et al., *The role and mechanisms of action of microRNAs in cancer drug resistance.* Clinical Epigenetics, 2019. **11**(1): p. 25.
60. Giovannetti, E., et al., *Molecular mechanisms underlying the role of microRNAs (miRNAs) in anticancer drug resistance and implications for clinical practice.* Critical Reviews in Oncology/Hematology, 2012. **81**(2): p. 103-122.
61. Kozomara, A., M. Birgaoanu, and S. Griffiths-Jones, *miRBase: from microRNA sequences to function.* Nucleic Acids Res, 2019. **47**(D1): p. D155-d162.
62. Jonas, S. and E. Izaurralde, *Towards a molecular understanding of microRNA-mediated gene silencing.* Nature Reviews Genetics, 2015. **16**(7): p. 421-433.
63. Shu, J., et al., *Dynamic and Modularized MicroRNA Regulation and Its Implication in Human Cancers.* Scientific Reports, 2017. **7**(1): p. 13356.
64. Ergin, K. and R. Çetinkaya, *Regulation of MicroRNAs*, in *miRNomics: MicroRNA Biology and Computational Analysis*, J. Allmer and M. Yousef, Editors. 2022, Springer US: New York, NY. p. 1-32.
65. O'Brien, J., et al., *Overview of MicroRNA Biogenesis, Mechanisms of Actions, and Circulation.* Frontiers in Endocrinology, 2018. **9**.
66. Denli, A.M., et al., *Processing of primary microRNAs by the Microprocessor complex.* Nature, 2004. **432**(7014): p. 231-235.
67. Saliminejad, K., et al., *An overview of microRNAs: Biology, functions, therapeutics, and analysis methods.* Journal of Cellular Physiology, 2019. **234**(5): p. 5451-5465.
68. Hill, M. and N. Tran, *miRNA interplay: mechanisms and consequences in cancer.* Dis Model Mech, 2021. **14**(4).
69. Mohr, A.M. and J.L. Mott, *Overview of microRNA biology.* Semin Liver Dis, 2015. **35**(1): p. 3-11.
70. Luna Buitrago, D., R.C. Lovering, and A. Caporali, *Insights into Online microRNA Bioinformatics Tools.* Non-Coding RNA, 2023. **9**(2): p. 18.
71. Sharma, Y., et al., *Host miRNA and immune cell interactions: relevance in nano-therapeutics for human health.* Immunologic Research, 2022. **70**(1): p. 1-18.
72. Duval, M., P. Cossart, and A. Lebreton, *Mammalian microRNAs and long noncoding RNAs in the host-bacterial pathogen crosstalk.* Semin Cell Dev Biol, 2017. **65**: p. 11-19.
73. Pedersen, I. and M. David, *MicroRNAs in the immune response.* Cytokine, 2008. **43**(3): p. 391-4.
74. Potenza, N., et al., *Molecular mechanisms governing microRNA-125a expression in human hepatocellular carcinoma cells.* Scientific Reports, 2017. **7**(1): p. 10712.
75. Aguilar, C., M. Mano, and A. Eulalio, *Multifaceted Roles of microRNAs in Host-Bacterial Pathogen Interaction.* Microbiology Spectrum, 2019. **7**(3): p. 10.1128/microbiolspec.bai-0002-2019.
76. Das, K., O. Garnica, and S. Dhandayuthapani, *Modulation of Host miRNAs by Intracellular Bacterial Pathogens.* Frontiers in Cellular and Infection Microbiology, 2016. **6**.
77. Chandan, K., M. Gupta, and M. Sarwat, *Role of Host and Pathogen-Derived MicroRNAs in Immune Regulation During Infectious and Inflammatory Diseases.* Frontiers in Immunology, 2020. **10**.
78. Gu, H., et al., *Salmonella produce microRNA-like RNA fragment Sal-1 in the infected cells to facilitate intracellular survival.* Scientific Reports, 2017. **7**(1): p. 2392.

79. Ferreira, G.S., et al., *A standardised framework to identify optimal animal models for efficacy assessment in drug development.* PLoS One, 2019. **14**(6): p. e0218014.
80. Domínguez-Oliva, A., et al., *The Importance of Animal Models in Biomedical Research: Current Insights and Applications.* Animals, 2023. **13**(7): p. 1223.
81. Robinson, N.B., et al., *The current state of animal models in research: A review.* International Journal of Surgery, 2019. **72**: p. 9-13.
82. Almeqdadi, M., et al., *Gut organoids: mini-tissues in culture to study intestinal physiology and disease.* Am J Physiol Cell Physiol, 2019. **317**(3): p. C405-c419.
83. Leung, C.M., et al., *A guide to the organ-on-a-chip.* Nature Reviews Methods Primers, 2022. **2**(1): p. 33.
84. Murphy, S.V. and A. Atala, *3D bioprinting of tissues and organs.* Nat Biotechnol, 2014. **32**(8): p. 773-85.
85. de Dios-Figueroa, G.T., et al., *3D Cell Culture Models in COVID-19 Times: A Review of 3D Technologies to Understand and Accelerate Therapeutic Drug Discovery.* Biomedicines, 2021. **9**(6): p. 602.
86. Ryu, N.E., S.H. Lee, and H. Park, *Spheroid Culture System Methods and Applications for Mesenchymal Stem Cells.* Cells, 2019. **8**(12).
87. Benien, P. and A. Swami, *3D tumor models: History, advances and future perspectives.* Future oncology (London, England), 2014. **10**: p. 1311-27.
88. Tevlek, A., et al., *Spheroid Engineering in Microfluidic Devices.* ACS Omega, 2023. **8**.
89. Pinto, B., et al., *Three-Dimensional Spheroids as In Vitro Preclinical Models for Cancer Research.* Pharmaceutics, 2020. **12**: p. 1186.
90. Bundesministerium für wirtschaftliche Entwicklung und Zusammenarbeit; Referat Pandemieprävention, O.H., Tiergesundheit, Biodiversität *Initativthema „One Health" in der Entwicklungszusammenarbeit.* BMZ Papier, 2021. **1**.
91. Tacconelli, E., et al., *Discovery, research, and development of new antibiotics: the WHO priority list of antibiotic-resistant bacteria and tuberculosis.* The Lancet Infectious Diseases, 2018. **18**(3): p. 318-327.
92. Van Deun, K., et al., *Colonization strategy of Campylobacter jejuni results in persistent infection of the chicken gut.* Veterinary Microbiology, 2008. **130**(3): p. 285-297.
93. Sperandio, B., et al., *Virulent Shigella flexneri affects secretion, expression, and glycosylation of gel-forming mucins in mucus-producing cells.* Infect Immun, 2013. **81**(10): p. 3632-43.
94. Byrd, J.C., et al., *Inhibition of gastric mucin synthesis by Helicobacter pylori.* Gastroenterology, 2000. **118**(6): p. 1072-1079.
95. Bergstrom, K.S., et al., *Modulation of intestinal goblet cell function during infection by an attaching and effacing bacterial pathogen.* Infect Immun, 2008. **76**(2): p. 796-811.
96. Larsson, J.M., et al., *Altered O-glycosylation profile of MUC2 mucin occurs in active ulcerative colitis and is associated with increased inflammation.* Inflamm Bowel Dis, 2011. **17**(11): p. 2299-307.
97. Gong, A., et al., *The lncRNA MEG3 mediates renal cell cancer progression by regulating ST3Gal1 transcription and EGFR sialylation.* J Cell Sci, 2020. **133**(16).
98. He, Y., et al., *Targeting PI3K/Akt signal transduction for cancer therapy.* Signal Transduction and Targeted Therapy, 2021. **6**(1): p. 425.
99. Larson, C.L., et al., *The fibronectin-binding motif within FlpA facilitates Campylobacter jejuni adherence to host cell and activation of host cell signaling.* Emerg Microbes Infect, 2013. **2**(10): p. e65.

100. Krause-Gruszczynska, M., et al., *The signaling pathway of Campylobacter jejuni-induced Cdc42 activation: Role of fibronectin, integrin beta1, tyrosine kinases and guanine exchange factor Vav2.* Cell Commun Signal, 2011. **9**: p. 32.
101. Xi, D., et al., *The glycosyltransferase ST3GAL2 is regulated by miR-615-3p in the intestinal tract of Campylobacter jejuni infected mice.* Gut Pathogens, 2021. **13**(1): p. 42.
102. Krishn, S.R., S.K. Batra, and S. Kaur, *Advances in miRNA-Mediated Mucin Regulation.* Current Pharmacology Reports, 2015. **1**(6): p. 355-364.
103. Krishn, S.R., S.K. Batra, and S. Kaur, *Advances in miRNA-Mediated Mucin Regulation.* Curr Pharmacol Rep, 2015. **1**(6): p. 355-364.
104. Thu, C.T. and L.K. Mahal, *Sweet Control: MicroRNA Regulation of the Glycome.* Biochemistry, 2020. **59**(34): p. 3098-3110.
105. Agrawal, P., et al., *Mapping posttranscriptional regulation of the human glycome uncovers microRNA defining the glycocode.* Proc Natl Acad Sci U S A, 2014. **111**(11): p. 4338-43.
106. Shan, Y., et al., *LncRNA SNHG7 sponges miR-216b to promote proliferation and liver metastasis of colorectal cancer through upregulating GALNT1.* Cell Death Dis, 2018. **9**(7): p. 722.
107. Serino, G., et al., *Role of let-7b in the regulation of N-acetylgalactosaminyltransferase 2 in IgA nephropathy.* Nephrol Dial Transplant, 2015. **30**(7): p. 1132-9.
108. Liu, B., et al., *LINC01296/miR-26a/GALNT3 axis contributes to colorectal cancer progression by regulating O-glycosylated MUC1 via PI3K/AKT pathway.* J Exp Clin Cancer Res, 2018. **37**(1): p. 316.
109. Qu, J.J., X.Y. Qu, and D.Z. Zhou, *miR-4262 inhibits colon cancer cell proliferation via targeting of GALNT4.* Mol Med Rep, 2017. **16**(4): p. 3731-3736.
110. Stiegelbauer, V., et al., *miR-196b-5p Regulates Colorectal Cancer Cell Migration and Metastases through Interaction with HOXB7 and GALNT5.* Clin Cancer Res, 2017. **23**(17): p. 5255-5266.
111. Li, Q., et al., *Downregulation of N-Acetylglucosaminyltransferase GCNT3 by miR-302b-3p Decreases Non-Small Cell Lung Cancer (NSCLC) Cell Proliferation, Migration and Invasion.* Cell Physiol Biochem, 2018. **50**(3): p. 987-1004.
112. Shanks, N., R. Greek, and J. Greek, *Are animal models predictive for humans?* Philos Ethics Humanit Med, 2009. **4**: p. 2.
113. Salama, N.R., M.L. Hartung, and A. Müller, *Life in the human stomach: persistence strategies of the bacterial pathogen Helicobacter pylori.* Nat Rev Microbiol, 2013. **11**(6): p. 385-99.
114. Ansari, S. and Y. Yamaoka, *Animal Models and Helicobacter pylori Infection.* J Clin Med, 2022. **11**(11).
115. Heimesaat, M.M., et al., *Campylobacter jejuni infection induces acute enterocolitis in IL-10-/- mice pretreated with ampicillin plus sulbactam.* European Journal of Microbiology and Immunology, 2022. **12**(3): p. 73-83.
116. Ryan, S.-L., et al., *Drug Discovery Approaches Utilizing Three-Dimensional Cell Culture.* ASSAY and Drug Development Technologies, 2016. **14**: p. 19-28.
117. Koledova, Z., *3D Cell Culture: An Introduction.* Methods Mol Biol, 2017. **1612**: p. 1-11.
118. Sato, T., et al., *Single Lgr5 stem cells build crypt-villus structures in vitro without a mesenchymal niche.* Nature, 2009. **459**(7244): p. 262-265.
119. Taelman, J., M. Diaz, and J. Guiu, *Human Intestinal Organoids: Promise and Challenge.* Frontiers in Cell and Developmental Biology, 2022. **10**.

120. Yan, J., et al., *Intestinal organoids to model Salmonella infection and its impact on progenitors.* Scientific Reports, 2024. **14**(1): p. 15160.
121. Llanos-Chea, A., et al., *Bacteriophage Therapy Testing Against Shigella flexneri in a Novel Human Intestinal Organoid-Derived Infection Model.* J Pediatr Gastroenterol Nutr, 2019. **68**(4): p. 509-516.
122. Co, J.Y., et al., *Controlling the polarity of human gastrointestinal organoids to investigate epithelial biology and infectious diseases.* Nature Protocols, 2021. **16**(11): p. 5171-5192.
123. Herter, S., et al., *A novel three-dimensional heterotypic spheroid model for the assessment of the activity of cancer immunotherapy agents.* Cancer immunology, immunotherapy : CII, 2017. **66**.
124. Dolznig, H., et al., *Organotypic spheroid cultures to study tumor-stroma interaction during cancer development.* Drug Discovery Today: Disease Models, 2011. **8**: p. 113-119.
125. Rosenblum, D. and S. Naik, *Epithelial-immune crosstalk in health and disease.* Curr Opin Genet Dev, 2022. **74**: p. 101910.
126. Wittkopf, N., M.F. Neurath, and C. Becker, *Immune-epithelial crosstalk at the intestinal surface.* Journal of Gastroenterology, 2014. **49**(3): p. 375-387.
127. Zhao, L., W. Song, and Y.G. Chen, *Mesenchymal-epithelial interaction regulates gastrointestinal tract development in mouse embryos.* Cell Rep, 2022. **40**(2): p. 111053.
128. Mosa, M.H., et al., *Dynamic Formation of Microvillus Inclusions During Enterocyte Differentiation in Munc18-2–Deficient Intestinal Organoids.* Cellular and Molecular Gastroenterology and Hepatology, 2018. **6**(4): p. 477-493.e1.
129. Lea, T., *Caco-2 Cell Line*, in *The Impact of Food Bioactives on Health: in vitro and ex vivo models*, K. Verhoeckx, et al., Editors. 2015, Springer International Publishing: Cham. p. 103-111.
130. Gheytanchi, E., et al., *Morphological and molecular characteristics of spheroid formation in HT-29 and Caco-2 colorectal cancer cell lines.* Cancer Cell International, 2021. **21**(1): p. 204.
131. Yu, B., et al., *Overlapping cytokines in H. pylori infection and gastric cancer: A tandem meta-analysis.* Frontiers in Immunology, 2023. **14**.
132. Eckmann, L. and M.F. Kagnoff, *Cytokines in host defense against Salmonella.* Microbes and Infection, 2001. **3**(14): p. 1191-1200.
133. Iwashita, J., et al., *mRNA of MUC2 is stimulated by IL-4, IL-13 or TNF-alpha through a mitogen-activated protein kinase pathway in human colon cancer cells.* Immunol Cell Biol, 2003. **81**(4): p. 275-82.
134. Wilson, D.L., et al., *Genetic diversity in Campylobacter jejuni is associated with differential colonization of broiler chickens and C57BL/6J IL10-deficient mice.* Microbiology (Reading), 2010. **156**(Pt 7): p. 2046-2057.
135. Wiesner, R.S., D.R. Hendrixson, and V.J. DiRita, *Natural transformation of Campylobacter jejuni requires components of a type II secretion system.* J Bacteriol, 2003. **185**(18): p. 5408-18.
136. Konkel, M.E., et al., *Factors that influence the interaction of Campylobacter jejuni with cultured mammalian cells.* Journal of Medical Microbiology, 1992. **37**(1): p. 30-37.
137. Ayllón, N., et al., *Comparative Proteomics Reveals Differences in Host-Pathogen Interaction between Infectious and Commensal Relationship with Campylobacter jejuni.* Front Cell Infect Microbiol, 2017. **7**: p. 145.

9. Acknowledgement

I would like to take this opportunity to express my heartfelt gratitude to everyone who has supported me throughout my doctorate journey. Words cannot fully convey how much your help and advice mean to me.

First and foremost, I am sincerely grateful to my supervisor, PD Dr. Soroush Sharbati, for your guidance, expertise, encouragement and unwavering support. Thank you for navigating me through many highs and lows, for never letting me give up and for shaping me into the scientist I am today. Thank you for giving me the opportunity to work on a topic I am truly passionate about.

I would like to thank Prof. Dr. Dr. Ralf Einspanier for granting me the invaluable chance to conduct my doctoral thesis at the Institute of Veterinary Biochemistry. Thank you for allowing me to experience what academic research and teaching are truly like.

I am sincerely grateful to Prof. Dr. Burkhard Kleuser for reviewing and evaluating my thesis.

I would like to thank Dr. Greta Gölz, for your invaluable advice and guidance and for stepping up to help whenever it was needed. I am thankful for Dr. Carlos Hanisch for giving me the opportunity to continue my research and supporting me through the first 1.5 years and for your reviewing the 2. Paper.

I would also like to address my heartful thankfulness to Barbara Kutz-Lohroff for her kind words and advice both inside and outside the lab. Thank you for always lending a hand and providing assistance.

I extent my sincere thanks to the entire Institute of Veterinary Biochemistry team. Thank you everyone for minorly or majorly contributed to this research. The biggest thank you goes to Clara Räckel. Thank you for being the best colleague and friend a person could ask for. Thank you for all the laughter and lab dance parties, even during tough times. Thank you for making this experience one of the best of my life.

I am deeply grateful for my family. Without the constant, unconditional love and support of my parents and my brother, I would not have reached this point today. Thank you, Mama, for listening to all my complaints, thoughts and worries, for all the encouragement and for the countless hours of proofreading. Thank you, Papa, for always being there to help with IT issues, even at the last minute.

And last but certainly not least, thank you Thilo, for standing by my side throughout this journey. Your unwavering support, love and the way you lifted me up when I needed it made this experience so much easier. I could not have done it without you.

10. Scientific Activity

Articles:

Kraski, A., Mousavi, S., Heimesaat, M.M. *et al.* miR-125a-5p regulates the sialyltransferase ST3GAL1 in murine model of human intestinal campylobacteriosis.*Gut Pathog* **15**, 48 (2023). DOI: https://doi.org/10.1186/s13099-023-00577-6

Kraski, A., Migdał, P., Klopfleisch, R. *et al.* Structured multicellular intestinal spheroids (SMIS) as a standardized model for infection biology. *Gut Pathog* **16**, 47 (2024). DOI: https://doi.org/10.1186/s13099-024-00644-6

Talks:

DVH Fachgruppe Physiologie und Biochemie, Gießen, 24.-26.06.2022
Title: Intestinales 3D Zellkultur-Modell für microRNA induzierte Muzin-artige *O*-Glykosylierung nach *Campylobacter jejuni* Infektionen

BB3R Autumn School 2022 – Alternatives to animal testing, Berlin, 10.-12.10.2022
Title: Intestinal Co-Culture Spheroids as a standardized 3D Cell Culture Model

Junior Scientist Zoonosis Meeting 2023, Münster, 15.-16.06.2023
Title: miRNA mediated regulation of the sialyltransferase ST3GAL1 and its role in intestinal *Campylobacter jejuni* Infections

Poster:

Junior Scientist Zoonosis Meeting 2023, Münster, 15.-16.06.2023
Title: miRNA mediated regulation of the sialyltransferase ST3GAL1 and its role in intestinal *Campylobacter jejuni* Infections